Broad Remodeling of the Acetylproteome by SIRT3 Manipulation Fails to Affect Insulin Secretion or β-cell Metabolism in the Absence of Dietary Overnutrition

by

Brett Steven Peterson

Department of Pharmacology and Cancer Biology
Duke University

Date:_____
Approved:

_____
Christopher Newgard, Supervisor

_____
Donald McDonnell, Chair

_____
Matthew Hirschey

_____
Deborah Muoio

_____
David D'Alessio

Dissertation submitted in partial fulfillment of
the requirements for the degree of Doctor
of Philosophy in the Department of
Pharmacology and Cancer Biology in the Graduate School
of Duke University

2018

ABSTRACT

Broad Remodeling of the Acetylproteome by SIRT3 Manipulation Fails to Affect Insulin Secretion or β-cell Metabolism in the Absence of Dietary Overnutrition

by

Brett Steven Peterson

Department of Pharmacology and Cancer Biology
Duke University

Date:_____
Approved:

_____
Chris Newgard, Supervisor

_____
Donald McDonnell, Chair

_____
Matthew Hirschey

_____
Deborah Muoio

_____
David D'Alessio

An abstract of a dissertation submitted in partial
fulfillment of the requirements for the degree
of Doctor of Philosophy in the Department of
Pharmacology and Cancer Biology in the Graduate School of
Duke University

2018

Copyright by
Brett Steven Peterson
2018

Abstract

SIRT3 is an NAD^+-dependent mitochondrial protein deacetylase purported to influence cellular and systemic metabolism through modulation of the mitochondrial acetylproteome. Fuel-stimulated insulin secretion from pancreatic islets involves mitochondrial metabolism and might be susceptible to SIRT3-mediated effects. To investigate this idea, we used CRISPR/Cas9 technology to obtain complete SIRT3 knockout in the INS-1 832/13 insulinoma cell line. In the context of this SIRT3 knockout cell line, we "re-expressed" wild-type SIRT3, β-Galactosidase, or one of three catalytically inactive mutant forms of SIRT3 to generate lines representing a wide range of SIRT3 expression and mitochondrial protein deacetylase activity. We performed large-scale acetylproteome profiling by mass spectrometry on the different lines, and observed wide-spread, SIRT3-dependent changes in acetylation of enzymes involved in fatty acid oxidation, the TCA cycle, and the electron transport chain. Remarkably, despite these broad changes, the cell lines had indistinguishable insulin secretion responses to glucose or pyruvate, and exhibited no differences in function or viability in response to metabolic or ER stress-inducing agents. Moreover, metabolomic profiling revealed that, when compared to SIRT3-null cell lines, expression of wild-type SIRT3 does not result in appreciable changes in a host of organic acid, amino acid or fatty acid-derived acylcarnitine metabolites during glucose stimulation.

We also studied mice with global SIRT3 knockout (SIRT3 KO) fed a standard chow (STD) or high-fat/high-sucrose (HFHS) diet. Importantly, we performed these studies in the C57Bl/6J background in which we replaced the mutant alleles of nicotinamide nucleotide transhydrogenase (*Nnt*) present in the "J" substrain, with the wild-type alleles in order to restore endogenous NNT function. SIRT3 KO and wild-type (WT) mice fed a STD diet exhibited no differences in insulin secretion during oral or IP glucose tolerance tests, and the function of islets isolated from these mice was indistinguishable in islet perifusion studies conducted with a broad array of secretagogues. Only when chronically fed a HFHS diet did SIRT3 KO animals exhibit a modest impairment in insulin secretion, but without an effect on glycemic control. Our broad conclusion is that major changes in mitochondrial protein acetylation in response to manipulation of SIRT3 are not sufficient to cause changes in islet function or metabolism. However, under conditions of chronic nutritional stress (feeding of a HFHS diet for 12 weeks), a negative effect on function appears, suggesting that islets may be more susceptible to nutrition-induced factors (oxidative stress, local cytokine production, etc.) when SIRT3 is absent. Further studies will be required to identify factors that may interact with SIRT3 deficiency and mitochondrial protein hyperacetylation to increase the risk of β-cell dysfunction.

Dedication

I dedicate this dissertation to my grandparents, Robert and Signe Peterson. The work described herein would not have been possible had they not selflessly dedicated themselves to providing their children – and their children's children – with opportunity and continuous support for over half a century. They are true champions of hard work and education, and I hope they find satisfaction and gratification in knowing that my Doctorate of Philosophy is, in large part, fruit of their labor.

Contents

Abstract iv

Dedication vi

List of Tables x

List of Figures xi

List of Abbreviations xiii

Acknowledgements xvii

1. Introduction 1

1.1 The Islets of Langerhans and the Pancreatic β-cell 2

1.2 Type 2 Diabetes (T2D) 3

1.3 Glucose-Stimulated Insulin Secretion (GSIS) 4

1.4 Mitochondrial Function of the β-cell in GSIS and T2D 6

1.5 Mitochondrial Protein Acetylation and Sirtuins 7

1.6 Nonenzymatic Acetylation is a Carbon Stress 9

1.7 The Impact of Global SIRT3 Loss on Metabolic Homeostasis 10

1.8 SIRT3, Mitochondrial Protein Acetylation, and the β-cell 13

1.8.1 Standard Nutrition Conditions 14

1.8.2 Overnutrition Conditions 15

1.8.3 Discrepancies & Limitations of the Existing Literature 19

1.9 Project Goals 24

2. Experimental Procedures 32

2.1 Cell Culture and Reagents 32

2.2 siRNA- and Ad-shRNA-Mediated Target Suppression 33

2.3 CRISPR/Cas9n 34

2.4 Lentiviral Constructs and Lentivirus 35

2.5 Cell Fractionation and Immunoblot Analysis 36

2.6 RNA Isolation and Quantitative PCR (qPCR) 38

2.7 Fuel-Stimulated Insulin Secretion (FSIS) 38

2.8 Acetylproteomics 39

2.9 Metabolomics 46

2.10 Animals 46

2.11 Islet Isolation and Perifusion 48

2.12 Statistical Analysis 49

3. Developing a Tractable *in vitro* β-cell Model for the Interrogation of Mitochondrial Protein Acetylation 54

3.1 Clonal Variability in 832/13 β-cell Subclones with Complete CRISPR/Cas9n-Dependent Loss of SIRT3 57

3.2 Stable Integration of Different SIRT3 Transgenes in Expanded SIRT3 KO Cells Yields Polyclonal Cell Lines with Concordant GSIS Responses 62

4. Defining the SIRT3-Targeted Mitochondrial Acetylproteome of the β-cell and its Impact on Fuel-Stimulated Insulin Secretion (FSIS) 71

4.1 SIRT3 KO β-cells with Re-Expressed Wild-Type SIRT3 Have Deacetylated Mitochondrial Proteins but No Differences in Fuel-Stimulated Insulin Secretion (FSIS) 72

4.2 Metabolic Pathways that Impart Control Over Fuel-Stimulated Insulin Secretion (FSIS) are Represented in the SIRT3-Targeted Acetylproteome 74

4.3 Manipulation of Mitochondrial Protein Acetylation Has No Impact on the Effect of Glucose to Change Metabolite Levels in the β-cell 76

4.4 Differences in the SIRT3-Targeted Acetylproteome Do Not Impact β-cell Viability or Function in the Presence of Stress-Inducing Agents 78

5. Interrogating the Impact of Global SIRT3 Loss *in vivo* Under Conditions of Standard Nutrition and Chronic Overnutrition 89

5.1 Effects of Global SIRT3 Knockout on Insulin Secretion and Glycemic Control in Mice Fed STD or HFHS Diets are Modest 91

5.2 Islets from SIRT3 KO Animals Fed a STD Diet Exhibit Normal Insulin Secretion, whereas Islets from SIRT3 KO Animals Fed a HFHS Diet Secrete Less Insulin in Response to a Wide Array of Secretagogues 93

6. Discussion 103

7. Conclusions 114

Appendix A 117

References 118

Biography 129

List of Tables

Table 1: siRNA duplex sequences 50

Table 2: Adenovirus shRNA target sequences 50

Table 3: CRISPR/Cas9n guide RNA (gRNA) sequences 51

Table 4: qPCR primer sequences 52

Table 5: *Sirt3* genotyping primer sequences 53

Table 6: *Nnt* genotyping primer sequences 53

Table 7: Summary of diet-induce obesity (DIO) study 95

List of Figures

Figure 1: β-cell functional mass coordinates systemic metabolic homeostasis. 27

Figure 2: A decline in β-cell functional mass is a precipitating event in T2D.....28

Figure 3: Mitochondria are central to GSIS. 29

Figure 4: SIRT3 is the main mitochondrial protein deacetylase. 30

Figure 5: Hypothesized role for SIRT3 in the GSIS response of the pancreatic β-cell.....31

Figure 6: Equal suppression of SIRT3 protein by different SIRT3-specific siRNA oligonucleotides (siSIRT3) or an adenovirus-delivered SIRT3-specific shRNA (Ad-shSIRT3) has discordant effects on GSIS. 64

Figure 7: Application of CRISPR/Cas9n results in complete and sustained loss of SIRT3 protein, but SIRT3 KO 832/13 subclones exhibit discordant GSIS responses. 65

Figure 8: Discordance in the expression of mitochondrial sirtuins, canonical components of the GSIS machinery, and insulin further preclude model reliability. 66

Figure 9: Selection of cells with *hINS* expression yields similar GSIS responses in polyclonal populations. 67

Figure 10: Normally distributed functional heterogeneity independent of intervention confirms subclonal discordance is an inherent byproduct of monoclonal derivation.....68

Figure 11: Transgenic overexpression of different forms of SIRT3 in a SIRT3 KO background cell line produces an *in vitro* model with a theoretical maximal delta in SIRT3 expression. 69

Figure 12: Stable integration of different SIRT3 transgenes in an expanded cell population yields functionally concordant cell lines.....70

Figure 13: Graphical summary of the model design and the comparisons being made between the transgenic WT, KO, and HY cell lines. 81

Figure 14: Differences in mitochondrial protein acetylation are not associated with differences in insulin secretion.....83

Figure 15: SIRT3 targets 33% of the proteins identified in the mitochondrial acetylproteome of the β-cell. 84

Figure 16: Quantifying acetylation abundance reveals the degree to which SIRT3 deacetylates specific lysines and specific proteins..... 85

Figure 17: Glucose-stimulated changes in intracellular metabolites are unaffected by changes in the SIRT3-targeted β-cell acetylproteome..... 86

Figure 18: Changes in the SIRT3-targeted β-cell acetylproteome do not affect responses to cell stress agents. 87

Figure 19: Extended culture in media supplemented with 10 mM pyruvate as a potential acetylating agent does not influence FSIS. 88

Figure 20: Genotyping confirms the presence of wild-type *Nnt* in the mouse line generated for study. 94

Figure 21: Isolated islets from SIRT3 KO animals exhibit hyperacetylated proteins under both the STD diet-fed and HFHS diet-fed conditions. 96

Figure 22: Global SIRT3 deletion does not impair glucose tolerance or insulin tolerance in mice fed a STD diet..... 97

Figure 23: Global SIRT3 deletion does not impair glucose tolerance or insulin tolerance in mice fed a HFHS diet, despite a modest difference in the plasma insulin response following an intraperitoneal (IP) glucose bolus. 98

Figure 24: Perifusion of islets isolated from mice fed a STD diet reveals that insulin secretion in response to multiple secretagogues and potentiators is largely unchanged by global deletion of SIRT3..... 100

Figure 25: Perifusion of islets isolated from mice fed a HFHS diet reveals that SIRT3 KO mice secrete less insulin in response to multiple secretagogues and potentiators..... 102

List of Abbreviations

AA, amino acid

Ad-shRNA, adenovirus expressing shRNA

Ad-shSCR, adenovirus expressing control shRNA

Ad-shSIRT3, adenovirus expressing SIRT3-directed shRNA

ADP, adenosine diphosphate

ATP, adenosine triphosphate

BCA, bicinchoninic acid assay

BSA, bovine serum albumin

CoA, coenzyme A

CRISPR, clustered regularly interspaced short palindromic repeats

DIO, diet-induced obesity

DNA, deoxyribonucleic acid

DTT, dithiothreitol

ELISA, enzyme-linked immunosorbent assay

ER, endoplasmic reticulum

ETC, electron transport chain

FAO, fatty acid oxidation

FBS, fetal bovine serum

FFA, free fatty acid

FSIS, fuel-stimulated insulin secretion

GC, gas chromatography

GCK, glucokinase

GIP, glucose-dependent insulinotropic polypeptide

GL, glycerolipid

GLP-1, glucagon-like peptide 1

GLUT2, glucose transporter 2

gRNA, guide RNA

GRP78, 78 kDa glucose-regulated protein

GSH, glutathione

GSIS, glucose-stimulated insulin secretion

GSSG, glutathione disulfide

HAT, histone acetyltransferase

HbA1c, haemoglobin A1c

HBSS, HEPES balanced salt solution

HDAC, histone deacetylase

HFHS, high-fat/high-sucrose (used in reference to diet)

IDH1/ICDc, isocitrate dehydrogenase – cytosolic isoform

IP, intraperitoneal

ipGTT, IP glucose tolerance test

ITT, insulin tolerance test

K_{ATP} channel, ATP-dependent potassium (K^+) channel

KO, knockout

LC, liquid chromatography

LCAD, long-chain acyl-CoA dehydrogenase

LSIS, leucine-stimulated insulin secretion

mRNA, messenger RNA

MS, mass spectrometry

NAD^+, nicotinamide adenine dinucleotide

$NADP^+$, nicotinamide adenine dinucleotide phosphate

NAM, nicotinamide

O/P, oleate/palmitate

oGTT, oral glucose tolerance test

PBS, phosphate-buffered saline

PDH, pyruvate dehydrogenase

PPP, pentose phosphate pathway

PSIS, pyruvate-stimulated insulin secretion

PTM, post-translational modification

RIPA, radioimmunoprecipitation assay

RNA, ribonucleic acid

ROS, reactive oxygen species

S-AMP, adenylosuccinate

shRNA, short hairpin RNA

siRNA, small interfering RNA

siSCR, control siRNA

siSIRT3, SIRT3-directed siRNA

SOD2, superoxide dismutase 2

STD, standard (used in reference to diet)

T2D, type 2 diabetes

TBS, tris-buffered saline

TBS-T, TBS w/ Tween-20

TCA, tricarboxylic acid

TSA, trichostatin A

TUNEL, terminal deoxynucleotidyl transferase dUTP nick-end labeling

WT, wild-type

Acknowledgements

I'd like to thank Chris Newgard for his mentorship and the opportunity to work in his lab. Truthfully, I'm not sure I would have allowed the 24-year-old version of me to join my lab (if I had one). Chris's faith in me and my work has been paramount to the completion of this project, and for that I am extremely grateful. I'd also like to thank Matt Hirschey for his mentorship and making me an honorary member of the Hirschey Lab. I'm appreciative of Matt routinely challenging me to "think deeply" and "think critically" - it played an important role in my graduate training. Additionally, I'd like to thank the members of the Newgard Lab, the Hirschey Lab, and my committee for all of their support throughout graduate school.

I'd like to thank Eoin McDonnell for dragging me with him when he decided to dive headfirst into the world of CRISPR in 2014. Together, we built these new tools from scratch, and their successful application is the backbone of my dissertation. And though, just four years later, you can buy these reagents off-the-shelf, I'll always be proud of what we accomplished as graduate students. I'd like to thank Jon Campbell for being extraordinarily generous with his time. As junior faculty at Duke University, Jon had an entire laboratory to assemble and grants to write. And yet, when I walked into his office and asked him to help me with my mouse-work in early 2017, his response was, "How's tomorrow at noon sound?" This was routine for a little over a year and, invariably, Jon

would drop whatever he was doing to help me. His generosity was vital to the completion of this project – I can't thank him enough.

I need to thank Chad and Jessica Paddock for being friends that I don't deserve, but I'm very grateful to have. Since June of 2016, along with three dogs and their baby girl, Laura, we've lived under the same roof as one big, happy family – it's made the frustrations of graduate school and basic research all the more bearable. Without their friendship, kindness, and generosity, I would not have completed this degree. I will never be able to adequately express how much their friendship means to me.

Thank you to my entire family, from my siblings to my grandparents – your cheerleading has been an enormous source of support. A special "thank you" to my parents, Karen and Steven, for working harder than I think I will ever understand to provide me the opportunity to receive the education that I have. My mom has run a childcare center out of our house in Massachusetts for over 25 years. And for over 25 years she has faithfully performed the thankless task of waking up at 4:30 AM to make sure everybody else's day starts off right with coffee made and lunches packed. And she does this before the first of several families drop their children off for childcare at 7:15 AM. Her ability to grind-out these long days has never ceased to amaze and inspire me.

Neither of my parents had college degrees when I was born in 1987, but it was a different time, and they were making enough money to support two kids and pay a mortgage – and I never once felt poor. But they recognized the value of an education and

wanted the set an example for their kids. So, while working a full-time job, my dad pursued his Bachelor of Science in Electrical Engineering degree – no small task. I have vivid childhood memories of waking up in the middle of the night to go to the bathroom or get a drink, and finding my dad passed-out, face-first in a textbook at the dining room table – and he'd have to wake up shortly thereafter to go to work. In 1998, at the age of 36, and with what was now four kids, he graduated *summa cum laude*. On days when I think "it's too hard", I conjure the image of my dad passed-out in that textbook, and it helps me carry on.

Finally, I need to thank my girlfriend Stacey. Stace and I have been together for 6 years – the closest we've lived to each other in that time is 750 miles. We met at Northeastern University in Boston, Massachusetts. I came to Duke for graduate school, and since Stace was an aspiring Physician Assistant she planned to apply to Duke's program, which is one of the best in the country – the plan was perfect, and we'd only "do long-distance" for a little over two years with an easy hour-and-half flight from BOS to RDU. She got her interview for Duke University's Physician Assistant program in November, 2013 to start the following year – the plan was still perfect. But, she ended up getting wait-listed, which I assure you, was not just my loss, but Duke's. Shortly thereafter, the University of Colorado, Denver granted her admission – 1,500 miles away. So, she went, we survived, and what is now six years later, we're a few weeks away from starting our life together. Needless to say, I'm pretty excited – I think we deserve it.

So, six-and-a-half years, five different homes, three different cars, two different laboratories, countless flights, thousands of hours of FaceTime, two knee surgeries, a sinus surgery, and one crazy rescue-dog later, this chapter has come to a close.

1. Introduction

The pancreatic β-cell of the islets of Langerhans plays a critical role in the maintenance of systemic metabolic homeostasis. β-cells are highly specialized to synthesize and secrete insulin, a master anabolic hormone. In addition to regulating lipid and amino acid metabolism, insulin is the primary mediator of glycemic control, via its ability to stimulate glucose uptake and utilization in peripheral tissues (Figure 1). In the β-cell, enhanced secretion of insulin under anabolic (fed) conditions is largely driven by the intracellular metabolism of glucose, a process referred to as glucose-stimulated insulin secretion (GSIS). The importance of a robust GSIS response is made clear in overt type 2 diabetes (T2D). In the early phases of T2D development, insulin secretion is often increased to offset insulin resistance, temporarily preserving glycemic control. But as the disease progresses, normal GSIS is lost and pancreatic β-cell mass declines, resulting in loss of glycemic control (Figure 2). Given the rapid increase in world-wide prevalence of T2D over the past several decades, a deeper understanding of the molecular mechanisms that control GSIS in the normal islet, and how these become perturbed to promote β-cell dysfunction in T2D, have been a focus of our group and the premise for the work described herein.

1.1 The Islets of Langerhans and the Pancreatic β-cell

The pancreas is comprised of exocrine tissue, which secretes digestive enzymes, as well as endocrine tissue that secretes hormones critical to the control of systemic metabolism and fuel homeostasis. The endocrine tissue, historically referred to as the "islets of Langerhans" (hereafter referred to as "pancreatic islets") was identified in 1869 by its discoverer, Paul Langerhans (Langerhans, 1869). "Islet" describes "a small island" or cluster of endocrine cells that are estimated to constitute about 1% of the total mass of the pancreas. In 1922, Frederick Banting demonstrated that islet-containing "pancreatic extracts" harbored an "internal secretion" that controlled blood sugar, later identified as the hormone, insulin (Banting and Best, 1922; Banting et al., 1922). Subsequent research from different groups have since shown that pancreatic islets are comprised of several distinct hormone-secreting cell types; 1) insulin-secreting beta-cells (β-cells); 2) glucagon-secreting alpha-cells (α-cells) (Baum et al., 1962); 3) somatostatin-secreting delta-cells (δ-cells) (Goldsmith et al., 1975); 4) ghrelin-secreting epsilon-cells (ε-cells) (Prado et al., 2004); and 5) pancreatic polypeptide-secreting PP cells (Kimmel et al., 1975). The ability to synthesize and secrete a suite of unique hormones with distinct effects on metabolism, place the pancreatic islets as master coordinators of systemic metabolic homeostasis.

1.2 Type 2 Diabetes (T2D)

T2D is widely considered a public health emergency given its increasing prevalence throughout the world (IDF, 2017). The disease is characterized by the dysregulated metabolism of glucose, lipid, and protein, due in large part to changes in secretion and action of the major pancreatic islet hormones, glucagon and insulin (Defronzo et al. 2015). T2D is preceded by prediabetes, a condition diagnosed based on elevated fasting blood glucose concentrations, impaired glucose tolerance, or an increase in glycated haemoglobin A1c (HbA1c) levels. These symptoms are indicative of a loss of glycemic control, largely occurring early in the disease as a consequence of peripheral insulin resistance. Interestingly, a significant portion of prediabetic subjects can remain prediabetic for long periods and resist conversion to T2D due to a sustained pancreatic islet β-cell adaptive response. The adaptive response slowly raises circulating insulin to compensate for insulin resistance and to prevent overt hyperglycemia (Figure 2). Whereas compensation and euglycemia can be maintained for long periods, subjects destined for T2D eventually experience a decline in pancreatic islet β-cell function and mass, and this failure catalyzes the descent into overt T2D (Defronzo et al., 2015) (Figure 2). While overt T2D is transiently manageable through pharmacologic interventions that enhance insulin sensitivity (metformin) or enhance insulin secretion and curb appetite (incretin hormones), these approaches lose efficacy over time and subjects eventually have no

recourse other than insulin injection. At this stage, patients experience a dramatic decrease in quality of life and an increased risk of developing T2D comorbidities including neuropathy, retinopathy, nephropathy, and cardiovascular disease. As such, protection and augmentation of the functional mass of the insulin-secreting β-cell continues to be a central goal in diabetes research, and future success demands a deeper understanding of the disease-dependent molecular mechanisms that impair GSIS.

1.3 Glucose-Stimulated Insulin Secretion (GSIS)

The canonical model of glucose stimulated insulin secretion is biphasic. In the first/K_{ATP} channel-dependent/triggering phase, glucose enters the β-cell via plasma membrane facilitated glucose transporters (Thorens et al., 1988), is rapidly phosphorylated by the high K_m glucokinase (GCK) (Iynedjian et al., 1989; Matschinsky and Ellerman, 1968), and undergoes glycolysis to yield pyruvate. Glucose-derived pyruvate then enters the mitochondria and increases the intracellular ATP:ADP ratio via oxidative phosphorylation through the tricarboxylic acid (TCA) cycle and the electron transport chain (ETC). The increase in the ATP:ADP ratio inhibits ATP-dependent K^+ channels (K_{ATP} channels) resulting in plasma membrane depolarization, which leads to subsequent activation of voltage-gated Ca^{2+} channels, influx of Ca^{2+}, and stimulation of granule exocytosis (Ashcroft et al., 1984; Bryan et al., 2005; Henquin et al., 2003; Newgard

and Matschinsky, 2001) (Figure 3). The second/K_{ATP} channel-independent/amplifying phase of insulin secretion, although requiring the closure of K_{ATP} channels as an initiating event, is largely independent of first phase mechanisms and has been estimated to account for over 60% of the GSIS response (Henquin et al., 2003). Several mechanisms have been proposed to regulate the amplifying phase of insulin secretion (Prentki et al., 2013). Mounting evidence supports a model in which mitochondrial production and subsequent efflux of citrate and/or isocitrate into the cytosol, followed by oxidative decarboxylation of isocitrate by the cytosolic isocitrate dehydrogenase (IDH1 or ICDc) is required for the full second phase response (Jensen et al., 2006; Jensen et al., 2008; Joseph et al., 2006; Ronnebaum et al., 2006). Further, recent literature has demonstrated that the byproduct of the oxidative decarboxylation reaction catalyzed by IDH1, NADPH, is the primary link between this step and second phase granule exocytosis by increasing the GSH:GSSG ratio (Ferdaoussi et al., 2015). Other implicated mechanisms include glucose-stimulated production of adenylosuccinate (S-AMP) (Gooding et al., 2015), signaling by intermediates of the pentose phosphate pathway (PPP) (Spegel et al., 2013), glycerolipid/free fatty acid (GL/FFA) cycling (Prentki and Madiraju, 2012), and others (Prentki et al., 2013).

1.4 Mitochondrial Function of the β-cell in GSIS and T2D

The involvement of increases in ATP:ADP and NADPH:$NADP^+$ ratios position mitochondrial function as a central coordinator of the GSIS response (Figure 3). Indeed, preventing mitochondrial import and oxidation of glucose-derived pyruvate significantly blunts the glucose-dependent shifts in these ratios and both phases of GSIS (Patterson et al., 2014). As such, perturbations of mitochondrial metabolic machinery have been proposed as a candidate-mechanism that facilitates the decline in β-cell function in T2D (Mulder, 2017). Supporting this hypothesis, examination of isolated pancreatic islets from T2D patients reveals impairment in glucose-induced increases in ATP:ADP ratios when compared to islets from non-diabetic donors (Anello et al., 2005). In addition, intracellular delivery of the glucose-derived TCA cycle intermediate, isocitrate, to dissociated islets of T2D donors potently stimulates insulin granule-exocytosis, whereas glucose is not effective (Ferdaoussi et al., 2015). Taken together, these data could be explained by a mitochondria-localized impairment of either the glucose-induced production, or cytosolic efflux, of citrate/isocitrate in T2D islets. Despite these observations, the identity of the primary lesion/s underlying mitochondrial dysfunction of the pancreatic islet β-cell in T2D remains unclear.

1.5 Mitochondrial Protein Acetylation and Sirtuins

Lysine acetylation is a reversible post-translational modification (PTM) that was first appreciated for its dynamic role in the regulation of transcriptional activity (Verdin and Ott, 2015). This regulatory mechanism is mediated by histone acetyltransferases (HATs) that use acetyl-CoA as a substrate to modify histones, and by histone deacetylases (HDACs) that remove the acetyl moiety, thereby restoring baseline transcriptional activity. Years after these initial discoveries, acetylation became recognized as a regulatory modification on non-histone proteins such as tubulin and the tumor suppressor p53 (Sterner and Berger, 2000), widening the potential biological impact of this PTM. Further expanding this potential, eighteen unique HDACs have now been identified in humans. These are grouped into three classes based on their homology to HDACs identified in *Saccharomyces cerevisiae* (yeast): RPD3 (class I), HDA1 (class II), and silent information regulator (Sir)2 (class III).

The histone deacetylase Sir2 and related proteins garnered significant interest following studies demonstrating a Sir2-dependent role in promoting longevity in *Saccharomyces cerevisiae* (yeast) (Kaeberlein et al., 1999; Lin et al., 2000), *Caenorhabditis elegans* (worms) (Tissenbaum and Guarente, 2001), and *Drosophila melanogaster* (flies) (Rogina and Helfand, 2004). Sir2 is dependent on NAD^+ (Imai et al., 2000), positioning this HDAC as a sensor of cellular metabolism (Guarente, 2000), and interestingly, the

longevity-promoting effects of calorie restriction have been attributed to NAD^+-mediated Sir2 activity in lower organisms (Lin et al., 2000; Rogina and Helfand, 2004). Mammals express seven unique NAD^+-dependent homologs of the Sir2 protein (SIRT1-SIRT7), and are broadly referred to as "sirtuins" (Sir2-"ins"). SIRT3, SIRT4, and SIRT5 localize to the mitochondria and exhibit unique deacylase activities (Anderson et al., 2017; Lombard et al., 2007; Schwer et al., 2002; Tan et al., 2014; Zhao et al., 2010), suggesting the existence of mitochondria-localized acylated substrates.

The discovery of mitochondrial protein acetylation in the first mammalian proteomics survey of acetyllysine-enriched cellular fractions was "totally unexpected" (Kim et al., 2006). While acetylation of histones and a handful of non-histone proteins was recognized as a potential regulatory PTM for DNA-protein binding, gene-transcription, subcellular localization, and substrate stability, the existence and impact of acetylation on mitochondrial proteins was unknown. The abundance of this post-translational modification (PTM) on metabolic enzymes in both fed and fasted mice pointed to a role for acetylation in regulating metabolism (Kim et al., 2006). Several subsequent studies continued to expand the mitochondrial acetylproteome in different models and model organisms, strengthening this hypothesis (Choudhary et al., 2009; Wang et al., 2010; Zhao et al., 2010). These studies also demonstrated that acetylation impacts the enzymatic activity of the modified substrate in a eukaryotic system (Zhao et al., 2010), and that the

aggregate acetylation status of metabolic pathways directs carbon flux in a prokaryotic system (Wang et al., 2010). Given that: 1) Sirtuin activity is linked to metabolism via NAD^+-dependence; and 2) mitochondria-localized SIRT3 exhibits deacetylase activity (Schwer et al., 2002), it was postulated that SIRT3 manages the mammalian mitochondrial acetylproteome. Indeed, models of SIRT3 gene ablation invariably exhibit global hyperacetylation of mitochondrial proteins in all examined tissues, demonstrating that mitochondrial protein acetylation and SIRT3 are ubiquitous and tightly linked (Dittenhafer-Reed et al., 2015; Hebert et al., 2013; Lombard et al., 2007; Rardin et al., 2013; Sol et al., 2012).

1.6 Nonenzymatic Acetylation is a Carbon Stress

Unlike the HAT-dependent acetylation of histones, mitochondrial protein acetylation is thought to occur non-enzymatically, a product of the permissive chemical conditions of the mitochondrial matrix, the matrix concentration of acetyl-CoA, and time (Wagner and Hirschey, 2014; Wagner and Payne, 2013). In light of these characteristics, it has been hypothesized that acetylation of mitochondrial proteins is a promiscuous and spurious modification representing a "carbon stress", with SIRT3 serving a protective, counteractive role (Wagner and Hirschey, 2014). To date, acetylation sites have been found on 63% of mitochondrial proteins in *Mus musculus* (mice), and manipulation of

SIRT3 expression is routinely leveraged as a powerful tool with which to study the functional impact of this modification (Baeza et al., 2016). In virtually all cases where the impact of SIRT3-dependent acetylation status on a specific substrate-protein has been examined, authors have reported a decrease in function (Baeza et al., 2016). SIRT3 substrate proteins are positioned in almost all mitochondrial metabolic pathways including the tricarboxylic acid (TCA) cycle, the electron transport chain (ETC), fatty acid oxidation (FAO), amino acid catabolism, acetate metabolism, and ketogenesis. Enzymes important for detoxification of reactive oxygen species (ROS) are also targets. Taken together, the broad consensus of the field during the performance of this dissertation research was that mitochondrial protein acetylation represents a stress condition resulting in impaired substrate activity, and thus has the potential to broadly impact mitochondrial function.

1.7 The Impact of Global SIRT3 Loss on Metabolic Homeostasis

Loss of SIRT3 and concomitant hyperacetylation of mitochondrial proteins are associated with decreases in mitochondrial energy production. SIRT3 KO mice have markedly reduced ATP (Ahn et al., 2008) and NADPH:total $NADP^+$ (Someya et al., 2010) in multiple tissues including the heart, kidney, liver, brain, and inner ear. Further, loss of SIRT3 and concomitant hyperacetylation of mitochondrial proteins has been implicated

in mediating systemic metabolic dysregulation. Under standard conditions, hyperacetylation of mitochondrial proteins in global SIRT3 KO mice promotes insulin resistance and glucose intolerance (Hirschey et al., 2011; Jing et al., 2011), as a result of increased oxidative stress in skeletal muscle (Jing et al., 2011). Follow up studies that further examined skeletal muscle revealed that hyperacetylation of the E1α subunit of pyruvate dehydrogenase (PDH E1α) in SIRT3 KO mice decreases the activity of this enzyme, and thus decreases carbohydrate metabolism (Jing et al., 2013). A compensatory increase of fatty acid oxidation in these animals is capable of sustaining ATP production, however this is likely at the expense of increased oxidative stress which others have shown can promote insulin resistance. Unlike the skeletal muscle, fatty acid oxidation is markedly impaired in the livers of SIRT3 KO mice (Hirschey et al., 2010). In healthy animals, fasting stimulates a transition from carbohydrate oxidation to lipid oxidation to sustain mitochondrial energy production. However, long-chain acyl-CoA dehydrogenase (LCAD), a critical enzyme in the fatty acid oxidation pathway, is hyperacetylated in SIRT3 KO mice and thus less active. Therefore, the liver of SIRT3 KO mice exhibits decreased metabolic flexibility under fasting conditions, reflected in impaired ATP production (Hirschey et al., 2010). Together, these studies suggest that, even under standard conditions, SIRT3 loss results in systemic metabolic dysregulation, explained at least in part by functional impairments in skeletal muscle and liver.

The impact of SIRT3 ablation has also been studied under conditions of nutritional stress, such as chronic feeding of nutrient-dense diets (either high-fat or high-fat/high-sucrose). ~12 weeks of ad libitum-feeding of a nutrient-dense diet promotes global hyperacetylation of mitochondrial proteins in both liver and skeletal muscle of wild-type animals and is associated with the development of metabolic disease (Hirschey et al., 2011; Lantier et al., 2015). Loss of SIRT3 exacerbates diet-induced glucose intolerance, insulin resistance, hyperlipidemia, and nonalcoholic steatohepatitis (Hirschey et al., 2011), at least with very long exposure to dietary stress. This was attributed to the hyperacetylation of LCAD and resultant decrease in enzymatic activity (Hirschey et al., 2010; Hirschey et al., 2011). In this model, the decrease in LCAD activity reduces fatty acid oxidation in the liver rendering it permissive to the diet-driven accumulation of lipid, which promotes steatohepatitis and hepatic insulin resistance. Additionally, skeletal muscle from diet-induced obese global SIRT3 KO animals exhibit impaired insulin-stimulated glucose uptake, which contributes to systemic metabolic dysregulation (Lantier et al., 2015).

Interestingly, diet-induced obese global SIRT3 KO animals exhibit a significantly increased plasma insulin response following an intraperitoneal (IP) glucose bolus and a trend to increase fasting insulin levels compared to diet-induced obese wild-type mice (Hirschey et al., 2011; Lantier et al., 2015). Given the natural history of β-cell adaptation and subsequent failure in the development of T2D (Figure 2), these observations could be

explained by accelerated disease development (Hirschey et al., 2011) and could support a role for SIRT3 and mitochondrial protein acetylation in the obesity-induced adaptive response of the β-cell.

1.8 SIRT3, Mitochondrial Protein Acetylation, and the β-cell

At the time that this dissertation research was initiated, several lines of evidence supported a possible role for SIRT3 in mediating changes in β-cell function during T2D development: 1) Increases in both the ATP:ADP and NADPH:$NADP^+$ ratios are central mediators of the GSIS response of the pancreatic β-cell (Ashcroft et al., 1984; Ferdaoussi et al., 2015); 2) Both carbohydrate and lipid metabolism, pathways that SIRT3 has been shown to regulate in other tissue, impart control over β-cell GSIS (Coore and Randle, 1964; Dobbins et al., 1998; Grodsky et al., 1963; Stein et al., 1996); 3) Chronic overnutrition, a condition that drives systemic metabolic dysregulation and in which β-cell function is perturbed, promotes mitochondrial protein hyperacetylation (Hirschey et al., 2011); 4) Loss of the mitochondrial deacetylase, SIRT3, exacerbates systemic metabolic dysregulation in the context of chronic overnutrition (Hirschey et al., 2011; Lantier et al., 2015); and 5) SIRT3 loss promotes an accelerated β-cell adaptation in response to chronic overnutrition (Hirschey et al., 2011; Lantier et al., 2015). This suggested that promoting mitochondrial protein acetylation in the β-cell via the manipulation of SIRT3 expression

might impair β-cell function in standard conditions and further exacerbate β-cell dysfunction in the presence of chronic overnutrition. In order to address this hypothesis, several groups have employed *in vivo*, *ex vivo*, and *in vitro* models in which to manipulate SIRT3 expression, and by inference, mitochondrial protein acetylation, in the pancreatic β-cell.

1.8.1 Standard Nutrition Conditions

In pancreatic islets isolated from C57Bl/6 mice, *Sirt3* mRNA levels positively correlate with insulin secretion (Caton et al., 2013). Islets isolated from mice fasted for 24 hours exhibit a significant reduction in *Sirt3* transcript along with decreases in both glucose- and leucine-stimulated insulin secretion (GSIS and LSIS, respectively). Additionally, incomplete and transient siRNA-mediated knockdown of SIRT3 in the INS-1 β-cell line under standard conditions increases production of reactive oxygen species (ROS), promotes caspase 3 activity, and impairs insulin secretion. Under standard conditions, incomplete and transient suppression of SIRT3 via siRNA resulted in dramatic decreases in cell viability and GSIS in both the NIT-1 and INS-1 β-cell (Zhang et al., 2016). This dysfunction was attributed to the hyperacetylation and proposed inhibition of 78 kDa glucose-regulated protein (GRP78) and resultant dysregulation of the palmitate-induced endoplasmic reticulum (ER) stress response. Islet function was also studied in

global SIRT3 KO mice on the 129Sv background (Zhou et al., 2017). Upon an oral glucose bolus, SIRT3 KO mice fed a standard chow diet were purported to have an impaired plasma insulin response compared to WT controls, although statistical analysis of this comparison is omitted from the publication (Zhou et al., 2017). Pancreatic islets isolated from these SIRT3 KO animals as well as MIN-6 β-cells with stable, but incomplete shRNA-mediated knockdown of SIRT3 have impaired glucose-stimulated ATP production and insulin secretion, ascribed to increased acetylation and reduced activity of superoxide dismutase 2 (SOD2). Together, these studies seemingly support the hypothesis that hyperacetylation of mitochondrial proteins is sufficient to perturb β-cell viability, glucose metabolism, and insulin secretion under standard conditions.

1.8.2 Overnutrition Conditions

Given that chronic overnutrition promotes mitochondrial protein acetylation, and hyperacetylation of mitochondrial proteins promotes β-cell dysfunction, it would follow that increasing the expression of SIRT3 should counteract overnutrition-induced β-cell dysfunction, whereas decreasing the expression of SIRT3 should exacerbate it. To date, the challenges of obtaining pancreatic islets from human T2D donors, and the relatively low sensitivity of acetyllysine antibodies for immunoblotting, have precluded the examination of mitochondrial protein acetylation in the context of human T2D disease

development. However, a decrease in *SIRT3* transcript has been reported in human T2D donor islets, suggesting that a resultant increase in mitochondrial protein acetylation could contribute to T2D pathogenesis (Caton et al., 2013). In order to address this hypothesis, the field has employed both rodent models of diet-induced obesity (DIO), as well as isolated islets and β-cell lines treated with elevated concentrations of glucose and fatty acids as an *ex vivo/in vitro* model of overnutrition; this *ex vivo/in vitro* model of β-cell dysfunction is sometimes referred to as a "glucolipotoxicity" (Poitout and Robertson, 2008).

C57Bl/6 mice fed a nutrient-dense diet for 16 weeks exhibited no changes in either GSIS or leucine-stimulated insulin secretion (LSIS) compared to mice fed standard chow, even though dietary stress promoted a trending increase in islet *Sirt3* mRNA. The authors interpreted this data as evidence that SIRT3 expression increases in order to sustain a healthy insulin secretion response in the face of overnutrition (Caton et al., 2013). In another study, pancreatic islets isolated from Sprague Dawley rats every week throughout a 12-week DIO challenge exhibited a positive correlation between plasma insulin and islet *Sirt3* transcript expression (Zhang et al., 2016). From week 0-8, both plasma insulin and islet *Sirt3* expression were increased, consistent with the β-cell adaptive response to DIO. From week 8-12 both plasma insulin and islet *Sirt3* expression decreased, consistent with β-cell failure. Given that these animals develop hallmarks of

T2D at the 8-week time point including diet-induced weight gain, increased circulating free fatty acids (FFAs) , and hyperglycemia, the correlative expression data suggests that islet SIRT3 is coupled to the β-cell adaptive response and subsequent failure in the development of overt T2D (Zhang et al., 2016). To model this in vitro, both NIT-1 and INS-1 β-cell lines were chronically cultured in elevated glucose and fatty acids. Under these conditions, GSIS is markedly impaired and is associated with a reduction in SIRT3 expression (Zhang et al., 2016). β-cell dysfunction was attributed to the palmitate-induced ER stress response mediated by GRP78. Under glucolipotoxic conditions, siRNA-mediated knockdown of SIRT3 resulted in hyperacetylation and a resultant decrease in GRP78 function, accompanying β-cell dysfunction in both NIT-1 and INS-1 β-cells. Conversely, overexpression of SIRT3 ameliorated palmitate-induced dysfunction while reducing acetylation of GRP78 and the ER stress response. Similarly, adenovirus-mediated overexpression of SIRT3 was sufficient to protect both NIT-1 β-cells and isolated rat islets from glucolipotoxic impairment of GSIS accompanied by reduced acetylation of multiple β-cell proteins as measured by immunoblot with an anti-acetyllysine antibody (Kim et al., 2015).

In other studies, wild-type and SIRT3 KO mice were challenged with a nutrient-dense diet for 30 weeks (Zhou et al., 2017). Consistent with previous studies in islets and other tissue, chronic overnutrition resulted in a significant reduction in SIRT3 protein in

islets of wild-type animals, and this correlated with a trending decrease in plasma insulin following an oral glucose bolus (statistical analysis of this comparison omitted from the publication) as well as significant impairment in GSIS from isolated pancreatic islets (Zhou et al., 2017). Importantly, chronic feeding of a nutrient-dense diet results in elevated stress responses and an increase in cell death in both genotypes when compared to standard diet-fed controls, with SIRT3 KO islets exhibiting exacerbated responses. This suggests a role for SIRT3, and thus mitochondrial protein acetylation, in combatting the stress of overnutrition. Similar to chronic overnutrition *in vivo*, isolated wild-type islets subjected to glucolipotoxicity have significantly reduced SIRT3 protein and an associated decrease in GSIS. Further, islets isolated from SIRT3 KO animals consistently exhibit exacerbated oxidative stress responses when chronically cultured in glucolipotoxic conditions, attributed to hyperacetylated, and thus less active, SOD2.

Together, these studies support the idea that SIRT3 plays an important role in mediating β-cell function under both standard nutrition and overnutrition conditions. Under standard conditions, loss of SIRT3 results in dysregulated β-cell metabolism and both oxidative and ER stress responses, presumably due to hyperacetylation of mitochondrial proteins and a resultant decrease in function. Additionally, conditions of overnutrition decrease SIRT3 expression in wild-type animals, promote hyperacetylation of mitochondrial proteins, and impair β-cell function. Overexpression of SIRT3 under

these conditions provides protection from overnutrition-induced dysfunction, while loss of SIRT3 is exacerbating. As such, the seeming consensus of the field that developed during the performance of this dissertation is that activation of SIRT3 to promote mitochondrial protein deacetylation might constitute a therapeutic strategy to augment/protect β-cell function during T2D development.

1.8.3 Discrepancies & Limitations of the Existing Literature

While the model supported by the existing literature is seemingly consistent with the hypothesized role or SIRT3 and mitochondrial protein acetylation in the β-cell, there are several discrepancies and limitations that preclude definitive conclusions. For example, different models of overnutrition have different effects on SIRT3 expression. In islets isolated from mice on a 129Sv background fed nutrient-dense diet for 30 weeks or islets isolated from Sprague Dawley rats fed a nutrient-dense diet for 12 weeks, SIRT3 expression is markedly ***decreased*** (Zhang et al., 2016; Zhou et al., 2017). Conversely, C57Bl/6 mice fed a nutrient-dense diet for 16 weeks exhibit a modest ***increase*** in *Sirt3* expression (Caton et al., 2013). Comparison of similar *in vitro* experiments reveals that media supplemented with 500 – 800 μM palmitate for 24 hours significantly decreases SIRT3 expression in NIT-1, INS-1, and MIN-6 β-cell lines in two studies (Zhang et al., 2016; Zhou et al., 2017), while a different study shows no change in *Sirt3* expression following

24 hour treatment with 500 μM palmitate in NIT-1 β-cells (Kim et al., 2015). It should also be noted that culture of cells in elevated palmitate is a poor surrogate of hyperlipidemic states *in vivo*. In circulation, monounsaturated fatty acids such as oleate are present in a 2:1 ratio with saturated fats such as palmitate. Additionally, given that palmitate alone acts as a detergent to induce non-specific cytotoxicity (Watt et al., 2012), it is difficult to interpret studies that examine cells subjected to this stress. In fact, in one study that purports a protective role for SIRT3 in β-cells under palmitate-induced stress , palmitate markedly decreases cell viability by as much as 50% and reduces functional mitochondria (as measured by MitoTracker staining) by as much as 80% (Zhou et al., 2017). The unifying theme of the existing literature is that overnutrition-induced impairment of β-cell dysfunction follows a replicable progression: First, overnutrition reduces islet/β-cell SIRT3 expression; Second, the decrease in SIRT3 expression permits aberrant hyperacetylation of mitochondrial proteins; Then third, hyperacetylation of mitochondrial proteins impairs β-cell function. However, these studies do not provide evidence that the initial decrease in SIRT3 is a primary lesion, rather than secondary to decrease in mitochondrial number or cell death. These data seemingly confound published relationship between overnutrition, SIRT3 expression, mitochondrial protein acetylation, and β-cell function.

Isolated islets from SIRT3 KO mice on a 129Sv background fed a standard diet have impaired GSIS (Zhou et al., 2017). Importantly, this decrease is independent of an increase in TUNEL staining or a decrease in β-cell area per pancreatic area. Although Zhou and colleagues (Zhou et al., 2017) show a statistically significant increase in caspase 3 cleavage in Figure 2I, this data does not repeat in Figure 7E or 7H of the same publication. Additionally, stable knockdown of SIRT3 in MIN-6 β-cells results in a 50% decrease in insulin secretion independent of caspase 3 cleavage. Therefore, these studies suggest that loss of SIRT3, and by inference hyperacetylation of mitochondrial proteins, is sufficient to impair β-cell function independent of cell death. However, the existing *in vitro* studies that employ siRNA to suppress SIRT3 measure insulin secretion in β-cell lines that exhibit hallmarks of cell death. For example, siRNA-mediated suppression of SIRT3 in INS-1 cell lines significantly increases caspase 3 activity and decreases insulin secretion (Caton et al., 2013), and siRNA-mediated suppression of SIRT3 in NIT-1 cells and INS-1 cells significantly decreases cell viability by 50% (Zhang et al., 2016). Therefore, the available literature has failed to disentangle the effects of SIRT3 knockdown on insulin secretion from β-cell death; dead cells secrete less insulin.

An even more important limitation of studies performed to date has been the lack of assessment of changes in global mitochondrial protein acetylation, the major mechanism through which SIRT3 is presumed to exert its biological effects. One paper

demonstrates an effect of overexpressed SIRT3 to deacetylate proteins in whole cell lysates of NIT-1 β-cells as measured by immunoblotting with an acetyllysine antibody (Fig. 1F of Kim et al., 2015), but there are several problems with this data. Given that: 1) Despite exclusively mitochondrial or cytosolic subcellular localization of the different overexpressed SIRT3 constructs (Fig. 1D of Kim et al., 2015), the acetyllysine banding profiles are identical, suggesting deacetylation of the same substrate proteins; 2) NIT-1 β-cells were cultured in trichostatin A (TSA) for 6 hours prior to harvest, which would effectively reveal class I and II HDAC acetylation sites that a transiently overexpressed SIRT3 is coincidentally capable of deacetylating; and 3) In our own hands, SIRT3-dependent differences in mitochondrial protein acetylation cannot be measured reliably in whole-cell lysates from insulinoma cell lines (e.g. INS-1 832/13) by immunoblot, but rather require preparation of mitochondria-enriched fractions. In short, the data available about the effects of manipulation of SIRT3 on the β-cell acetylproteome is both limited and difficult to interpret.

The absence of a defined SIRT3-targeted acetylproteome in β-cells is another limitation of the existing literature. In both the presence and absence of palmitate, transient overexpression of SIRT3 in both NIT-1 and INS-1 β-cells results in reduced acetylation of GRP78, whereas transient knockdown of SIRT3 results in hyperacetylation of GRP78 (Zhang et al., 2016). However, we cannot conclude from this work that GRP78

is a primary target of endogenous SIRT3 because: 1) Despite decreasing expression of endogenous SIRT3 protein in both NIT-1 and INS-1 β-cells (Fig. 2A of Zhang et al., 2016), and theoretically providing an abundant pool of acetyl-CoA as an acetylation source, palmitate treatment alone does not result in hyperacetylation of GRP78 (Fig. 5D and 5E of Zhang et al., 2016); and 2) The authors fail to address how SIRT3, a mitochondria-localized deacetylase, interacts with GRP78, an ER-localized chaperone protein. Further, the authors make conclusions about the role of GRP78 in mediating changes in islet phenotypes in response to SIRT3 manipulation, but neither prove a role for GRP78 or address the possible contributions of other proteins that may also have experienced changes in lysine acetylation.

Similarly, lysine 68 (K68) of SOD2 is hyperacetylated in both isolated islets from SIRT3 KO animals and MIN-6 β-cells with incomplete and stable shRNA-mediated knockdown of SIRT3 (Zhou et al., 2017). Re-expression of SIRT3 with an adenovirus vector in SIRT3 KO islets deacetylates K68 of SOD2. Notably, acetylation of SOD2 is not sufficient to promote an increase in markers of oxidative stress in either MIN-6 β-cells with stable SIRT3 knockdown or in islets isolated from SIRT3 KO mice (Fig. 5 and Fig. 7 in Zhou et al., 2017). Therefore, though SOD2 is a likely target of SIRT3 in the β-cell, it does not explain the deficit in GSIS observed with SIRT3 loss.

1.9 Project Goals

When I began this research project in 2012, there was no published literature linking SIRT3, mitochondrial protein acetylation, and β-cell function. Between 2013 and the writing of this dissertation, several studies reviewed above have been published concluding that SIRT3 plays a critical role in protecting and augmenting β-cell function in both standard or overnutrition conditions. However, as summarized in section 1.8.3, these studies are inconsistent and inconclusive. Further, with the exception of GRP78 and SOD2, the identity and function of islet proteins undergoing changes in acetylation state in response to manipulation of SIRT3 has not emerged. Given that SIRT3 is presumed to exert its measurable biological activity by modulating the acetylation status of substrate proteins, omitting this data is analogous to assigning biological relevance to the manipulation of kinases or phosphatases without demonstrating changes in substrate phosphorylation status. As such, a primary goal of this project was to develop and employ β-cell models in which we could measure SIRT3-dependent shifts in global mitochondrial protein acetylation, thereby filling a very large gap in the field.

Between 2006 and 2015, 700 mitochondrial proteins across several tissues and cell types were identified as acetylated, constituting 63% of the mitochondrial proteome (Baeza et al., 2016). Importantly, the most comprehensive examination of acetylation stoichiometry in a mammalian system, to date, revealed that most detected acetylated

peptides exhibit stoichiometry of less than 1% (Weinert et al., 2015). Bona fide sites of regulatory mitochondria protein acetylation are likely higher in stoichiometry (>1%) but found on fewer proteins. These potentially regulatory modifications coexist with spurious sites of acetylation that are lower in stoichiometry (<1%) but found on many proteins (Weinert et al., 2015). As such, despite the size of the mitochondrial acetylproteome, it's been proposed that only a handful of sites on a handful of proteins will have a measureable biological impact, and these are most likely the primary targets of SIRT3. Additionally, given the low stoichiometry of mitochondrial protein acetylation, it has been proposed that the cumulative product of the acetylation status of multiple proteins in a metabolic pathway could also result in a measurable biological effect (Baeza et al., 2016; Carrico et al., 2018). Given these hypotheses, another priority of this project was the development of a reliable model in which to apply acetylproteomics analysis in order to define the SIRT3-targeted mitochondrial acetylproteome of the β-cell.

In addition, the effect of SIRT3 ablation with and without chronic overnutrition on the mitochondrial acetylproteome has not been shown in primary pancreatic islets. Further, the impact of SIRT3 loss on primary islet function has not been measured by islet perifusion, a method of measuring insulin secretion that permits interrogating the effect of multiple secretagogues in series at high-resolution. Finally, comprehensive

measurements of changes in metabolic fuel metabolism in response to SIRT3 manipulation have not been attempted.

Taken together, the voids in the field are vast, and therefore the impact of mitochondrial protein acetylation on β-cell function remains unclear. To address these gaps, we employed several different *in vitro* tools for manipulating SIRT3 expression in the INS-1 832/13 β-cell line in order to study the effect of mitochondrial protein acetylation. These tools included SIRT3-specific siRNA and Ad-shRNA, *Sirt3*-targeted CRISPR/Cas9 gene-disruption, and stable integration of SIRT3 overexpression constructs. Further, in order to interrogate the impact of acetylation in primary islets, we generated a novel global SIRT3 KO mouse and studied islet function after chronic feeding of a standard (STD) chow or high-fat/high-sucrose (HFHS) diet. Ultimately, the project was designed to comprehensively assess the impact of mitochondrial protein acetylation on β-cell function under conditions of standard nutrition and overnutrition. The following chapters of this dissertation describe the design, methods, and data that seek to address these questions and add clarity to the field.

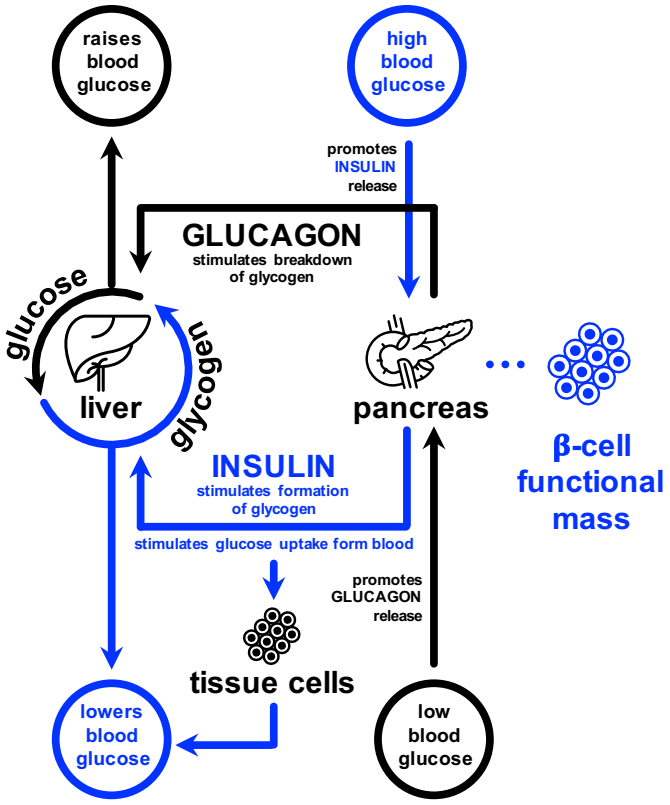

Figure 1: β-cell functional mass coordinates systemic metabolic homeostasis.

Following ingestion of a meal, a rise in blood glucose stimulates insulin secretion from islet β-cells located in the pancreas. The increase in circulating insulin then stimulates glucose uptake from the circulation and into peripheral tissues for energy production and glycogen storage. Glucose uptake also results in lowering of blood glucose to maintain euglycemia (Figure adapted from the International Diabetes Federation Atlas, 8th edn. (IDF, 2017)).

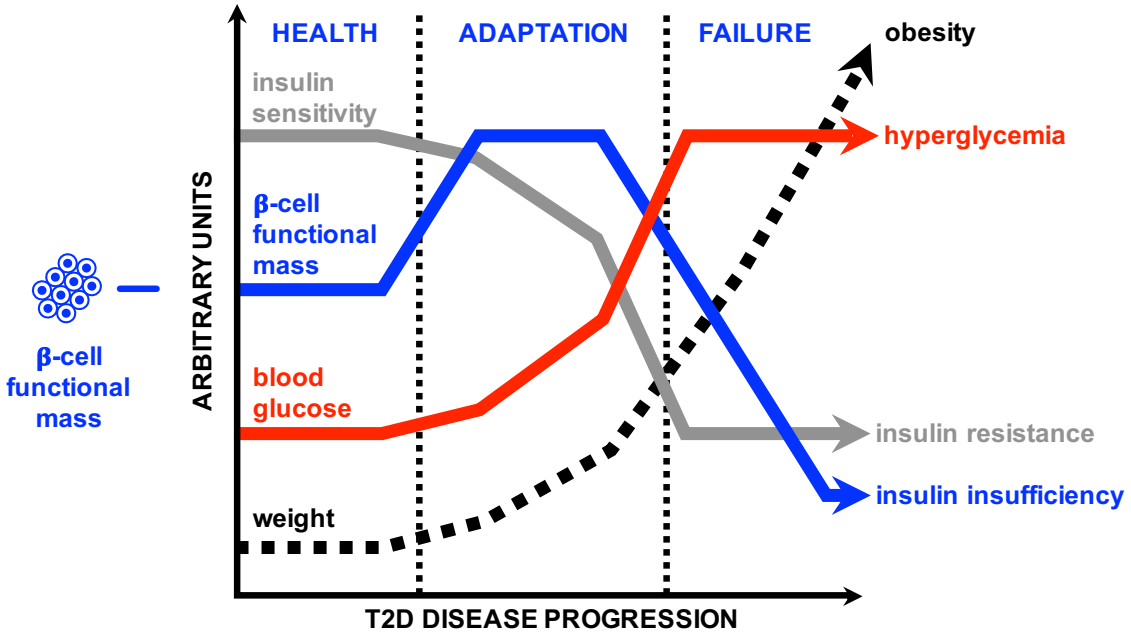

Figure 2: A decline in β-cell functional mass is a precipitating event in T2D.

The progression of the adaptive response of β-cell functional mass throughout the development of metabolic disease from health to adaptation and eventual failure (blue line) is promoted by underlying weight gain (dotted black line) and a decrease in insulin sensitivity (grey line). Early in development of type 2 diabetes (T2D), an adaptive increase in β-cell functional mass serves to maintain relative euglycemia despite increasing insulin resistance. A decline in β-cell functional mass marks the transition from adaptation to failure and results in hyperglycemia and overt T2D.

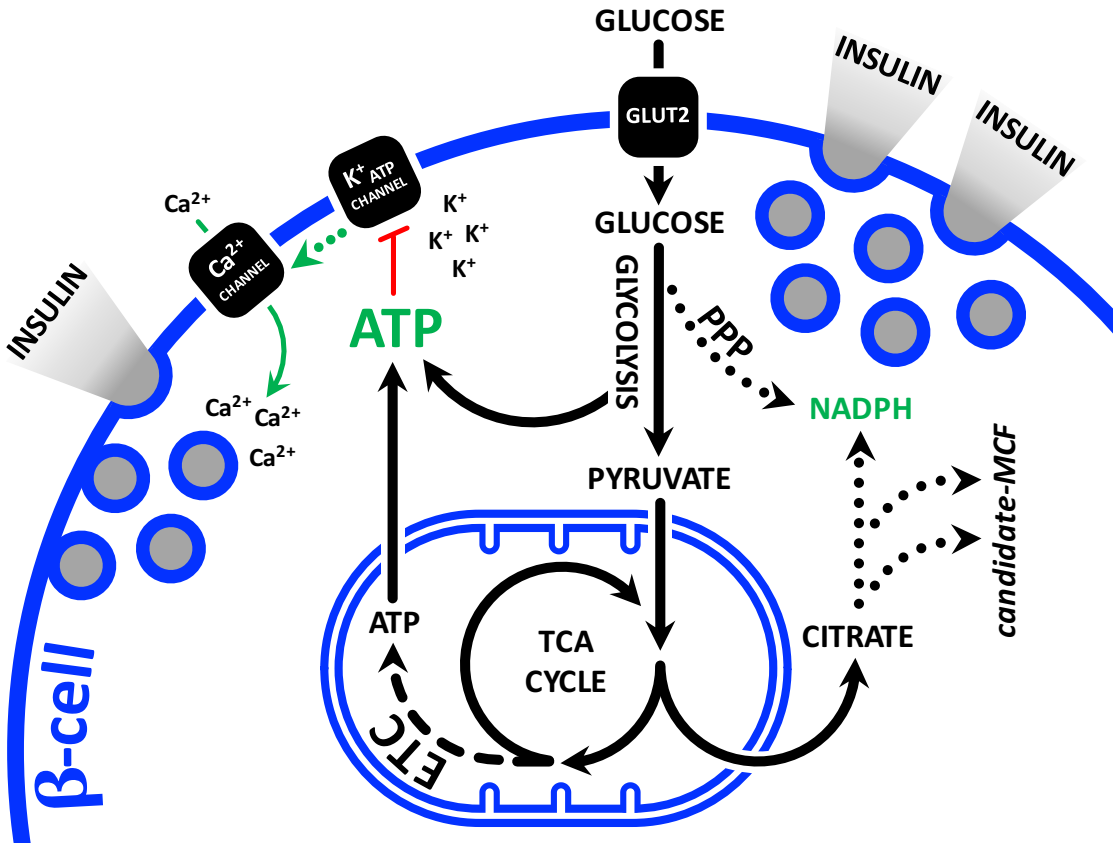

Figure 3: Mitochondria are central to GSIS.

Glucose enters the β-cell from the blood via the glucose transporter, GLUT2. Glycolysis then produces pyruvate which enters the mitochondria for oxidation and resultant ATP production via the tricarboxylic acid (TCA) cycle and the electron transport chain (ETC). ATP serves to close the K_{ATP} channel, which prevents efflux of potassium (K^+) and thus leads to plasma membrane depolarization. Depolarization of the plasma membrane results in an influx of calcium (Ca^{2+}) through voltage-gated Ca^{2+}-channels and promotes insulin granule exocytosis. Additionally, the glucose-dependent increase in TCA cycle activity results in efflux of citrate/isocitrate from the mitochondria. Cytosolic isocitrate dehydrogenase (ICDc or IDH1), then decarboxylates isocitrate to form α-ketoglutarate (α-KG) and NADPH. NADPH from this reaction also serves to promote insulin granule exocytosis.

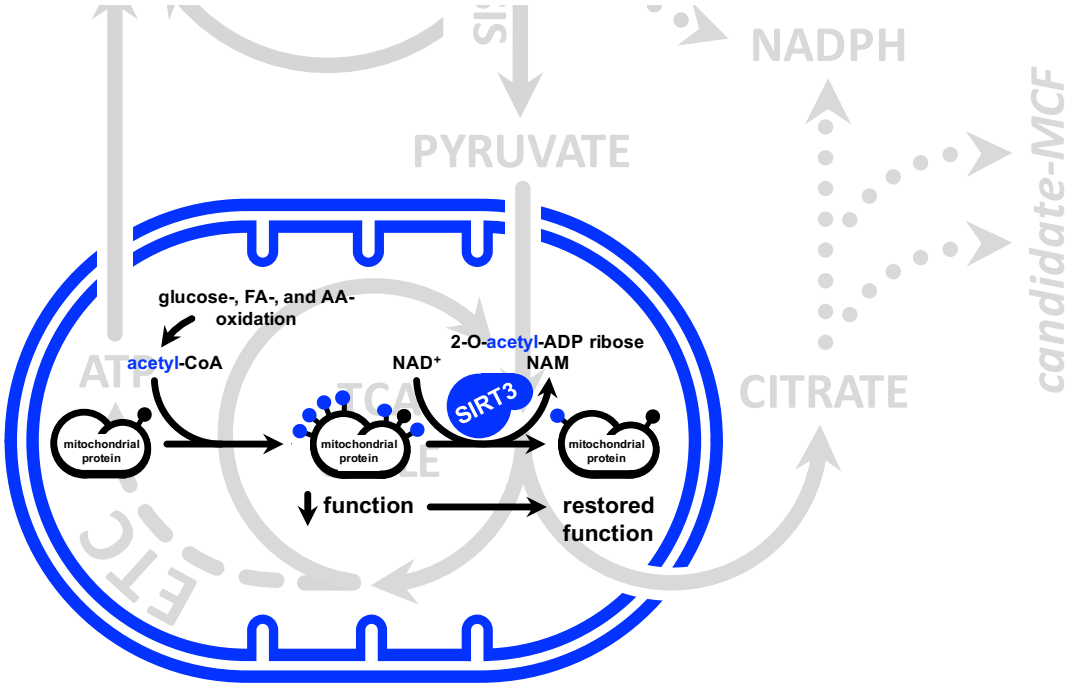

Figure 4: SIRT3 is the main mitochondrial protein deacetylase.

Mitochondrial protein acetylation is the result of a nonenzymatic reaction with acetyl-CoA, a byproduct of glucose-, fatty acid- (FA-), and amino acid- (AA-)oxidation. Mitochondrial proteins are thought to lose enzymatic and other functions upon acetylation. SIRT3 is an NAD^+-dependent mitochondrial protein deacetylase. SIRT3 catalyzes the NAD^+-dependent deacetylation of mitochondrial proteins to yield 2-O-acetyl-ADP ribose, NAM and the deacetylated substrate (Figure adapted from Wagner and Hirschey, 2014).

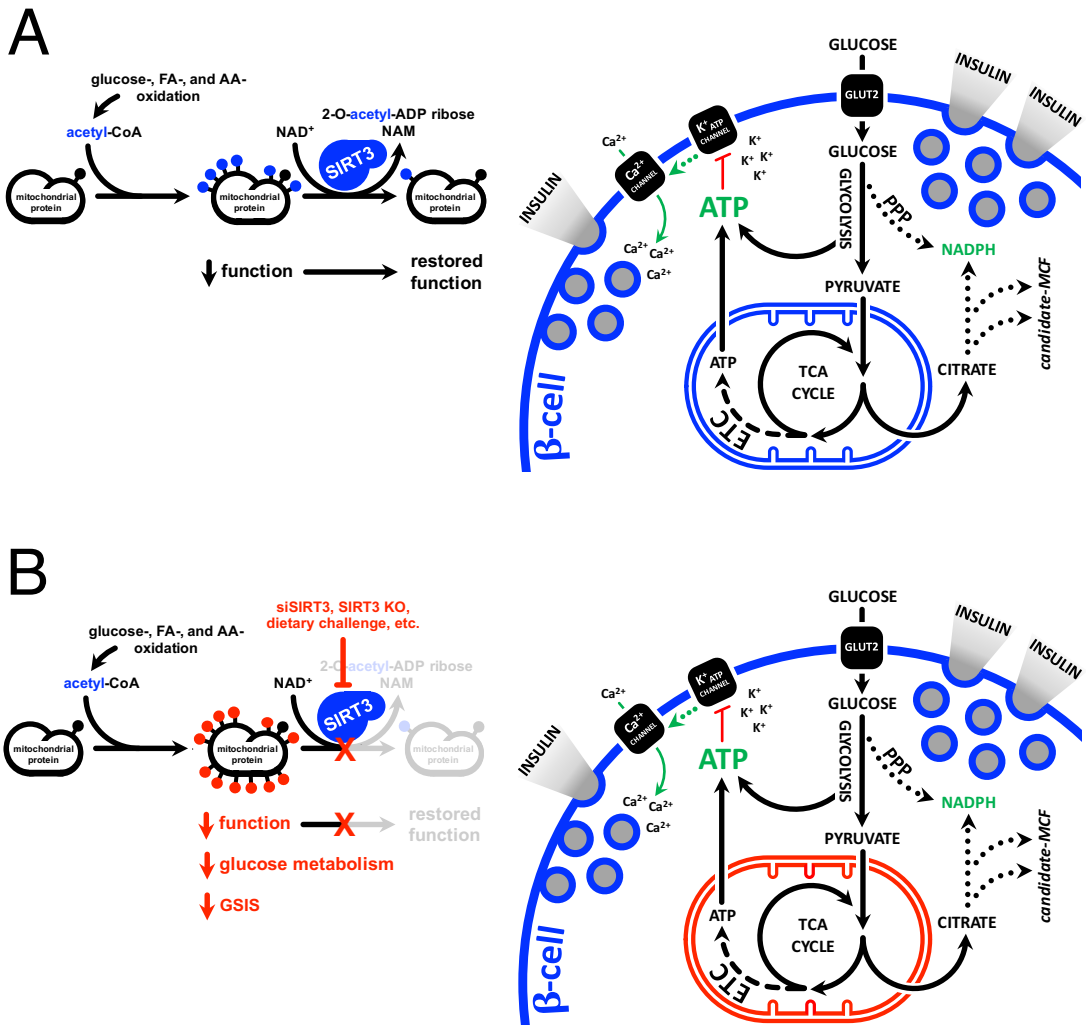

Figure 5: Hypothesized role for SIRT3 in the GSIS response of the pancreatic β-cell.

(A) SIRT3 serves to deacetylate mitochondrial proteins, presumably to maintain their enzymatic activity. It has been suggested that in performing this role, SIRT3 may preserve mitochondrial function and thus the GSIS response. (B) SIRT3 loss permits broad-scale mitochondrial protein acetylation, purportedly resulting in a sustained decrease in activity of target proteins. The model further suggests that decreased mitochondrial enzyme activity will impair mitochondrial metabolism of glucose-derived pyruvate and thus result in a decrease in GSIS.

2. Experimental Procedures

2.1 Cell Culture and Reagents

The INS-1-derived 832/13 rat insulinoma cell line was cultured as previously described (Hohmeier et al., 2000) unless otherwise indicated. For experiments using conditioned cell culture media: 1) Serum-deprived media was defined as RPMI-1640 with 11.1 mM glucose supplemented with 0.5% fetal bovine serum (FBS), 0.2% bovine serum albumin (BSA) (SIGMA #A7979), 10 mM HEPES, 2 mM glutamine, 1 mM sodium pyruvate, and 50 uM β-mercaptoethanol; 2) High-pyruvate media was defined as RPMI-1640 without glucose supplemented with 2.8 mM glucose, 0.5% FBS, 0.2% BSA, 10 mM HEPES, 2 mM glutamine, 10 mM sodium pyruvate, 50 uM β-mercaptoethanol, and 8.3 mM mannitol; 3) Glucolipotoxicity-inducing media was defined as RPMI-1640 with 11.1 mM glucose supplemented with 0.5 mM of 2:1 oleate:palmitate mixture conjugated to fatty acid-free BSA (O/P) (SIGMA #A9576), 0.5% fetal bovine serum (FBS), 0.2% bovine serum albumin (BSA), 10 mM HEPES, 2 mM glutamine, 1 mM sodium pyruvate, and 50 uM β-mercaptoethanol; 4) ER stress-inducing media was defined as RPMI-1640 with 11.1 mM glucose supplemented with 10 nM Thapsigargin, 0.5% fetal bovine serum (FBS), 0.2% bovine serum albumin (BSA), 10 mM HEPES, 2 mM glutamine, 1 mM sodium pyruvate,

and 50 uM β-mercaptoethanol. All reagents and solutions were obtained from Sigma-Aldrich unless otherwise indicated.

2.2 siRNA- and Ad-shRNA-Mediated Target Suppression

For siRNA duplex-mediated knockdown experiments, expression of SIRT3 was suppressed via introduction of 19-22 base pair siRNA duplexes (Integrated DNA Technologies) (Table 1). 832/13 cells were seeded in 24-well plates and transfected with 50 nM SIRT3-directed siRNA duplex or 50 nM siSCR control duplex using TransIT-LT1 (Mirus Bio #2300) reagent according to manufacturer's instructions. For experiments, cells were transfected for 24 hours, then cultured for an additional 48 hours in standard media prior to assay.

For Ad-shRNA-mediated knockdown experiments, expression of SIRT3 was suppressed via transduction with an adenovirus containing a SIRT3-directed shRNA sequence (Table 2). Adenoviruses containing siRNA sequences were constructed using vectors GI801 and pJM17 as previously described (Odegaard et al., 2010). Viruses were purified using a BD Biosciences Adeno-X Purification Kit (Clontech). For experiments, 832/13 cells were seeded in 24-well plates and transduced with either Ad-shSIRT3 or Ad-shSCR for 24 hours, then cultured for an additional 48 hours in standard media prior to assay.

2.3 CRISPR/Cas9n

For the generation of SIRT3 KO β-cell lines: 1) pSpCas9n(BB)-2A-Puro (PX462) was a kind gift from Feng Zhang (Addgene plasmid #48141); and 2) Oligonucleotide guide RNA (gRNA) sequences directed at the SIRT3 gene were designed using the Massachusetts Institute of Technology's "Optimized CRISPR Design" web tool (found online at http://crispr.mit.edu/), and purchased from Integrated DNA Technologies (IDT) (Table 3). Briefly, "pair 1" gRNA targeting sequences were used to generate SIRT3 KO 1 and SIRT3 KO 2 cell lines, while "pair 2" gRNA targeting sequences were used to generate SIRT3 KO 3 and SIRT3 KO 4 cell lines. gRNA targeting sequences were annealed to complementary RNA oligonucleotides and subsequently ligated into separate BbsI-digested PX462 vector backbones for a total of four (two pairs) of plasmids. Plasmids were transformed and amplified in Subcloning Efficiency DH5α Competent Cells (Thermo #18265017) and purified using the QIAprep Spin Miniprep Kit (QIAGEN #27104). 832/13 cells were cotransfected with either pair of SIRT3-targeting plasmids or an equal mass of empty vector as a control using TransIT-LT1 (Mirus Bio #2300) reagent according to manufacturer's instructions. Transfection media was replaced with full media 18 hours following transfection for an additional 24 hours of resistance marker expression. Full media was replaced with full media supplemented with 1.5 ug/mL Puromycin for selection and was refreshed every 24 hours for 48-96 hours. Selected cells were suspended

and plated at a limiting dilution in full media without Puromycin. Newly isolated monoclones were expanded and screened for SIRT3 protein expression by immunoblot with a SIRT3-specific antibody (Cell Signaling Technology #5490).

2.4 Lentiviral Constructs and Lentivirus

For the generation of lentiviral constructs: 1) The wild-type human SIRT3 (hSIRT3 WT) fusion protein open reading frame flanked by attR1 and attR2 sites was synthesized as a gBlock Gene Fragment from IDT; 2) The Gateway pDONR221 Vector (Thermo #12536017) was used according to manufacturer's instructions; and 3) The pLenti6.3/V5-DEST Gateway Vector Kit (Thermo #V53306) was used according to manufacturer's instructions. Briefly, the hSIRT3 WT gBlock Gene Fragment (gBlock JH506) was cloned into the pDONR221 vector according to manufacturer's instructions to generate the pDONR221/hSIRT3 WT plasmid (plasmid IS601). Using the pDONR221/hSIRT3 WT plasmid as a template, the QuikChange Lightning Multi Site-Directed Mutagenesis Kit (Agilent #210513) was used according to manufacturer's instructions to generate pDON221/hSIRT3 N229A, pDON221/hSIRT3 H248Y, and double-mutant pDON221/hSIRT3 NA/HY sequence-verified plasmids. pDONR221/hSIRT3 plasmids were recombined with pLenti6.3/V5-DEST vector to generate sequence-verified pLenti6.3/hSIRT3-V5 plasmids according to manufacturer's instructions. Lentivirus was

produced by transfecting either pLenti6.3/V5-GW/lacZ or one of the five different pLenti6.3/hSIRT3-V5 plasmids into HEK293T cells using the ViraPower Lentiviral Packaging Mix (Thermo #K497500) according to manufacturer's instructions. SIRT3 KO 1 and SIRT3 KO 3 β-cell lines were infected with the different lentiviruses in a confluent 25 cm^2 cell culture flask. Lentiviral media was replaced with full media 24 hours following infection for an additional 24 hours of resistance marker expression. Full media was replaced with full media supplemented with 2 ug/mL Blasticidin for selection and was refreshed every 48 hours until no death was observed. The two sets of five different stably infected polyclonal mixtures of β-cells were carried forward for study.

2.5 Cell Fractionation and Immunoblot Analysis

Mitochondrial enrichments: Confluent cells from a 175 cm^2 flask were washed with ice-cold PBS, lifted in 0.05% trypsin-EDTA, re-suspended in ice-cold PBS supplemented with 10% FBS and 10 mM NAM, and pelleted at 750 x g in a 4°C centrifuge. Cells were washed once more in ice-cold PBS supplemented with 10 mM NAM and pelleted. The pellet was re-suspended in 1 mL of ice-cold MSH buffer (220 mM mannitol, 70 mM sucrose, 5 mM HEPES, 10 mM NAM) and homogenized with 50 strokes in a Dounce homogenizer on ice. Following a 5-minute 750 x g centrifugation at 4°C, the supernatant was aliquoted in a separate tube and kept on ice. The remaining pellet was

re-suspended in 500 μL ice-cold MSH buffer and homogenized; the above steps were repeated twice more. Pooled supernatants were pelleted at 15,000 x g in a 4°C centrifuge and re-suspended in 500 μL ice-cold MSH for two subsequent wash steps. The pelleted mitochondria-enriched fraction was lysed in 30 μL of MSH buffer supplemented with 0.1% Triton X-100 and the Halt Protease Inhibitor Cocktail (Thermo #78430).

To prepare insulinoma and primary islet cell lysates, cells/ tissue were lysed in ice-cold RIPA buffer with Halt Protease Inhibitor Cocktail (Thermo #78430). Clarified lysates were resolved on 4-12% NuPAGE gels (Invitrogen) and transferred to nitrocellulose membranes (Bio-Rad). The membranes were first stained with Ponceau S for total protein images in the colorimetric channel of a Gel Doc imager (Bio-Rad). Ponceau S was thoroughly washed with TBS-T (TBS containing 0.1% Tween 20) prior to blocking the membrane with 5% milk in TBS-T. Following wash steps, membranes with resolved proteins were probed with the following primary antibodies: Anti-SIRT3 (Cell Signaling Technology #2627), anti-Total OXPHOS Cocktail (abcam #ab110413), anti-V5 Tag (Thermo #MA5-15253), anti-Citrate Synthase (Origene #TA308265), anti-Acetylated-Lysine (Cell Signaling Technology #9441), anti-UQCRSF1 (Abcam #14746), anti-β-actin (Cell Signaling Technology #8457), and anti-Caspase 3 (Cell Signaling Technology #9662). Primary antibodies were detected with the following secondary antibodies: Donkey anti-rabbit IRDye 800CW (Li-COR #926-32213) and donkey anti-mouse IRDye 680RD (Li-COR #926-

68072). Immunoblots were developed and quantified using an Odyssey CLx system (Li-COR).

2.6 RNA Isolation and Quantitative PCR (qPCR)

RNA was isolated from cells using the Qiagen RNeasy Mini Kit (Qiagen) and reverse transcribed with the iScript cDNA Synthesis Kit (Bio-Rad) according to manufacturer's instructions. Real-time quantitative PCR (qPCR) analysis was performed using iTaq Universal SYBR Green Supermix (Bio-Rad) and indicated primer sequences (Table 4). Human *INS* (*hINS*) gene expression was measured using TaqMan Gene Expression Assay Hs00355773_m1 (Thermo #4331182). qPCR assays were run using the ViiA 7 Real-Time PCR System (Thermo).

2.7 Fuel-Stimulated Insulin Secretion (FSIS)

For glucose- and pyruvate-stimulated insulin secretion experiments, collectively referred to as fuel-stimulated insulin secretion (FSIS), cells were seeded in 24-well plates (Corning) and cultured to confluence unless otherwise stated. Cells were pre-incubated in a HEPES balanced salt solution (HBSS) secretion buffer (114 mM NaCl, 4.7 mM KCl. 1.2 mM KH_2PO_4, 1.16 mM $MgSO_4$, 20 mM HEPES, 2.5 mM $CaCl_2$, 25.5 mM $NaHCO_3$, 0.2% BSA, pH 7.2) containing 2.8 mM glucose for 2 hours. Following pre-incubation, cells were

stimulated for 2 hours in secretion buffer containing either 2.8 mM glucose, 16.7 mM glucose, or 2.8 mM glucose supplemented with a range of sodium pyruvate concentrations (0.063 mM – 10 mM). Secretion buffer was sampled at the end of the 2-hour static incubation period, diluted as necessary, and assayed using a radioimmunoassay (RIA) with the Coat-A-Count kit (Diagnostic Products Corporation) for data in Figure 6, and the STELLUX Chemi rodent insulin ELISA kit (ALPCO) for all other insulin measurements. Cells were lysed in ice-cold RIPA buffer with Halt Protease Inhibitor Cocktail (Thermo #78430) and clarified lysates were assayed for total cellular protein using the BCA Protein Assay Kit (Thermo #23225). FSIS data was represented as insulin secreted per total cellular protein per hour.

2.8 Acetylproteomics

Sample preparation: Mitochondrial pellets were re-suspended in 300 μL of ice-cold 8M Urea Lysis Buffer (8 M urea in 50mM Tris, pH 8.0, 40 mM NaCl, 2 mM $MgCl_2$, 1x complete mini EDTA-free protease inhibitor tablet, 10 mM Nicotinamide, 10 μM TSA). The mitochondria were disrupted by a combination of pipetting and vortexing, and subsequent sonication with a probe sonicator in three 5 second bursts (power setting of 3), incubating on ice between each burst. Samples were centrifuged at 10,000 x g for 10 min at 4°C and the supernatant was retained. Protein concentration was determined by

BCA, and equal amounts of protein (500 μg, adjusted to 2.5 mg/mL with Urea Lysis Buffer) from each sample were reduced with 5 mM DTT at 37°C for 30 min, cooled to RT, alkylated with 15 mM iodoacetamide for 30 min in the dark and unreacted iodoacetamide quenched by the addition of DTT up to 15 mM. Each sample was digested with 5 μg LysC (100:1 w/w, protein to enzyme) at 37°C for 4 hours. Following dilution to 1.5 M urea with 50 mM Tris (pH 8.0), 5 mM $CaCl_2$, the samples were digested with trypsin (50:1 w/w, protein:enzyme) overnight at 37°C. The samples were acidified to 0.5% trifluoroacetic acid (TFA) and centrifuged at 4,000 x g for 10 min at 4°C to pellet insoluble material. The supernatant was desalted by solid phase extraction (SPE) with a Waters 50 mg tC18 SEP-PAK SPE column and the eluate was frozen and dried in a speed vac. Each sample was re-suspended in 100 μL of 200 mM triethylammonium bicarbonate (TEAB), mixed with a unique 10-plex Tandem Mass Tag (TMT) reagent (0.8 mg re-suspended in 50 μL100% acetonitrile), and shaken for 5 hours at room temperature. After samples were quenched with 0.8 μL 50% hydroxylamine and shaken for 15 additional minutes at RT, all nine samples were combined, frozen, and dried in a speed vac. The mixture was re-suspended in 1 mL 0.5% TFA and subjected to SPE with a Waters 100 mg tC18 SEP-PAK SPE column. The eluate was vortexed and split into aliquots containing ~ 5% of the total peptide mixture (250 μg) and a second aliquot containing ~ 95% (4.75 mg). Both aliquots were

frozen and dried in a speed vac. The 250 μg aliquot of the "input" material was saved at -80°C for quantification of unmodified peptides.

Acetylpeptide enrichment and input fractionation: The 4.75 mg aliquot was re-suspended in 1.4 mL 1X IAP Buffer and subjected to immunoprecipitation (IP) with PTMScan Acetyl Lysine Motif IAP Beads on a rotator overnight at 4°C. The next day, the antibody-peptide complexes were pelleted via centrifugation at 2,000 x g for 30 seconds and the precipitate was washed 2 times in 1 mL of IP buffer and 3 times in 1 mL water (centrifuging each time). Acetylpeptides were eluted twice with 100 μL of 0.15% TFA for 10 minutes each time, and the supernatants from each elution were combined, acidified to 0.5% TFA (and brought to a 1 mL volume), desalted on a 50 mg tC18 SEP-PAK SPE column, frozen, and dried in a speed vac. The "input" material was separated into 8 fractions using a High pH Reversed Phase Peptide Fractionation Kit (Pierce #84868). After column conditioning, 100 μg of peptide re-suspended in 300 μL 0.1% TFA was loaded onto a fractionation column and centrifuged at 3,000 x g for 2 minutes at RT. Sample was washed with 300 μL water followed by 300 μL of 5% acetonitrile (ACN), 0.1% TFA. Sample was eluted in 8 fractions containing increasing amount of ACN, frozen, and dried in a speed vac. Peptide fractions were re-suspended in 10 μL of 0.1% formic acid (FA) and quantified using the Quantitative Colorimetric Peptide Assay (Pierce, 23275).

Nano-LC-MS/MS: All samples were subjected to *nano*LC-MS/MS analysis using an EASY-nLC UPLC system (Thermo Fisher Scientific) coupled to a *Q Exactive Plus* Hybrid Quadrupole-Orbitrap mass spectrometer (Thermo Fischer Scientific) *via* an EASY-Spray (Thermo Fischer Scientific) nanoelectrospray ionization source. Prior to injection, the acetylpeptide sample was re-suspended in 22.5 μL 1% FA and each of the HPRP fractions of the input material were re-suspended in enough 0.1% FA to achieve a peptide concentration of approximately 0.15 μg/μL (which was determined precisely using the peptide quantitation assay described above). The acetylpeptide sample was analyzed with technical triplicate runs, with 6.5 μL of sample injected for each. The 8 input HPRP fractions were analyzed in singlicate, with 1 ug injections (roughly 7 μL for each based on the precise concentration). For each injection, the sample was first trapped on an Acclaim PepMap 100 C18 trapping column (3 μm particle size, 75 μm × 20 mm) with 18 μL of solvent A (0.1 % FA) at a variable flow rate dictated by max pressure of 500 Bar, after which the analytical separation was performed over a 105 minute gradient (flow rate of 300 nL/minute) of 5 to 40% solvent B (90% ACN, 0.1% FA) using an Acclaim PepMap RSLC C18 analytical column (2 um particle size, 75 μm × 500 mm column (Thermo Fischer Scientific) with a column temperature of 55ºC. MS^1 (precursor ions) was performed at 70,000 resolution, with an AGC target of $3x10^6$ ions and a maximum injection time of 60 ms. MS^2 spectra (product ions) were collected by data-dependent acquisition (DDA) of

the top 10 most abundant precursor ions with a charge greater than 1 per MS1 scan, with dynamic exclusion enabled for a window of 30 seconds. Precursor ions were filtered with a 0.7 m/*z* isolation window and fragmented with a normalized collision energy of 30. MS2 scans were performed at 35,000 resolution, with an AGC target of $1x10^5$ ions and a maximum injection time of 60 ms.

Raw data processing: Raw LC-MS/MS data have been deposited to the ProteomeXchange Consortium via the PRIDE partner repository (Vizcaino et al., 2016) with the dataset identifier to be issued. Raw LC-MS/MS data were processed in Proteome discoverer v2.2 (PD2.2, Thermo Fisher Scientific), using both the Sequest HT (Yates, 2015) and MS Amanda 2.0 (Dorfer et al., 2014) search engines. Data were searched against the UniProt rat complete proteome database of reviewed (Swiss-Prot) and unreviewed (TrEMBL) proteins, which consisted of 29,979 sequences on the date of download (9/20/2017). Default search parameters included oxidation (15.995 Da on M) as a variable modification and carbamidomethyl (57.021 Da on C) and TMT (229.163 Da on peptide N-term and K). To assess labeling efficiency as a quality control measure, the input fraction was re-searched with N-terminal TMT as a variable modification, confirming N-terminal labeling of 91% of all PSMs. Acetylpeptide runs added acetyl (42.01057 Da on K) as a variable modification and changed TMT to a variable modification on K (remaining fixed on peptide N-term). Data were searched with a 10 ppm precursor mass and 0.02 Da

product ion tolerance. The maximum number of missed cleavages was set to a default value of 2 (but changed to 4 for acetyl runs) and enzyme specificity was trypsin (full). Considering each data type (acetyl, input) separately, peptide spectral matches (PSMs) from each search algorithm were filtered to a 1% false discovery rate (FDR) using the Percolator (Kall et al., 2007) node of PD2.2. For acetyl data, site localization probabilities were determined for acetyl lysines using the ptmRS algorithm (Taus et al., 2011). PSMs were grouped to unique peptides while maintaining a 1% FDR at the peptide level and using a 90% site localization threshold for acetyl lysines. Peptides from all samples (acetyl, input) were grouped to proteins together using the rules of strict parsimony and proteins were filtered to 1% FDR using the Protein FDR Validator node of PD2.2. Reporter ion intensities for all PSMs having co-isolation interference below 50% (of the ion current in the isolation window) and average reporter S/N>2.5 were summed together at the peptide group and protein level, but keeping quantification for each data type (acetyl, input) separate. Peptides shared between protein groups were excluded from protein quantitation calculations.

Statistical analysis: Protein and peptide groups tabs in the PD2.2 results were exported as tab delimited .txt. files, opened in Microsoft EXCEL, and analyzed as described previously (McDonnell et al., 2016). First, peptide group reporter intensities for each peptide group in the input material were summed together for each TMT channel,

each channel's sum was divided by the average of all channels' sums, resulting in channel-specific loading control normalization factors to correct for any deviation from equal protein/peptide input into the ten-sample comparison. Reporter intensities for peptide groups from the acetyl fraction and for proteins from the input fraction were divided by the loading control normalization factors for each respective TMT channel. Analyzing the acetylpeptide and protein datasets separately, all loading control-normalized TMT reporter intensities were converted to log2 space, and the average value from the nine samples was subtracted from each sample-specific measurement to normalize the relative measurements to the mean. For each cell line (WT, KO, HY), condition average and standard deviation were calculated. For each comparison (WT/HY, WT/KO, HY/KO), Log2 fold change, p-value (two-tailed student's t-test, assuming equal variance), and adjusted p-value ($P_{adjusted}$, Benjamini Hochberg FDR correction) were calculated (Benjamini et al., 2001; Lesack and Naugler, 2011). For protein-level quantification, only Master Proteins—or the most statistically significant protein representing a group of parsimonious proteins containing common peptides identified at 1% FDR—were used for quantitative comparison. Acetylpeptide measurements were calculated both alone (referred to as "relative abundance") and with normalization to any change in the corresponding Master Protein (referred to as "relative occupancy"), calculated by

subtracting Log2 Master Protein values from acetylpeptide quantitation values on a sample-specific basis.

2.9 Metabolomics

Cells were seeded in 21 cm^2 cell culture dishes (Greiner). Organic acids, amino acids, and acylcarnitines were analyzed using a stable isotope dilution technique. Organic acids were quantified using methods described previously (Jensen et al., 2006) employing a Trace Ultra GC coupled to a ISQ MS operating under Xcalibur 2.2 (Thermo Fisher Scientific, Austin, TX). Amino acid and acylcarnitine measurements were made by flow injection tandem mass spectrometry using sample preparation methods described previously (An et al., 2004; Ferrara et al., 2008). Data were acquired using a Waters TQD mass spectrometer equipped with a Acquity UPLC system and controlled by the MassLynx 4.1 operating system (Waters, Milford, MA).

2.10 Animals

SIRT3 KO mice on a 129Sv background were a kind gift from Professor Eric Verdin, Buck Institute. They were re-derived upon arrival at Duke University in the C57Bl/6J strain (JAX Stock No: 000664) and continually back-crossed onto this background for greater than 10 generations to generate C57Bl/6J SIRT3 mice. These mice were then

crossed with the C57Bl/6NJ strain (JAX Stock No: 005304) until homozygous for wild-type nicotinamide nucleotide transhydrogenase (*Nnt*), to generate breeders for the C57Bl/6J/*Nnt* wild-type SIRT3 KO line used in this study. Successful transfer of two alleles of wild-type *Nnt* was confirmed by genotyping (Figure 20A and 20B) using indicated primer sequences (Table 5 and 6). At 11-14 weeks of age, male mice were fed either a standard diet (Lab Diet #5053) or a high-fat/high-sucrose diet (Research Diets #D12451) for 12 weeks. For glucose-tolerance tests, mice were fasted for 5 hours before administering 1.5 mg/g body weight of glucose via oral gavage (oGTT) or intraperitoneal injection (ipGTT). Blood glucose was measured from tail vein blood at 0, 10, 20, 30, 60, 90, and 120 minutes post-bolus. Tail vein blood was collected at 0, 10, and 30 minutes post-bolus for plasma insulin measurements. For insulin tolerance tests (ITT), mice were fasted for 5 hours before administering 0.5 mU/g body weight Humalog (Eli Lilly) via intraperitoneal injection. Blood glucose was measured at 0, 10, 20, 30, 60, and 90 minutes post-injection. Blood glucose was measured with a Bayer Contour glucometer. Plasma insulin was assayed using the STELLUX Chemi Rodent Insulin ELISA (ALPCO). All animal protocols were approved by the Institutional Animals Use and Care Committee at Duke University.

2.11 Islet Isolation and Perifusion

Primary islets were isolated from mice as previously described (Lamont et al., 2012). Sixty size-matched islets were handpicked into 0.275 mL chambers containing KRBPH (135 mM NaCl, 3.6 mM KCl, 1.5 mM $CaCl_2$, 0.5 mM NaH_2PO_4, 0.5 mM $MgSO_4$, 5 mM HEPES, 5 mM $NaCO_3$, 1% BSA, pH 7.4). Islets were perifused for 48 minutes of equilibration in KRBPH with 2.8 mM glucose at a flow rate of 200 μL per minute using the Biorep Perifusion system. Following equilibration, islets were perifused at a flow rate of 200 μL per minute with KRBPH supplemented with the following secretagogues/ potentiators for the following times: 1) 2.8 mM glucose for 8 minutes; 2) 16.7 mM glucose for 16 minutes; 3) 2.8 mM glucose for 16 minutes; 4) 11.1 mM glucose for 12 minutes; 5) 11.1 mM glucose with 0.5 mM O/P for 12 minutes; 6) 11.1 mM glucose for 12 minutes; 7) 11.1 mM glucose with 0.03 nM GLP-1 for 12 minutes; 8) 11.1 mM glucose for 12 minutes; 9) 11.1 mM glucose with 0.3 nM GIP for 12 minutes; 10) 11.1 mM glucose for 12 minutes; 11) 2.8 mM glucose for 12 minutes; and 12) 2.8 mM glucose with 30 mM KCl for 12 minutes. Perifusion media was collected at 1 minute-intervals for measurement of insulin concentrations. Insulin was detected with the AlphaLISA Biomarker Detection Kit (PerkinElmer) and the EnVision 2105 Multimode Plate Reader (PerkinElmer). Data is represented as ng insulin secreted per mL of buffer.

2.12 Statistical Analysis

Analysis for all studies was performed using GraphPad Prism6 unless otherwise stated. Data are presented as the mean ± SE unless otherwise stated. Data were analyzed busing a Two-Way ANOVA with Bonferroni post hoc corrections for multiple comparisons or the two-tailed unpaired, Student's t test unless otherwise stated.

Table 1: siRNA duplex sequences

(Lowercase) Base pairs added as 3′ overhangs.
(Bold) Base pairs intentionally mismatched.

control siRNA (siSCR)	5′	UAAUCACGGAUAGGGUCUCtt	3′
	3′	ttAUUAGUGCCUAUCCCAGAG	5′
SIRT3 siRNA 1 (siSIRT3 1)	5′	UAGUGAGCGACAUUGGGCCtg	3′
	3′	ttAUCACUCGCUGUAACCCGG	5′
SIRT3 siRNA 2 (siSIRT3 2)	5′	GUCUGUACUGGCGUUGUGAAAUtt	3′
	3′	ttCAGACAUGACCGCAACACUUUg	5′
SIRT3 siRNA 3 (siSIRT3 3)	5′	UUUCUGUACCGAUUCAGACaa	3′
	3′	ttAAAGACAUGGCUAAGUCUG	5′
SIRT3 siRNA 4 (siSIRT3 4)	5′	GGAAAGUCGCACAGGAGAUutt	3′
	3′	ttCCUUUCAGCGUGUCCUCUAG	5′
SIRT3 siRNA 5 (siSIRT3 5)	5′	GUACAGUGCUGCUUUCUGA**U**Att	3′
	3′	ttCAUGUCACGACGAAAGACU**G**U	5′

Table 2: Adenovirus shRNA target sequences

control Ad-shRNA (Ad-shSCR)	5′	TAATCACGGATAGGGTCTC	3′
SIRT3 Ad-shRNA (Ad-shSIRT3)	5′	GGAGTGGCCTCTACAGCAA	3′

Table 3: CRISPR/Cas9n guide RNA (gRNA) sequences

pair 1: *Sirt3*-directed gRNA 1	5′	ACATTGGGCCTGTAGTGCCC	3′
pair 1: *Sirt3*-directed gRNA 2	5′	CCTTCGGCTGCTTCACGACA	3′
pair 2: *Sirt3*-directed gRNA 1	5′	GCTTCAACCAGCTTTGAGGC	3′
pair 2: *Sirt3*-directed gRNA 2	5′	CTACGTGCACGGTCTGTCGA	3′

Table 4: qPCR primer sequences

rat *CypB* (S)	5′	GAACAGCAAGTTCCATCGTGTC	3′
rat *CypB* (AS)	5′	CTCACCATAGATGCTCTTTCCTC	3′
rat *Sirt3* (S)	5′	CAAACATGGGCCAGACCACAACAT	3′
rat *Sirt3* (AS)	5′	ACACGTGGAGCTCCTTTGTATGGT	3′
rat *Sirt4* (S)	5′	GCCCTTAATAGACCCACAGTG	3′
rat *Sirt4* (AS)	5′	CTCTAGGATGCAGACAGTAAGC	3′
rat *Sirt5* (S)	5′	TACATCGAAAGGCTGGCACCAAGA	3′
rat *Sirt5* (AS)	5′	AGTTCTCAGCAACATTGCCACACG	3′
rat *Glut2* (S)	5′	TTCTTTGGTGGGTGGCTTGG	3′
rat *Glut2* (AS)	5′	GCTTCTTCCAGCAATGATGAGAGC	3′
rat *Gck* (S)	5′	AGACCTGGGAGGAACCAACTTCAG	3′
rat *Gck* (AS)	5′	TCAAAGAGCATCTCGGCAGTGC	3′
rat *Kir6.2* (S)	5′	TCCACTCCTTTTCGTCTGCCTTC	3′
rat *Kir6.2* (AS)	5′	ATGCTGTTACCACCCACACCGTTC	3′
rat *Sur1* (S)	5′	GCTGTTCTTCTGTTCCTTGCCCTC	3′
rat *Sur1* (AS)	5′	TTGGTCTGGAATGCTCCTCTCAGG	3′
rat *Ins2* (S)	5′	GGACCCACAAGTGGCACAAC	3′
rat *Ins2* (AS)	5′	TAGAGAGAGCAGATGCTGGTGC	3′

Table 5: *Sirt3* genotyping primer sequences

mouse wild-type: forward	5′	CTTCTGCGGCTCTATACACAG	5′
mouse KO: forward	5′	TACTGAATATCAGTGGGAACG	5′
reverse	5′	TCGAACAAGGCTTTATCTTCC	5′

Table 6: *Nnt* genotyping primer sequences

mouse wild-type: forward	5′	GGGCATAGGAAGCAAATACCAAGTTG	5′
mouse mutant: forward	5′	GTGGAATTCCGCTGAGAGAACTCTT	5′
reverse	5′	GTAGGGCCAACTGTTTCTGCATGA	5′

3. Developing a Tractable *in vitro* β-cell Model for the Interrogation of Mitochondrial Protein Acetylation

The development of *in vitro* models with which to study molecular mechanisms has been essential to our understanding of basic biology. Historically, tumors have been amenable starting material for the derivation of cell lines that can be propagated and studied in tissue culture. With their genetic predisposition for rapid proliferation, culture of cancer cell lines has proven a tractable model in which to uncover the molecular mechanisms that promote many cancers. Development of tractable *in vitro* models for studying β-cell biology has presented a unique challenge, given the limited regenerative capacity of primary islet β-cells, and the difficulty in obtaining transformed lines that retain expression of the high K_m glucose transporter (GLUT2) and glucokinase (GCK) proteins that are essential for regulating glucose metabolism, and thus insulin secretion, over the normal physiological range. In 1977, researchers from Harvard Medical School, New England Deaconess Hospital (NEDH), and the University of Massachusetts Medical School, took the first steps towards a solution (Chick et al., 1977). After almost 2 years following whole-body irradiation of an NEDH albino rat, a pancreatic tumor was observed and later excised for transplantation and subcutaneous propagation in other rats. The presence of insulin within secretory granules suggested that this tumor (insulinoma) retained at least some characteristics of primary β-cells. As such, the

researchers recognized that the tumors could be "a means for establishing a permanent line of insulin-producing cells in tissue culture" (Chick et al., 1977).

By 1992, several β-cell lines had been developed. These included the RINm5F β-cell line derived from the NEDH rat insulinoma tumor (Praz et al., 1983), the β-TC β-cell line derived from tumors excised from transgenic mice expressing large T-antigen under control of the insulin promoter as a transforming agent (Efrat et al., 1988), and the HIT β-cell line generated via transformation of hamster islet cells (Ashcroft et al., 1986). While these new *in vitro* models proved useful in many respects, their inevitable tendency to lose their differentiated state and become less responsive to glucose with increasing passage raised several caveats and made them cumbersome to work with. In 1992, Claes Wollheim's group made a serendipitous discovery during the course of co-culture experiments with lymphocytes and cells derived from the NEDH rat insulinoma (Asfari et al., 1992). They noticed the formation of a morphologically distinct group of cells during the course of these experiments. Subsequent characterization revealed that they retained many quantitative and qualitative characteristics of primary islet β-cells including GSIS within the physiological range of blood glucose (2.8 – 20 mM). Further, these cells, now named "INS-1 cells", retained their glucose sensitivity for 80 passages, far longer than previously published β-cell lines (Asfari et al., 1992). While the development of INS-1 cells created a useful tool, the range of glucose responsiveness of these cells (2-3-fold) was far

less than observed in experiments with primary rodent or human islets. Moreover, even this modest response was found to wane over prolonged culture periods and successive cell passaging.

In 2000, our group addressed this technical challenge with the development of novel INS-1-derived β-cell lines. The guiding hypothesis was that INS-1 cells represented a mix of glucose unresponsive and responsive cells, and that time in culture led to disproportional expansion of glucose-unresponsive cells within the polyclonal mixture. To overcome this, a transfection strategy was applied in which a plasmid containing the human insulin gene (*hINS*) and a neomycin resistance marker was used to stably transfect parental INS-1 cells to derive new monoclonal populations. This led to the isolation of a set of clonal lines with remarkable functional heterogeneity in terms of GSIS, supporting the idea that INS-1 cells are indeed polyclonal. Importantly, this approach yielded several subclones with robust GSIS, including the INS-1 832/13 cell line, which exhibited a 13-fold GSIS response to 12 mM glucose compared to 2.8 mM glucose (spanning the physiological range) (Hohmeier et al., 2000). Upon publication of the paper describing these cells, 832/13 rapidly became a widely used resource in the field, such that approximately 225 papers in which these cells were used for experiments have been published to date.

Based on this background, the 832/13 cell line seemed an ideal starting point for studies seeking to understand the role of SIRT3 in regulation of β-cell function. Initial

challenges with siRNA-mediated methods of SIRT3 knockdown necessitated the development of a novel CRISPR/Cas9-mediated SIRT3 knockout model. And though I revealed significant technical issues with our original CRISPR/Cas9 approach, I was ultimately able to resolve them. The specific problem, and steps taken to circumvent it, are described in this chapter.

3.1 Clonal Variability in 832/13 β-cell Subclones with Complete CRISPR/Cas9n-Dependent Loss of SIRT3

Our initial strategy for assessing the role of the SIRT3-targeted acetylproteome on β-cell function was similar to the transient siRNA-mediated SIRT3 knockdown approach reported in two previous studies (Caton et al., 2013; Zhang et al., 2016). While these studies used a single transfectable SIRT3-specific siRNA oligonucleotide, we tested several different oligonucleotides (Table 1), as well as a recombinant adenovirus containing a SIRT3-specific shRNA sequence (Ad-shRNA) (Table 2). However, suppression of SIRT3 expression by these methods in the 832/13 β-cell line revealed key obstacles: 1) Suppression of SIRT3 protein expression was limited, such that several different targeting sequences (siRNA oligonucleotides or Ad-shRNA) suppressed SIRT3 protein by 50% or less (Figure 6A and 6B); 2) This level of suppression was insufficient to cause measurable changes in the mitochondrial acetylproteome, as analyzed by immunoblot of mitochondria-enriched cellular subfractions with a pan anti-acetyllysine

antibody (data not shown); and 3) Different targeting sequences, despite similar suppression of SIRT3 expression, had significantly different effects on β-cell function. While one sequence impaired GSIS, others either augmented GSIS or had no effect (Figure 6C).

We reasoned that the incomplete and transient knockdown of SIRT3 achieved with the siRNA/shRNA approach, possibly coupled with non-specific effects of the targeting sequences, contributed to the inconclusive findings regarding the role of the SIRT3-targeted acetylproteome in β-cell function. In order to address these challenges, we applied a CRISPR/Cas9 gene-editing technique (Ran et al., 2013) to generate cell lines with complete, sustained, and specific loss of the endogenous rat SIRT3 (rSIRT3) protein. 832/13 cells were cotransfected with two plasmids containing the CRISPR/Cas9 D10A mutant nickase (Cas9n) enzyme and one of two unique pairs of chimeric guide RNA (gRNA) molecules targeting the *Rattus norvegicus Sirt3* gene. Following transient antibiotic selection, limiting dilution for monoclonal derivation, and clonal expansion, complete and sustained loss of SIRT3 protein was confirmed in several 832/13 subclones by immunoblotting with a SIRT3-specific antibody (Figure 7A).

β-cell function was assessed by measuring GSIS. The SIRT3 KO 832/13 β-cell subclones were exposed to either a basal (2.8 mM) or stimulatory (16.7 mM) concentration of glucose for 2 hours, and insulin secretion was assayed by measuring its accumulation

in the media (Figure 7B-7D). To our surprise, GSIS was markedly different among several clones with complete SIRT3 ablation. We initially explored if this variability was associated with compensatory expression of other mitochondrial sirtuins (Figure 8A), differences in expression of canonical components of the GSIS machinery (Figure 8B), and/or differences in expression of insulin (Figure 8C). Although there was some variability in the expression of mitochondrial sirtuins and GSIS regulatory components amongst SIRT3 KO monoclones, there were no obvious patterns that related to differences in insulin secretion. Differences in insulin expression were more dramatic, including the virtual absence of *hINS* expression in several of the 832/13 subclones. Three possible explanations for this variability were considered: 1) Cas9n has off-target effects in the 832/13 cell line and promotes heterogeneity; 2) The INS-1 832/13 β-cell line, though isolated as a monoclone (Hohmeier et al., 2000), has since experienced genetic drift leading to loss of the *hINS1* in some clones and functional variability across the clonal population; and/or 3) Functional heterogeneity is an inherent and unavoidable byproduct of monoclonal derivation. Based on the predicted specificity of the CRISPR/Cas9n system (Ran et al., 2013), we focused on the second two possibilities.

Since the characterization of the INS-1 832/13 β-cell line (Hohmeier et al., 2000), studies have been conducted largely under the presumption that these cells have remained a monoclonal population. This is a safe assumption when using transient

genetic engineering tools such as siRNA-mediated knockdown, delivery of overexpression plasmids by transient transfection, or adenovirus-mediated overexpression or siRNA delivery. However, use of stable transfection methods such as lentivirus for genomic integration of shRNA or overexpression plasmids requires several assumptions, including: 1) If the population of cells used for study is polyclonal, their heterogeneity is normally distributed; and 2) The transfection/transduction/infection efficiency is sufficiently high. In order to successfully apply CRISPR/Cas9n as a method of achieving complete gene knockout as described here, we needed a deeper understanding of INS-1 832/13 β-cell line clonal variability.

We performed a set of experiments to investigate 832/13 subclone variability (Figure 9A). New subclones were derived independent of CRISPR/Cas9n transfection and their function compared following clonal expansion. Of note, 832/13 cells were originally derived from parental INS-1 cells using a stable transfection-strategy with a plasmid that both directed *hINS* expression and contained a neomycin resistance gene for antibiotic selection with G418 (Hohmeier et al., 2000). We therefore hypothesized, that if variability in *hINS* expression was driving clonal variability, functional concordance could be restored to monoclones by reselection of neomycin-resistant clones. To test this, we split a single culture of 832/13 cells into two separate flasks to be carried in parallel. One flask went untreated (no Tx) and the other was treated with neomycin (G418). Selected cells

maintained as a polyclonal population maintained similar and robust GSIS response compared to untreated cells (Figure 9B), and exhibited the predicted enrichment of the *hINS* transcript (Figure 9C). However, derivation of ten new monoclones from either the unselected 832/13 population (Figure 10A and 10B) or the neomycin-selected 832/13 population (Figure 10D and 10E) resulted in functional heterogeneity independent of *hINS* gene expression (Figure 10C and 10F, respectively). Lastly, we chose a newly expanded 832/13 subclone, 1327/06, from the neomycin-selected population, and derived twenty new monoclones (1327/06a-1327/06t). Again, this yielded subclones with widely variable GSIS responses (Figure 10G and 10H), with those responses arraying in a normal distribution (Figure 10I). Taken together, these findings demonstrate that the clonal heterogeneity of the 832/13 cell line persists even following antibiotic selection, that normally distributed functional heterogeneity exists even when subclones are further derived from a new parental 832/13 subclone, and that caution should be used when employing selected monoclonal cell lines for either stable transfection studies or CRISPR/Cas9 gene-disruption. These findings are likely not unique to INS-1-derived cell lines, and may have impacted assays of SIRT3 function in other β-cell lines such as MIN-6 studied by stable transfection methods in other laboratories (Zhou et al., 2017).

3.2 Stable Integration of Different SIRT3 Transgenes in Expanded SIRT3 KO Cells Yields Polyclonal Cell Lines with Concordant GSIS Responses

The foregoing observations suggested the need to develop a different *in vitro* model in which we could reliably evaluate the effects of the SIRT3-targeted acetylproteome on β-cell function. Based on findings summarized in Figure 10G-10I, we developed a strategy (Figure 11A) to generate an *in vitro* model in a polyclonal cell line-setting such that phenotypes represent the average of the normal functional distribution. Given the complete absence of the main mitochondrial deacetylase, SIRT3, we reasoned that the previously generated SIRT3 KO cell lines would be maximally permissive to mitochondrial protein acetylation. Therefore, these cells would be ideal parental cell lines in which to introduce different forms of SIRT3 with or without deacetylase activity. Two expanded SIRT3 KO monoclones (SIRT3 KO 1 and SIRT3 KO 3) were used as parental cell lines in which we stably overexpressed a V5-tagged wild-type form of human SIRT3 (hSIRT3 WT-V5), β-Galactosidase (β-Gal-V5), or three different catalytically inactive forms of human SIRT3 (hSIRT3 N229A-V5, hSIRT3 H248Y-V5, and hSIRT3 NA/HY-V5) (Figure 11B) (Schwer et al., 2002). These cell lines are referred to hereafter as "WT", "KO", "NA", "HY", and "DM" (double-mutant), respectively. Following antibiotic selection, these two sets of five different polyclonal cell lines were expanded for further study.

We validated the presence of the different constructs by immunoblot analysis (Figure 11C). Only the overexpression of a catalytically active form of SIRT3 (hSIRT3 WT-V5) would be predicted to cause a decrease in mitochondrial protein acetylation in the parental SIRT3 KO cells, whereas overexpression of either β-Gal-V5 or the SIRT3 mutant gene products that lack deacetylase activity – and thus remain effectively "SIRT3-null" – should exhibit comparatively elevated mitochondrial protein acetylation. Notably, SIRT3 protein was completely undetectable in KO cells, whereas the WT, NA, HY, or DM cell lines had levels of hSIRT3-V5 protein that were approximately 70-fold higher than the endogenous rSIRT3. As expected, analysis of GSIS revealed no significant differences amongst the two sets of SIRT3-null β-cell lines, thus validating our strategy (Figure 12A-12C and 12D-12F). Surprisingly, the WT cell line (hSIRT3 WT-V5 overexpression in SIRT3 KO cells) exhibited GSIS identical to the four SIRT3-null cell lines. These findings suggest that either the overexpressed hSIRT3 WT-V5 fusion protein did not deacetylate mitochondrial proteins in the parental SIRT3 KO β-cells under standard culture conditions, or that changes in the SIRT3-targeted acetylproteome do not influence GSIS.

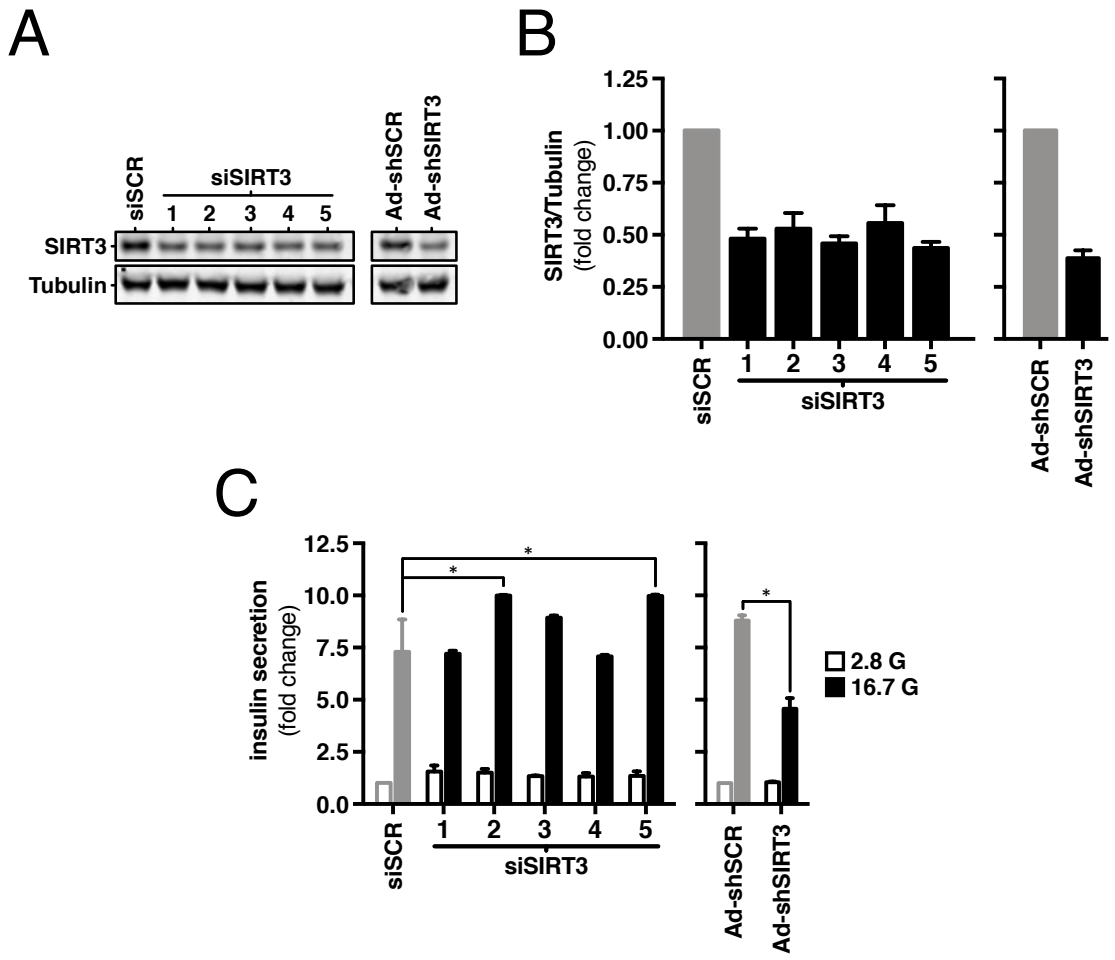

Figure 6: Equal suppression of SIRT3 protein by different SIRT3-specific siRNA oligonucleotides (siSIRT3) or an adenovirus-delivered SIRT3-specific shRNA (Ad-shSIRT3) has discordant effects on GSIS.

(A) Immunoblot detection of SIRT3 and Tubulin in 832/13 cells following 72-hour transfection or transduction. (B) Immunoblot quantification of SIRT3 expression. Fold change values normalized to respective control (siSCR or Ad-shSCR) set to 1. n=3 independent experiments. (C) Glucose-stimulated insulin secretion in response to 2.8 mM glucose (2.8 G) or 16.7 mM glucose (16.7 G). Fold change values normalized to respective control (siSCR or Ad-shSCR) treated with 2.8 mM glucose (2.8 G). n=2 independent experiments. Data represent mean ± SE. Statistical comparisons made using a Two-Way ANOVA with Bonferroni's multiple comparisons test. *$p \leq 0.05$ effect of SIRT3 knockdown.

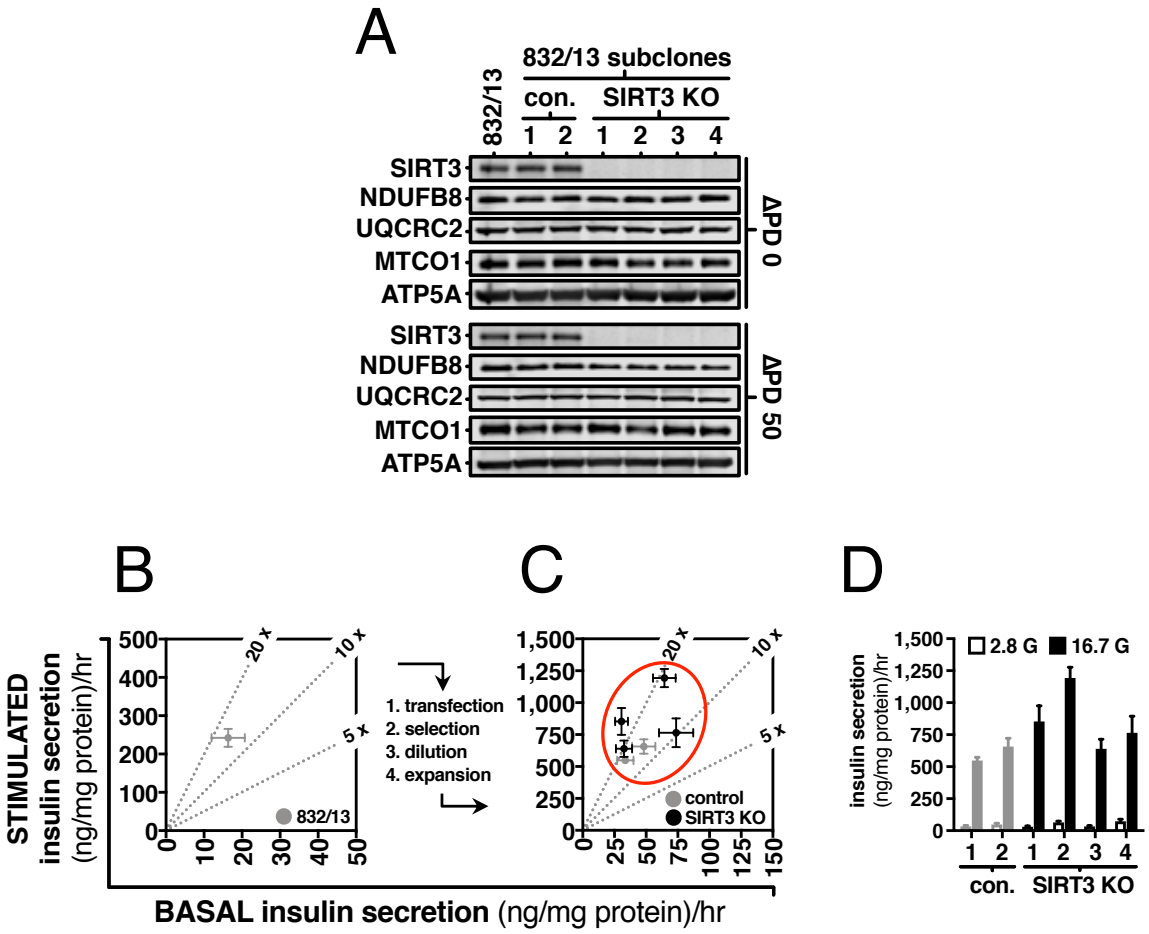

Figure 7: Application of CRISPR/Cas9n results in complete and sustained loss of SIRT3 protein, but SIRT3 KO 832/13 subclones exhibit discordant GSIS responses.

(A) Immunoblot detection of SIRT3 and mitochondrial markers (NDUFB8, UQCRC2, MTCO1, ATP5A) at initial point of freeze-down (ΔPD 0) and following 50 passage-doublings (ΔPD 50). (B-C) GSIS. X-axis (BASAL insulin secretion): insulin secretion in response to 2.8 mM glucose. Y-axis (STIMULATED insulin secretion): insulin secretion in response to 16.7 mM glucose. "5 x", "10 x", and "20 x" mark 5-, 10-, and 20-fold GSIS, respectively (dotted grey lines). Individual points represent one cell line. n= 4 independent experiments. (D) GSIS. Conventional presentation of data from Figure 1C. Data represent mean ± SE.

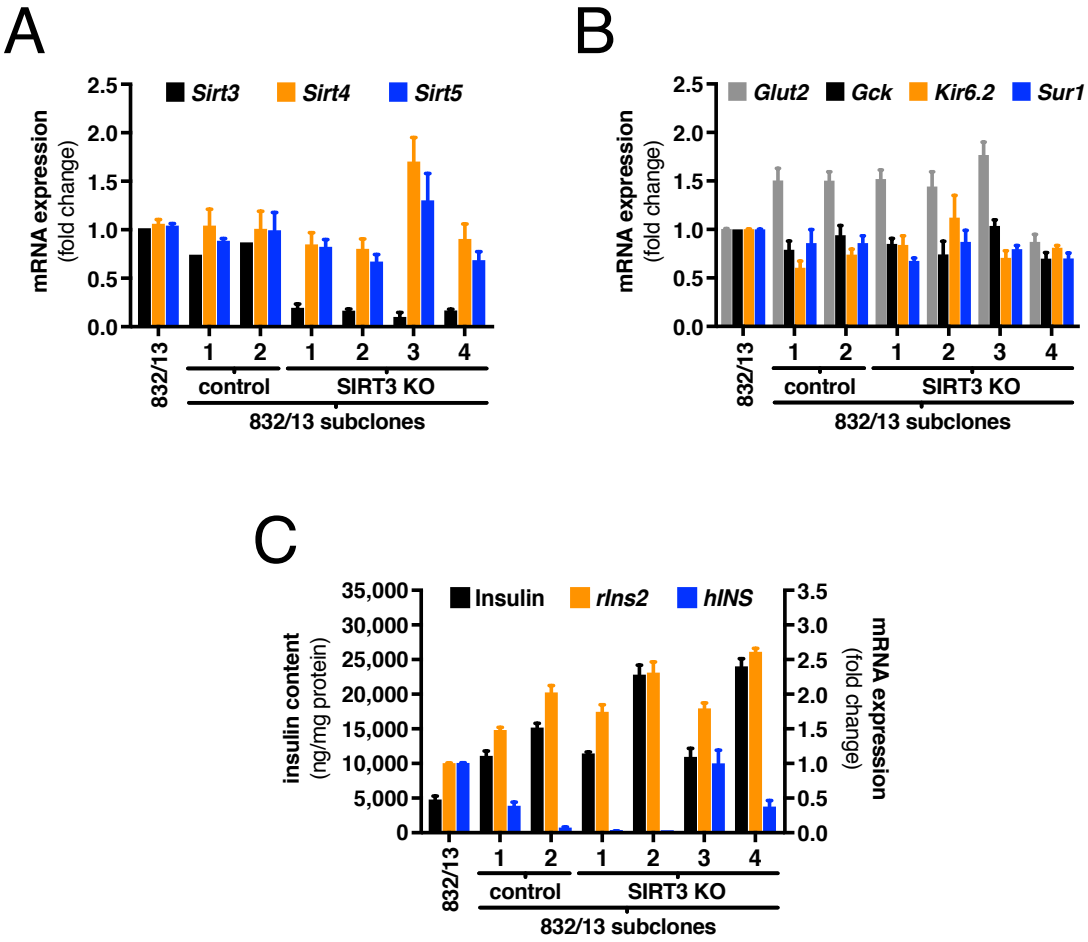

Figure 8: Discordance in the expression of mitochondrial sirtuins, canonical components of the GSIS machinery, and insulin further preclude model reliability.

(A-C) Expression of key genes in the CRISPR/Cas9n-generated subclones. (A) mRNA expression of mitochondrial sirtuins: *Sirt3*, *Sirt4*, and *Sirt5*. (B) mRNA expression of GSIS machinery: High K_m glucose transporter (*Glut2*), glucokinase (*Gck*), and subunits of the K_{ATP} channel, *Kir6.2* and *Sur1*. (C) Insulin content and expression of the endogenous rat Insulin-2 (*rIns2*) transcript and the transgenic human insulin (*hINS*) transcript. n=3-6 independent experiments. Data represent mean ± SE.

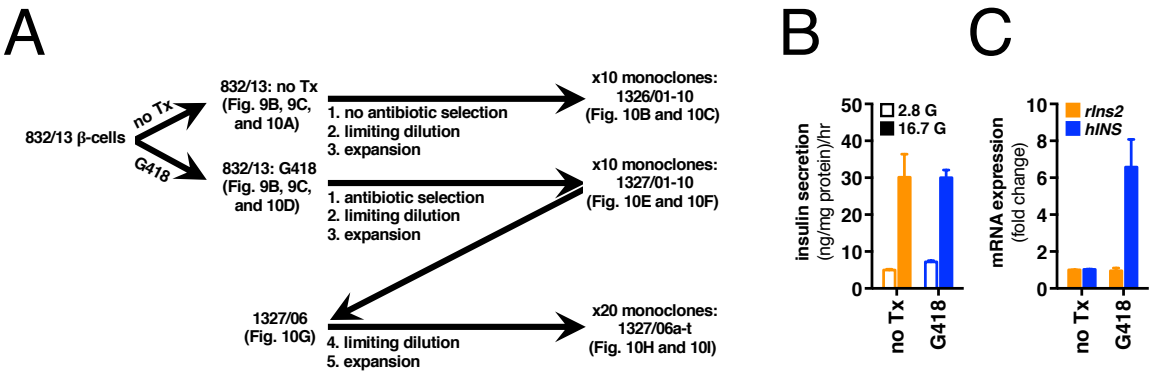

Figure 9: Selection of cells with *hINS* expression yields similar GSIS responses in polyclonal populations.

(A) Outline of experimental strategy used to interrogate clonal functional heterogeneity. (B) Insulin secretion in response to 2.8 mM glucose (2.8 G) or 16.7 mM glucose (16.7 G) in polyclonal parental 832/13 populations either unselected (no Tx) or G418-selected (G418). (C) mRNA expression of *rIns2* and *hINS* in polyclonal parental 832/13-derived cells either unselected (no Tx) or G418-selected (G418). n=3 independent experiments. Data represent mean ± SE.

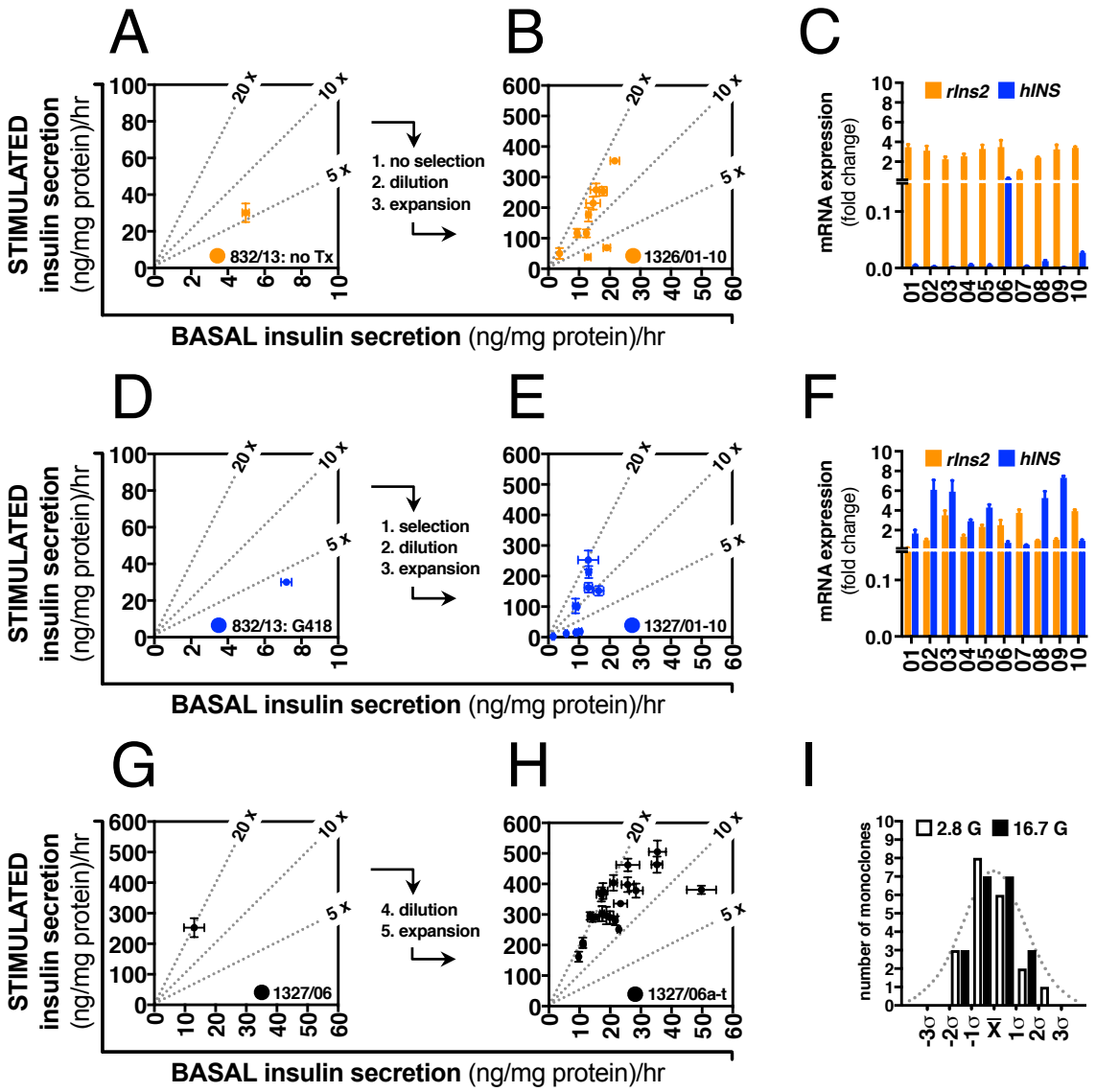

Figure 10: Normally distributed functional heterogeneity independent of intervention confirms subclonal discordance is an inherent byproduct of monoclonal derivation.

(A-C) Unselected (no Tx) 832/13 cells and subclones. (D-F) G418-selected 832/13 cells and subclones. (G-I) Newly derived 1327/06 cells and subclones. (A-B, D-E, and G-H) GSIS. X-axis (BASAL insulin secretion): insulin secretion in response to 2.8 mM glucose. Y-axis (STIMULATED insulin secretion): insulin secretion in response to 16.7 mM glucose. (C and F) mRNA expression *rIns2* and *hINS* in B, unselected subclones (1326/01-10) and E, selected subclones (1327/01-10). (I) GSIS distribution of 1327/06 subclones (1327/06a-t) binned by z-score. n=3 independent experiments. Data represent mean ± SE.

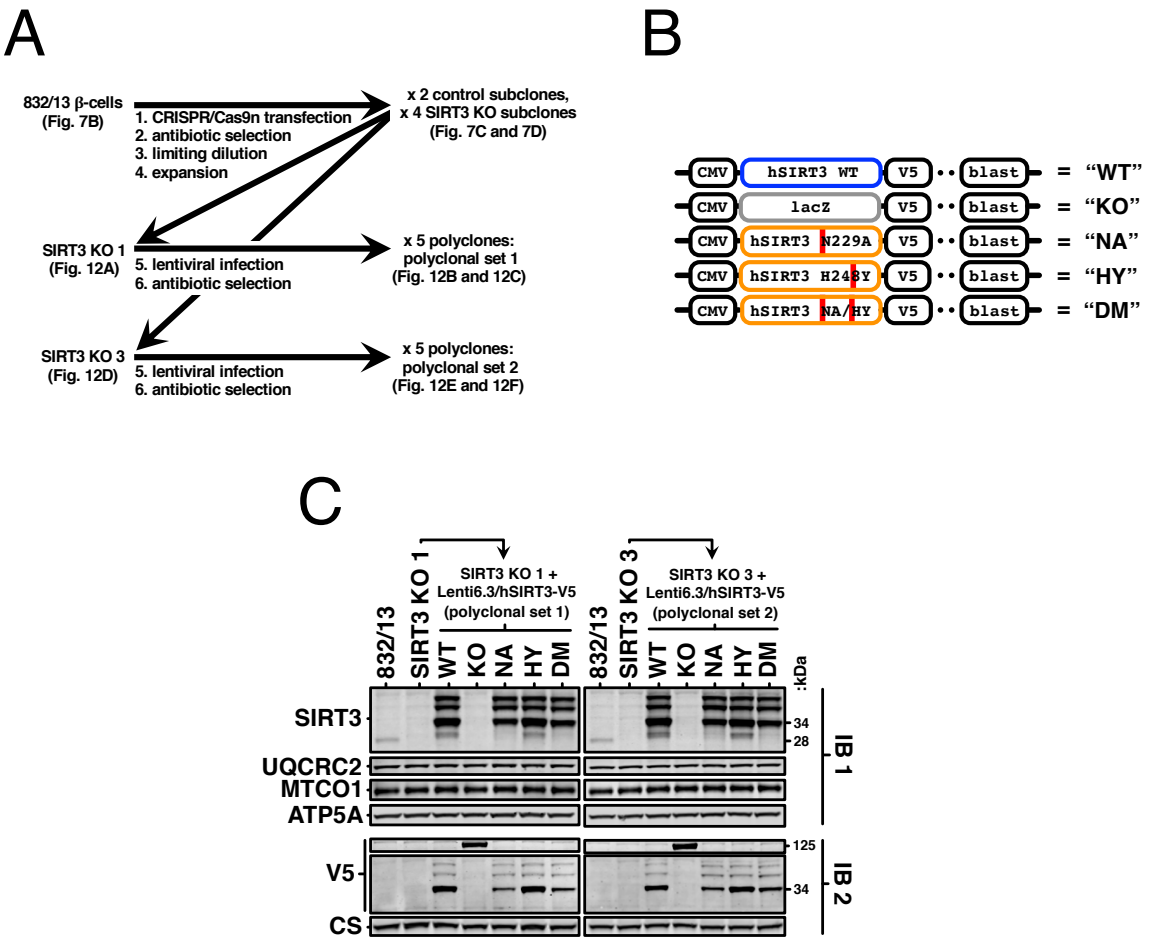

Figure 11: Transgenic overexpression of different forms of SIRT3 in a SIRT3 KO background cell line produces an *in vitro* model with a theoretical maximal delta in SIRT3 expression.

(A) Outline of experimental strategy used to engineer stable cell lines. (B) Diagram of the different lentiviral constructs used to infect SIRT3 KO cells and the corresponding name of resulting polyclonal cell lines. (C) Immunoblot detection of the different overexpressed hSIRT3-V5 fusion proteins or β-Gal-V5, as well as mitochondrial markers (UQCRC2, MTCO1, ATP5A, CS) in 832/13 parental β-cells, SIRT3 KO subclones, and two polyclonal sets of transgenic cell lines: WT—re-expression of catalytically active hSIRT3 WT-V5 in SIRT3 KO line; KO—expression of β-Gal-V5 in SIRT3 KO line; NA—re-expression of catalytically inactive hSIRT3 N229A-V5 mutant in SIRT3 KO line; HY—re-expression of catalytically inactive hSIRT3 H248Y-V5 mutant in SIRT3 KO line; and DM—re-expression of catalytically inactive hSIRT3 NA/HY-V5 double-mutant in SIRT3 KO line.

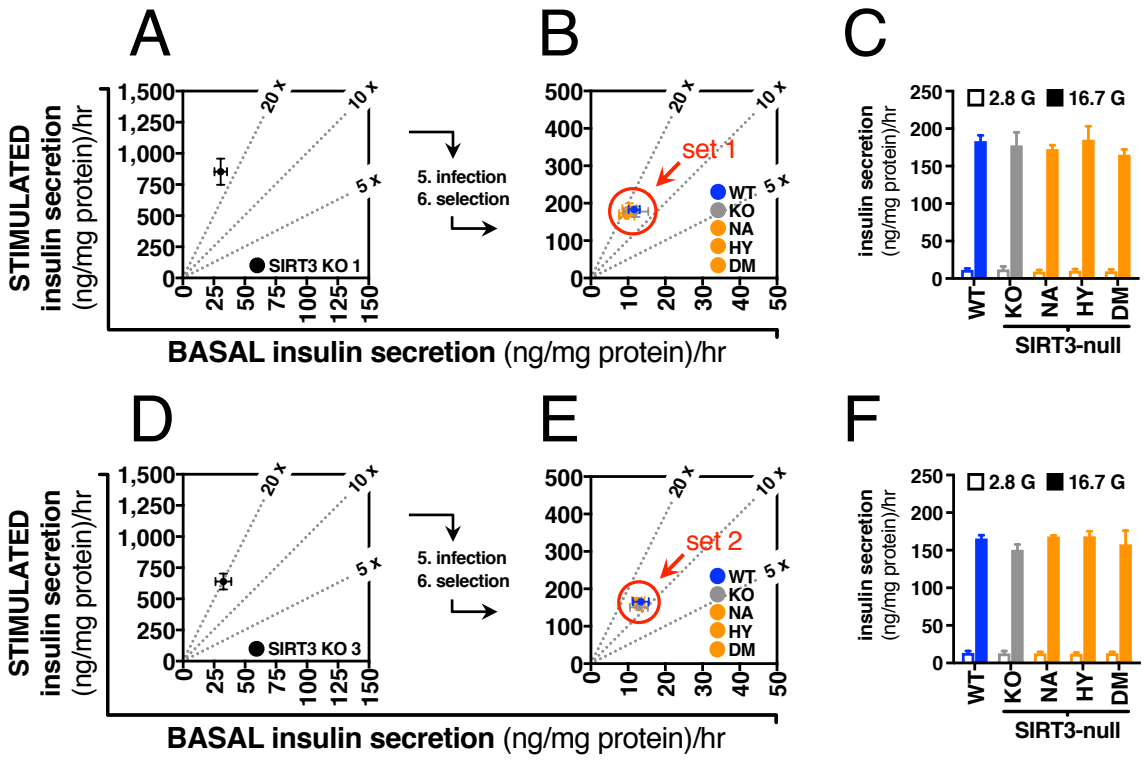

Figure 12: Stable integration of different SIRT3 transgenes in an expanded cell population yields functionally concordant cell lines.

(A-F) GSIS. X-axis (BASAL insulin secretion): insulin secretion in response to 2.8 mM glucose. Y-axis (STIMULATED insulin secretion): insulin secretion in response to 16.7 mM glucose. n=3 independent experiments. Individual points represent one cell line. (C and F) GSIS. Conventional presentation of data from Figure 1B and 1E, respectively. Data are mean ± SE. Statistical comparisons made using a Two-Way ANOVA with Bonferroni's multiple comparisons test. *p≤0.05 effect of cell line.

4. Defining the SIRT3-Targeted Mitochondrial Acetylproteome of the β-cell and its Impact on Fuel-Stimulated Insulin Secretion (FSIS)

We performed preliminary experiments to test the capacity of the two polyclonal sets of cell lines to tolerate serum deprivation for extended time periods in culture. We consistently observed that, under these conditions, polyclonal set 2 adhered more strongly to the bottom of cell culture flasks and plates than polyclonal set 1. Therefore, for experimental practicality, we chose polyclonal set 2 for further study. Additionally, we concluded that further characterization on WT, KO, and one cell line expressing a catalytically inactive form of SIRT3 (NA, HY, or DM) was sufficient. Interestingly, hSIRT3 N229A-V5 and hSIRT3 NA/HY-V5 fusion proteins exhibit banding patterns that are different from the hSIRT3 WT-V5 fusion protein: 1) The 34 kDa band corresponding to the dominant form of epitope-tagged mitochondrial hSIRT3 (Cooper et al., 2009) is less abundant in NA and DM cell lines; and 2) A less abundant 30 kDa band is virtually absent in NA and DM cell lines. We note that the constructs used to engineer these transgenes underwent mutagenesis in independent reactions and were each sequence-verified. Therefore, the differences in expression are likely a product of the N229A mutation found in the hSIRT3 N229A-V5 and hSIRT3 NA/HY-V5. Indeed, data from a previous study shows a similar discrepancy in hSIRT3 N229A-FLAG expression that was not discussed (Schwer et al., 2002). In contrast to the N229A constructs, hSIRT3 H248Y-V5 exhibited an

identical degree of expression as well as the same banding pattern in the HY cell line as hSIRT3 WT-V5 in the WT cell line. As such, the HY cell line was chosen as the best negative control for addressing the specific effects of deacetylase activity in the WT cell line. Simultaneous characterization of the WT, KO, and HY cell lines permits two comparisons (Figure 13). First, compared to KO cells with hyperacetylated mitochondrial proteins, does re-introduction of mitochondrial deacetylase activity via overexpressed hSIRT3 WT-V5 impact β-cell function (comparison 1)? Second, is this impact on β-cell function a product of differences in mitochondrial protein acetylation or due to some other mechanism of SIRT3 overexpression that is independent of deacetylase activity (comparison 2)?

4.1 SIRT3 KO β-cells with Re-Expressed Wild-Type SIRT3 Have Deacetylated Mitochondrial Proteins but No Differences in Fuel-Stimulated Insulin Secretion (FSIS)

SIRT3 is the predominant mitochondrial protein deacetylase (Lombard et al., 2007). To understand how manipulation of SIRT3 expression affected protein acetylation in our engineered β-cell lines, we began by preparing mitochondrial subfractions from each cell line for immunoblot analysis with a pan acetyllysine antibody following culture in three conditions: 1) Standard media (RPMI 1640, INS-1 supplement, 10% FBS), confluent for 1 day; 2) Serum-deprived media (RPMI 1640, INS-1 supplement, 0.5% FBS, 0.2% BSA), confluent for 1 day; and 3) Serum-deprived media (RPMI 1640, INS-1

supplement, 0.5% FBS, 0.2% BSA), confluent for 6 days. As predicted (Figure 13), we observed that when compared to KO cells, WT cells exhibited markedly less mitochondrial protein acetylation, while HY and KO cells had similar acetylation profiles (Figure 14A). We also found that the SIRT3-null cell lines cultured in serum-deprived media for 6 days exhibited global increases in mitochondrial protein acetylation by immunoblot relative to the other culture conditions. Increased acetylation could reasonably be attributed to the lengthened culture time over which acetyl-CoA could non-enzymatically acetylate proteins, as previously proposed (Wagner and Payne, 2013; Weinert et al., 2015). However, we cannot rule out that the increased acetyllysine signal could be influenced by protein abundance, at least for a subset of the immunoblot-detected proteins.

Recent work on GSIS points to important roles for extramitochondrial metabolic pathways including glycolysis, the pentose-phosphate pathway, and cytosolic metabolism of citrate and isocitrate (Ferdaoussi et al., 2015; Huang and Joseph, 2014; Spegel et al., 2013). We therefore studied pyruvate-stimulated insulin secretion (PSIS) in addition to GSIS, reasoning that pyruvate has a more direct path to mitochondrial metabolism that could unveil functional differences in our cell lines with different levels of SIRT3 activity. In β-cells that were confluent for 1 day in either standard culture media or serum-deprived media, we found no differences in insulin secretion in response to 2.8

mM glucose (2.8 G), 1 mM pyruvate (1 P), or 16.7 mM glucose (16.7 G) (Figure 14B). In β-cells that were confluent for 6 days in serum deprived media, the condition that yielded the greatest changes in immunoblot acetyllysine signals in the KO and HY cell lines (Figure 14A), both GSIS and insulin secretion responses to a full pyruvate dose curve (0.063 mM – 10 mM) were identical in all three cell lines (Figure 14C), with no differences in EC50 for pyruvate (Figure 14D).

4.2 Metabolic Pathways that Impart Control Over Fuel-Stimulated Insulin Secretion (FSIS) are Represented in the SIRT3-Targeted Acetylproteome

To further probe the apparent discrepancies between our findings and those reported in the existing literature (Caton et al., 2013; Zhang et al., 2016; Zhou et al., 2017), we next used a large-scale mass spectrometry-based proteomics approach to identify proteins with significant differences in lysine acetylation in the β-cell lines with varying levels of SIRT3 activity. We prepared mitochondria-enriched fractions from WT, KO, and HY cell lines cultured at confluence in serum-deprived media for 6 days and performed TMT-based quantitative acetylproteomics (Figure 15A) using previously described methods (McDonnell et al., 2016). We identified 1,216 acetylpeptides at 1% *qualitative* FDR, which mapped to 1,220 unique sites of acetylation on 539 proteins (representatives from parsimonious protein groups). From the 865 acetylpeptides that contained reliable

quantitative information, we further assessed 626 uniquely acetylated lysines that mapped to 242 validated (MitoCarta 2.0 (Calvo et al., 2016)) mitochondrial proteins (Figure 15B). When compared to the KO cell line, 140 of the 626 unique lysines had a statistically significant decrease in relative acetylation abundance at *quantitative* 10% FDR in the WT β-cell line, while only 1 lysine reached this degree of statistical significance in the HY cell line. Because the one significantly deacetylated lysine in the HY cell line was also identified in the 140 significantly deacetylated lysines in the WT cell line, it was considered a false-positive (well within our estimated 10% quantitative FDR). The remaining 139 sites were defined as SIRT3 targets. We note that multiple proteins exhibited a trend to decrease in the HY cells compared to KO cells. These changes were not statistically significant, but may suggest some residual deacetylase activity in the hSIRT3 HY-V5 mutant. Overall, hSIRT3 WT-V5 significantly deacetylated 139 (22%) of the identified acetylated lysines and thus potentially impacted the function of 81 (33%) of the identified acetylated mitochondrial proteins (Figure 15B). We manually cross-referenced the 81 identified proteins with the UniProt database to assign the proteins to different metabolic pathways (Figure 15C). We found changes in acetylation among proteins critical for mitochondrial energy production in the β-cell including several involved in fatty acid oxidation (FAO), the tricarboxylic acid cycle (TCA), and the electron transport chain (ETC). Additionally, we found proteins that help regulate protein quality control

(PROTEIN QC) and proteins involved in detoxification of reactive oxygen species (ROS detox.). Notably, while GRP78 was not detected in our analysis of mitochondrial enrichments, we did identify K130 of SOD2 as a SIRT3 target (Figure 16E). However, K68 of SOD2, the previously identified site of acetylation (Zhou et al., 2017), was not identified in our analysis. Further breakdown of the SIRT3-targeted pathways (Figure 15C) into their individual protein components illustrates the differences in relative acetylation abundance of unique lysines on specific proteins (Figure 16A-E). In sum, our proteomics approach detected wide-spread differences in acetylation of multiple proteins in important mitochondrial pathways in cell lines engineered for different levels of SIRT3 activity, but these changes had no effect on glucose- or pyruvate-stimulated insulin secretion.

4.3 Manipulation of Mitochondrial Protein Acetylation Has No Impact on the Effect of Glucose to Change Metabolite Levels in the β-cell

The lack of a SIRT3-dependent impact on GSIS or PSIS suggests the possibility that the observed changes in acetylation do not impact glucose metabolism or generation of signaling intermediates required for GSIS. To directly address this possibility, we performed targeted GC/MS- and MS/MS-based metabolic profiling on WT, KO, and HY cell lines during glucose stimulation, by previously described methods (Ferrara et al.,

2008; Jensen et al., 2006). Switching of all three cell lines from 2.8 mM glucose to 16.7 mM glucose and incubation for 2 hours caused robust increases in all measured TCA cycle intermediates (pyruvate, citrate, alpha-ketoglutarate, succinate, fumarate, and malate) (Figure 17A), in agreement with previous work from our group (Jensen et al., 2006). While, when compared to KO cells, the level of α-KG during glucose stimulation was increased by 6.3% in WT cells ($p = 0.045$), and malate was increased by 11.5% and 16.1% in WT and HY cells, respectively ($p=0.034$ and $p=0.002$, respectively), these subtle changes failed to affect insulin secretion. Similarly, among 16 amino acids measured by MS/MS, two were robustly increased by glucose stimulation in all three cell lines (Ala and Glx, a combined measure of glutamate and glutamine), and one was decreased (Asx, a combined measure of aspartate and asparagine), with no glucose-induced changes in the other 13 amino acids, again consistent with our previous findings (Ferdaoussi et al., 2015). When compared to KO cells, Ala levels measured in glucose-stimulated WT cells were 9.2% higher ($p=0.033$), whereas levels of Glx in WT and HY cells were 8.8% and 9.3% higher, respectively ($p=0.05$ and $p=0.036$, respectively) (Figure 17B). In addition, measurement of 20 acylcarnitine species derived from mitochondrial metabolism of glucose, fatty acids, and amino acids, revealed no differences among the cell lines in response to glucose stimulation. All three cell lines exhibited a decrease in levels of the long-chain, fatty acid-derived acylcarnitines C16, C18, and C18:2 in response to glucose stimulation, consistent

with glucose-dependent production of malonyl-CoA to serve as an inhibitor of the CPT1 system that generates long-chain acylcarnitines for β-oxidation (Figure 17C). However, despite the representation of multiple fatty acid oxidation enzymes in the SIRT3-targeted acetylproteome of the β-cell (Figure 15C and 16A), no differences were found in lipid-derived acylcarnitine species among the three cell lines (Figure 17C). Overall, broad changes in mitochondrial protein acetylation in response to manipulation of SIRT3 had minimal impact on responses of mitochondrial metabolites to glucose stimulation.

4.4 Differences in the SIRT3-Targeted Acetylproteome Do Not Impact β-cell Viability or Function in the Presence of Stress-Inducing Agents

Chronic nutrient abundance is a major driver of metabolic diseases and cellular stress. In obesity leading to T2D, islet β-cells can be exposed to chronic hyperlipidemia and gradual elevations in glucose levels. A common *in vitro* model for simulating this stressful environment is culture of β-cell lines or isolated islets in elevated concentrations of glucose and fatty acids, sometimes referred to as "glucolipotoxicity" (Poitout and Robertson, 2008). Several groups have reported that siRNA-mediated suppression of SIRT3 renders β-cells more vulnerable to oxidative and ER stress when cultured in elevated concentrations of palmitate, whereas overexpression of SIRT3 is protective under these same conditions (Kim et al., 2015; Zhang et al., 2016; Zhou et al., 2017). Potential

limitations of these prior studies include the use of siRNA-mediated knockdown for producing only partial suppression of SIRT3, thus allowing for residual deacetylase activity, as well as the aforementioned technical challenges of palmitate treatment described in section 1.8.3. We therefore re-visited the relationship of nutritional stress and SIRT3 with our new panel of cell lines. We cultured WT, KO, and HY cells at confluence in serum-deprived media for 6 days to achieve the remodeling of the acetylproteome defined in Figure 16, then replaced this media with serum-deprived media containing 11.1 mM glucose and either 0.5 mM of a 2:1 mixture of oleate:palmitate (O/P) conjugated to BSA, or BSA alone, for an additional 48 hours. As expected, culture of cells under glucolipotoxic conditions caused a clear impairment of insulin secretion in response to 1 mM pyruvate (1 P) or 16.7 mM glucose (16.7 G) (Figure 18A). However, there were no differences in insulin secretion among the three cell lines, suggesting that management of the SIRT3-targeted acetylproteome is not involved in mediating changes in fuel-stimulated insulin secretion under glucolipotoxic conditions.

We also investigated the impact of SIRT3 on apoptotic signaling in response to nutritional stress and ER stress-inducing agents. Culture of the WT, KO, and HY cell lines under glucoliptoxic conditions caused a trend to increase caspase 3 cleavage in all three cell lines that did not achieve statistical significance (Figure 18B and 18C). To test the effect of an ER stress-inducer, we cultured the three cell lines at confluence in serum-deprived

media for 6 days, and then replaced this media with serum-deprived media containing 10 nM Thapsigargin (Tg) or DMSO for an additional 48 hours. Tg induced a clear increase in cleaved caspase 3 that was of a similar magnitude in the three cell lines (Figure 18B and 18C). These data support the conclusion that manipulation of the SIRT3-targeted acetylproteome does not impact β-cell death in response to glucolipotoxicity or ER stress.

Acetylation of mitochondrial proteins is thought to occur via a non-enzymatic mechanism, proportional to the matrix concentration of acetyl-CoA and length of exposure (Wagner and Payne, 2013; Weinert et al., 2015). In an attempt to maximize generation of acetyl-CoA, and thus non-enzymatic acetylation of proteins, all three cell lines were cultured at confluence in serum-deprived media containing 2.8 mM glucose and 10 mM pyruvate for 12 days. Immunoblot analysis confirmed significant SIRT3-dependent differences in acetylation of multiple proteins under these conditions (Figure 19A and 19B). However, both GSIS and insulin secretion in response to a broad range of pyruvate levels (0.063 mM – 10 mM) remained unchanged (Figure 19C and 19D). Thus, even under conditions of a chronic substrate stress designed to maximize the modifying agent (acetyl-CoA), the presence or absence of SIRT3 had no effect on glucose- or pyruvate-stimulated insulin secretion.

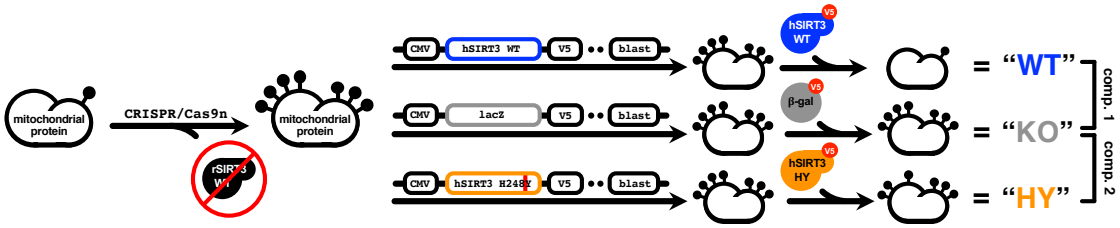

Figure 13: Graphical summary of the model design and the comparisons being made between the transgenic WT, KO, and HY cell lines.

From left to right, Baseline expression of endogenous wild-type SIRT3 (rSIRT3) in the 832/13 β-cell line serves to keep mitochondrial protein acetylation low. CRISPR/Cas9n-dependent disruption of rSIRT3 effectively ablates mitochondrial deacetylase activity, rendering mitochondrial proteins permissive to hyperacetylation. In theory expanded SIRT3 KO 1 and SIRT3 KO 3 β-cells have maximal *in vitro* mitochondrial protein acetylation prior to the transgenic expression of either hSIRT3 WT-V5, β-gal-V5, or hSIRT3 H248Y-V5. Expression of β-gal-V5 serves as the polyclonal surrogate for the starting SIRT3 KO 1 or SIRT3 KO 3 cell lines, to which WT and HY comparisons are made (comparison 1 and comparison 2, respectively). This model provides the unique capacity of ruling out false positive results that are unrelated to deacetylase activity, but are instead related to overexpression of a catalytically inactive SIRT3 protein. An additional advantage of this model is the wide range of SIRT3 expression; virtually absent compared to 70-fold overexpression when compared to endogenous rSIRT3 expression. This provides an extraordinarily large dynamic range over which to study the impact of mitochondrial protein acetylation *in vitro*.

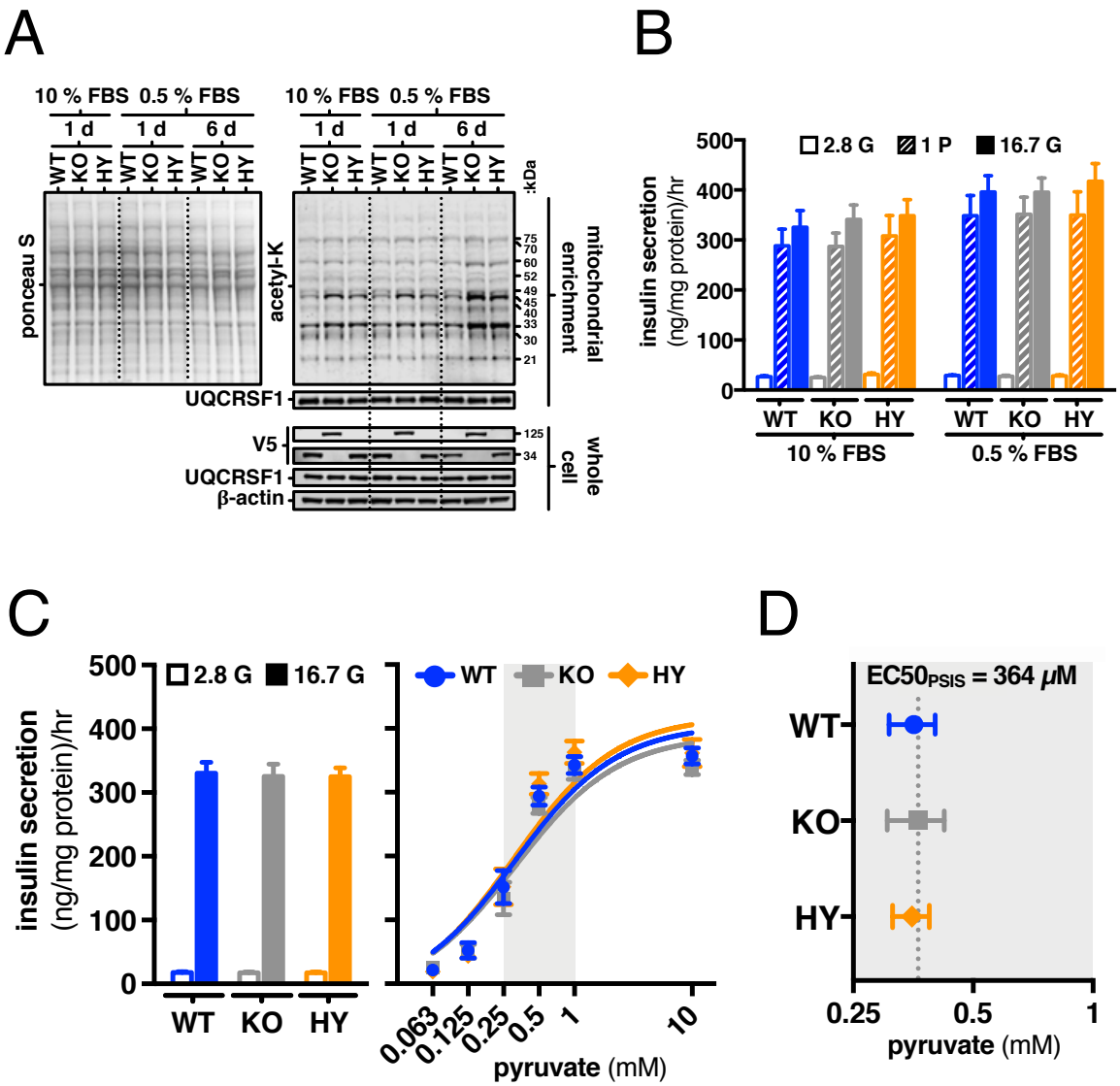
A
10 % FBS
0.5 % FBS
1 d
1 d
6 d
WT
KO
HY
ponceau S
acetyl-K
kDa
75
70
60
52
49
45
40
33
30
21
mitochondrial enrichment
UQCRSF1
V5
125
34
whole cell
UQCRSF1
β-actin
B
2.8 G
1 P
16.7 G
insulin secretion
(ng/mg protein)/hr
500
400
300
200
100
0
WT
KO
HY
10 % FBS
0.5 % FBS
C
2.8 G
16.7 G
insulin secretion
(ng/mg protein)/hr
WT
KO
HY
0.063
0.125
0.25
0.5
1
10
pyruvate (mM)
D
EC50PSIS = 364 μM
0.25
0.5
1
pyruvate (mM)

Figure 14: Differences in mitochondrial protein acetylation are not associated with differences in insulin secretion.

(A) Immunoblot detection of lysine acetylation (acetyl-K) in mitochondrial fractions. Cells cultured at confluence for 1 day (1 d) in either full media or serum-deprived media, or 6 days (6 d) in serum-deprived media. (B) Fuel-stimulated insulin secretion in response to 2.8 mM glucose (2.8 G), 2.8 mM glucose supplemented with 1 mM pyruvate (1 P), or 16.7 mM glucose (16.7 G) following culture at confluence for 1 day in respective culture conditions. n=3 independent experiments. (C) Insulin secretion following 6 days of culture at confluence in serum-deprived media. Left, Insulin secretion in response to 2.8 mM glucose (2.8 G) and 16.7 mM glucose (16.7 G). Right, Pyruvate-stimulated insulin secretion in response to 2.8 mM glucose supplemented with an array of pyruvate doses (63 uM – 10 mM pyruvate). Dose response curves are nonlinear fit [agonist] vs. response. (D) EC50 of PSIS curves in Figure 3*D*. n=3 independent experiments. Data represent means ± SE. Statistical comparisons made using a Two-Way ANOVA with Bonferroni's multiple comparisons test. *$p \leq 0.05$ effect of cell line.

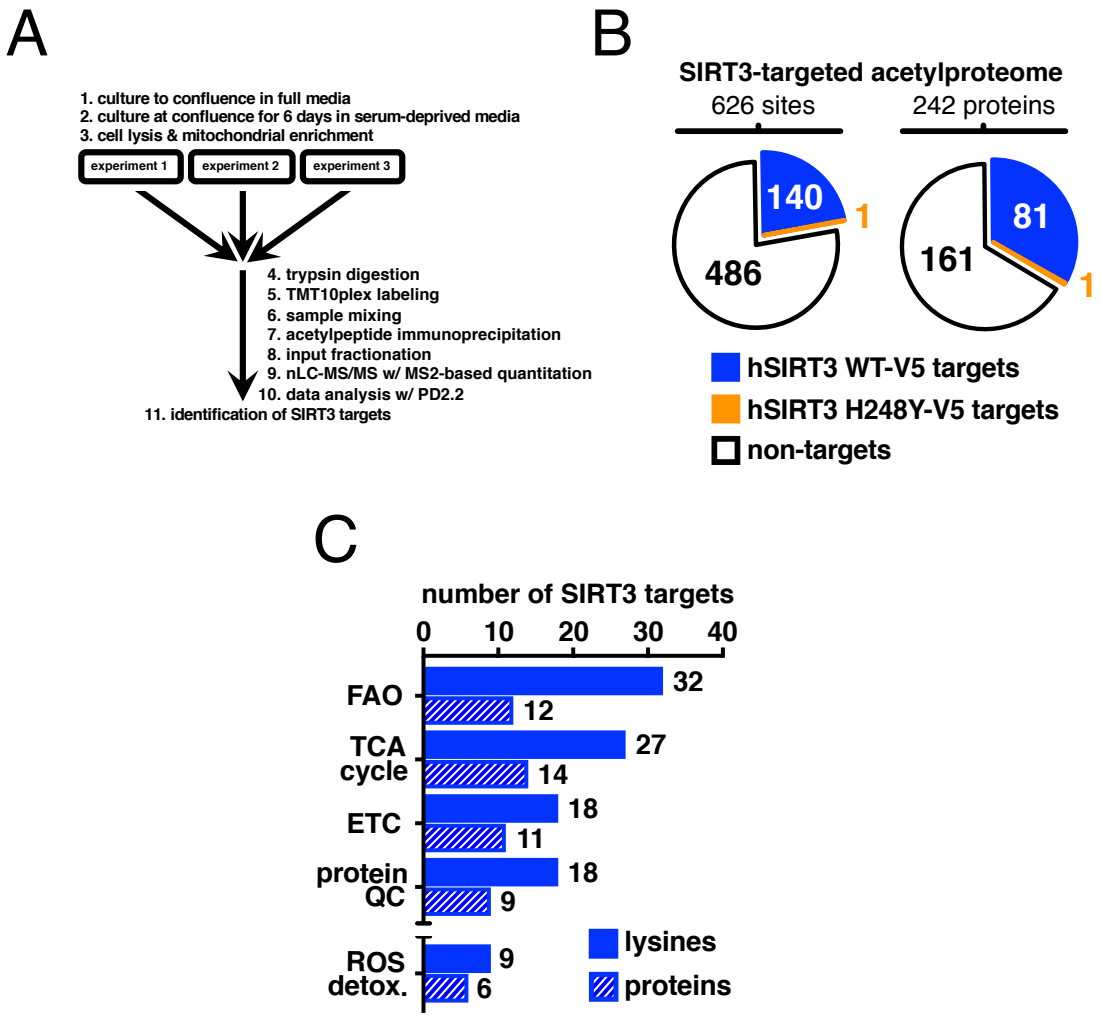

Figure 15: SIRT3 targets 33% of the proteins identified in the mitochondrial acetylproteome of the β-cell.

(A) Outline of the experimental strategy used to generate acetylproteomics data. (B) Summary of results, MS-based analysis of the SIRT3-targeted acetylproteome. Left, Summary of the 626 quantifiable acetyllysines and their significant deacetylation by hSIRT3 WT-V5, but not hSIRT3 H248Y-V5 (with one exception). Right, Summary of the 242 corresponding proteins targeted for deacetylation by hSIRT3 WT-V5 and hSIRT3 H248Y-V5. (C) Number of SIRT3-targeted lysines and proteins/subunits represented in manually identified pathways. Fatty acid oxidation (FAO), the tricarboxylic acid cycle (TCA cycle), the electron transport chain (ETC), protein quality control (PROTEIN QC), and reactive oxygen species detoxification (ROS detox.). n=3 independent experiments.

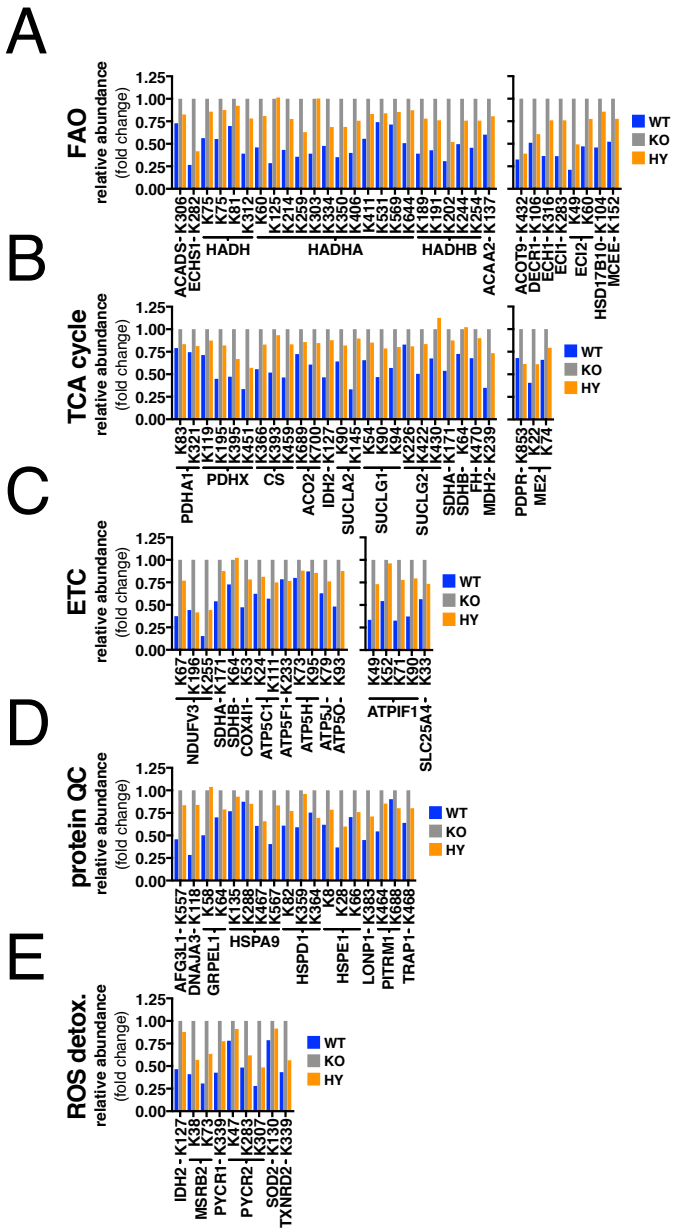

Figure 16: Quantifying acetylation abundance reveals the degree to which SIRT3 deacetylates specific lysines and specific proteins.

(A-E) Acetylation abundance of SIRT3-targeted lysines as defined in Figure 15B and stratified in respective pathways in Figure 15C. Data represented as acetylpeptide abundance relative to lysines in KO cells set to 1. n=3 independently prepped mitochondrial fractions.

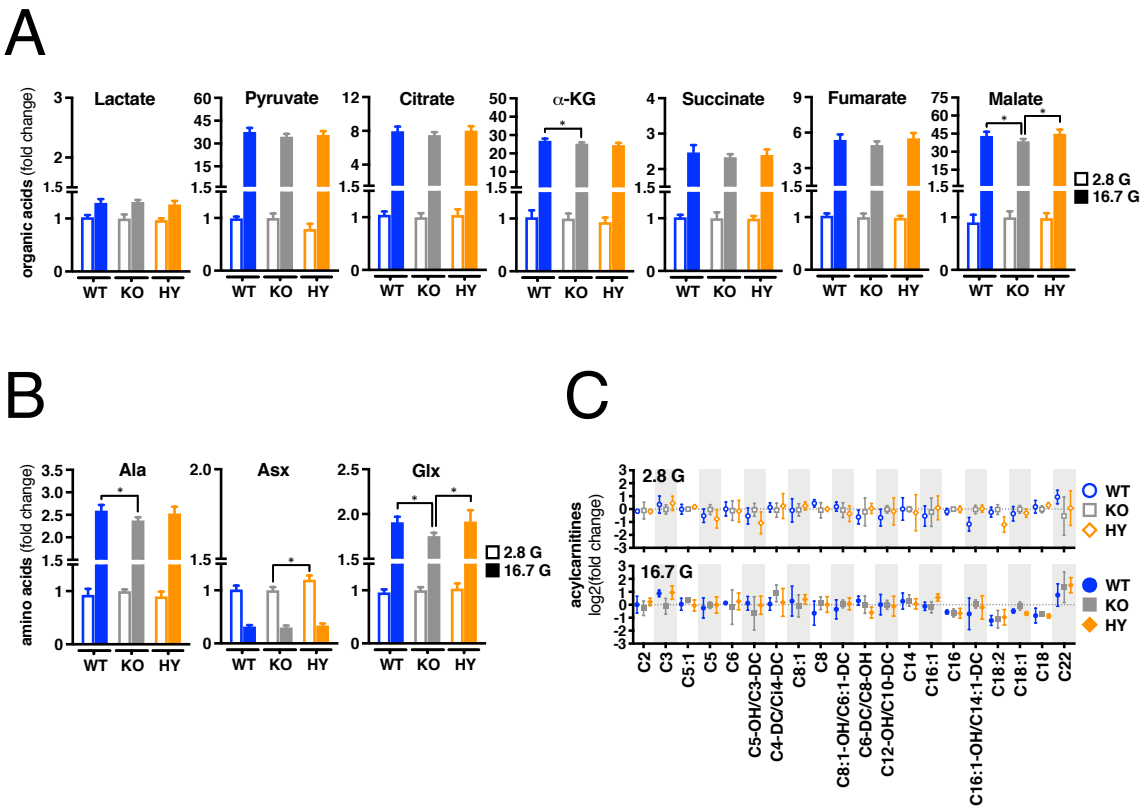

Figure 17: Glucose-stimulated changes in intracellular metabolites are unaffected by changes in the SIRT3-targeted β-cell acetylproteome.

Fold changes of intracellular (A) Organic acids and (B) Amino acids in response to treatment with 2.8 mM glucose (2.8 G) or 16.7 mM glucose (16.7 G); (C) Log2 fold changes of intracellular acylcarnitines in cells exposed to 2.8 mM glucose (2.8 G) or 16.7 mM glucose (16.7 G). Fold change values were normalized to KO cells treated with 2.8 mM glucose (2.8 G) set to 1. n=4 replicates. Data represented as mean ± SE. Statistical comparisons made using a Two-Way ANOVA with Bonferroni's multiple comparisons test. *p≤0.05 effect of cell line.

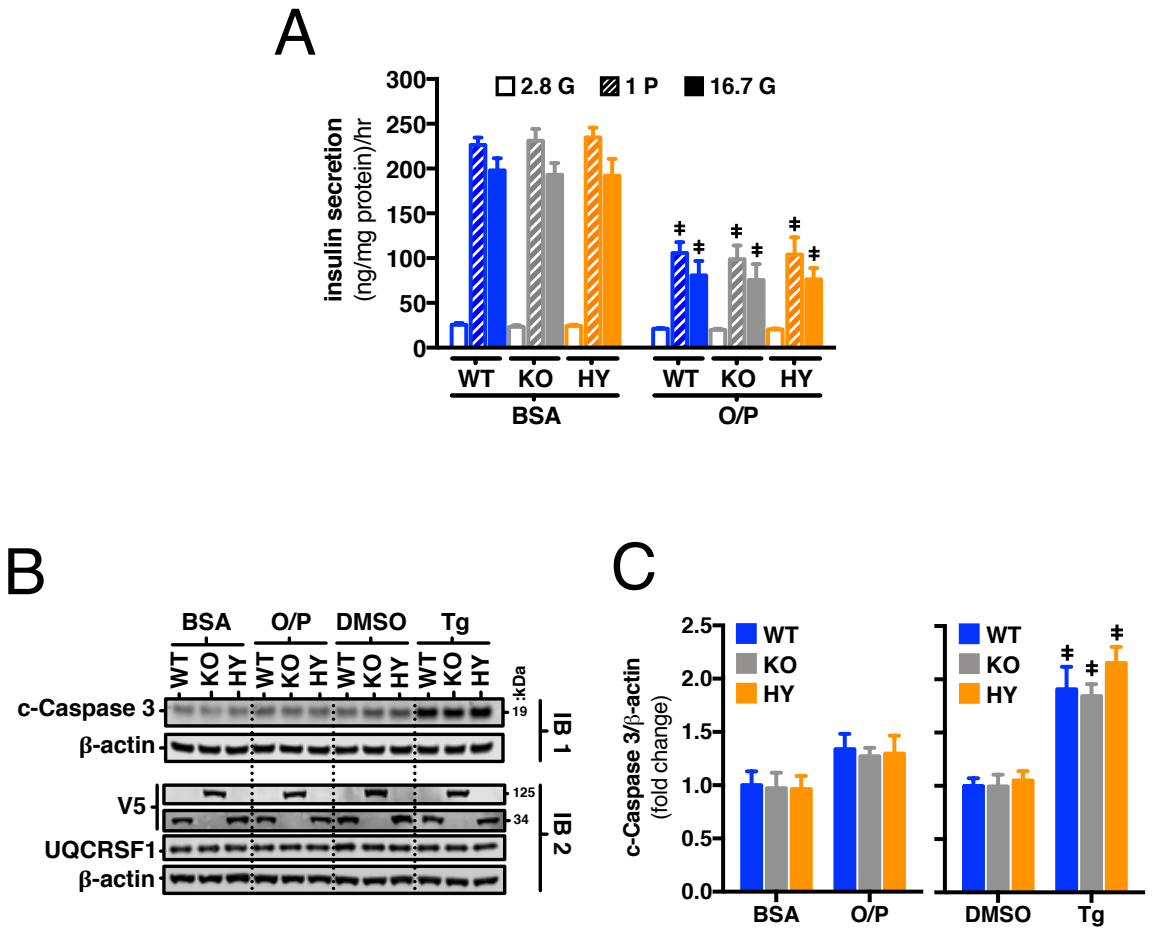

Figure 18: Changes in the SIRT3-targeted β-cell acetylproteome do not affect responses to cell stress agents.

(A) Insulin secretion in response to 2.8 mM glucose (2.8 G), 2.8 mM glucose supplemented with 1 mM pyruvate (1 P), or 16.7 mM glucose (16.7 G) following 48-hour treatment with BSA control (BSA) or 0.5 mM 2:1 oleate/palmitate (O/P) conjugated to BSA. n=3 independent experiments. (B) Immunoblot detection of cleaved caspase 3 (19 kDa) following 48-hour treatment with O/P vs. BSA, or DMSO vs. 10 nM Thapsigargin (Tg). (C) Immunoblot quantification of cleaved caspase 3 expression relative to KO cells set to 1. n=4 independent experiments. Data represent means ± SE. Statistical comparisons made using a Two-Way ANOVA with Bonferroni's multiple comparisons test. ‡p≤0.05 effect of treatment. *p≤0.05 effect of cell line.

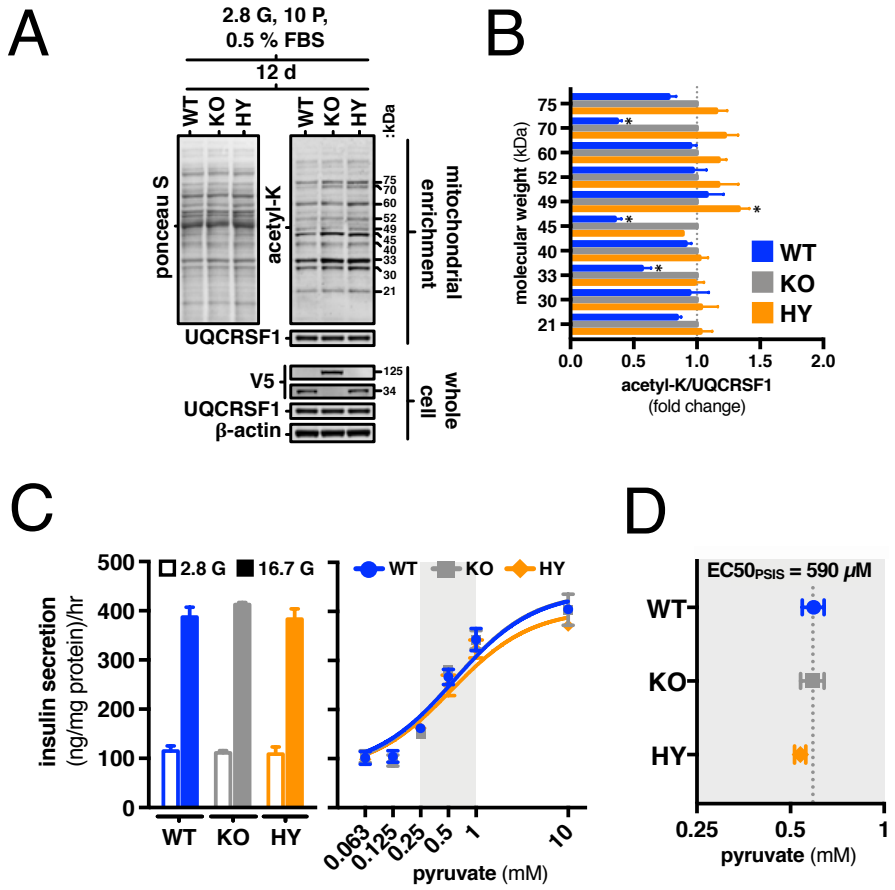

Figure 19: Extended culture in media supplemented with 10 mM pyruvate as a potential acetylating agent does not influence FSIS.

(A) Immunoblot detection of lysine acetylation (acetyl-K) in mitochondria-enriched fractions following 12-day (12 d) culture at confluence in high-pyruvate media. (B) Immunoblot quantification of lysine acetylation in mitochondria-enriched fractions relative to fractions from KO cells set to 1. n=3 independent experiments. (C) Insulin secretion following 12-day (12 d) culture at confluence in high-pyruvate media. Left, GSIS in response to 2.8 mM glucose (2.8 G) and 16.7 mM glucose (16.7 G). Right, Insulin secretion in response to 2.8 mM glucose supplemented with a range of pyruvate doses (63 uM – 10 mM). Dose response curves are nonlinear fit [agonist] vs. response. (D) EC50 of pyruvate response curves in Figure 3D. n=3 independent experiments. Data represent means ± SE. Statistical comparisons made using a Two-Way ANOVA with Bonferroni's multiple comparisons test. ‡p≤0.05 effect of treatment. *p≤0.05 effect of cell line.

5. Interrogating the Impact of Global SIRT3 Loss *in vivo* Under Conditions of Standard Nutrition and Chronic Overnutrition

Global SIRT3 KO mice have been widely used in defining the impact of mitochondrial protein acetylation on physiology. Prior to our study, studies of SIRT3 KO mice had been reported in the C57Bl/6 or 129Sv backgrounds. Early work examining C57Bl/6 global SIRT3 KO animals fed a standard chow diet reported these animals to be glucose intolerant compared to their wild-type (WT) controls at 24 weeks of age (Jing et al., 2011). Studies with the 129Sv global SIRT3 KO animals fed a standard chow diet showed identical glucose tolerance compared to their WT controls at 3 months of age, but glucose intolerance at 12 months of age (Hirschey et al., 2011). These data suggest that the duration of gene ablation or the aging process may mediate a SIRT3-dependent effect on metabolic dysregulation.

The addition of a nutrient-dense, high-fat/high-carbohydrate (primarily sucrose) diet, often referred as a "Western" diet accelerates the development of metabolic phenotypes in the 129Sv SIRT3 KO animal (Hirschey et al., 2011). In fact, when fed a nutrient-dense diet, SIRT3 KO animals exhibit increased insulin secretion, consistent with a diet-induced β-cell adaptive response, and insulin resistance at just 3 months of age when compared to WT controls. These differences become more dramatic at 12 months of age following 55 weeks of overnutrition. More recently, Lantier and colleagues (Lantier et

al., 2015) have demonstrated insulin resistance in 15-week old SIRT3 KO animals having been fed a nutrient-dense diet for 12 weeks. Based on this literature, it is challenging to dissect the relative contributions of strain background, chronic overnutrition and/or aging on SIRT3-dependent metabolic phenotypes, necessitating further studies.

Before beginning our own study on global SIRT3 knockout mice, we needed to address a potential confounding variable. Because SIRT3 KO animals were backcrossed onto the C57Bl/6 strain from The Jackson Laboratory, now referred to as the C57Bl/6J line, these animals harbored a mutation in the nicotinamide nucleotide transhydrogenase (*Nnt*) gene (Toye et al., 2005). The NNT enzyme catalyzes the reaction $NADH + NADP^+ \rightarrow NAD^+ + NADPH$ in the mitochondria. Critically, we recognized that the reaction's end products had the potential to impact mitochondrial protein acetylation in the pancreatic β-cell by limiting the NAD^+-dependent activity of SIRT3 (Schwer et al., 2002) and/or impairing NADPH-mediated GSIS (Ferdaoussi et al., 2015). Indeed, a side-by-side comparison of C57Bl/6 animals from The Jackson Laboratory (C57Bl/6J) reveals a defective insulin secretion response when compared to C57Bl/6 animals from the National Institutes of Health (NIH) that do not harbor the *Nnt* mutation (C57Bl/6N) (Fergusson et al., 2014). As such, we concluded that the best model in which to study SIRT3 and mitochondrial protein acetylation must contain wild-type *Nnt*. We therefore bred C57Bl/6J SIRT3 KO mice with C57Bl/6N wild-type mice purchased from The Jackson Laboratory (C57Bl/6NJ)

to produce C57Bl/6J breeders that were homozygous for the wild-type *Nnt* allele. The resulting animals used for study are referred to as "C57Bl/6J/*Nnt* wild-type" (Figure 20A and 20B).

5.1 Effects of Global SIRT3 Knockout on Insulin Secretion and Glycemic Control in Mice Fed STD or HFHS Diets are Modest

In order to examine the impact of global SIRT3 loss on islet function during the pathogenesis of metabolic disease leading to T2D, we designed a diet-induced obesity (DIO) study. We fed 11-14-week-old wild-type (WT) and SIRT3 knockout (SIRT3 KO) mice in the aforementioned C57Bl/6J/*Nnt* wild-type background either a standard chow (STD) or high-fat/high-sucrose (HFHS) diet for 12 weeks. At study end, the body weights of the HFHS diet-fed animals were significantly increased compared to the STD diet-fed animals, with no significant difference between genotypes. HFHS diet-fed mice had significant elevations in circulating glucose levels following 5 or 16 hours of fasting compared to STD diet-fed animals, again with no significant difference between genotypes. Interestingly, HFHS diet-feeding resulted in significant fasting hyperinsulinemia in WT animals, with only a trend to increase insulin levels in HFHS diet-fed SIRT3 KO animals, resulting in a genotype-dependent difference (Table 7).

We performed immunoblot analysis of pancreatic islets pooled from SIRT3 KO and WT mice with an acetyllysine antibody. These experiments revealed that islets from

SIRT3 KO mice had increased protein acetylation. This was true for islets from animals fed either the STD diet or the HFHS diet (Figure 21). Additionally, islets from SIRT3 KO, HFHS diet-fed mice exhibited modest increases in acetylation compared to islets from SIRT3 KO, STD diet-fed animals.

Glucose tolerance tests were performed to assess insulin secretion *in vivo*. In animals fed the STD diet, no genotype-specific differences were found in glucose or insulin excursions in response to oral or intraperitoneal glucose tolerance testing (oGTT and ipGTT, respectively) (Figure 22A and 22B). There were also no genotype-specific differences in insulin sensitivity as measured by an insulin tolerance test (ITT) (Figure 22C). Mice fed the HFHS diet had clear glucose intolerance and insulin resistance compared to mice fed the STD diet, but again with no genotype-specific differences (Table 7, Figure 23A-23C). However, HFHS diet-feeding did reveal lower insulin levels in SIRT3 KO mice in response to ipGTT, but not oGTT (Figure 23A and 23B), due mainly to a significant decrease in fasting insulin in these animals (Table 7). However, this impairment did not impact glycemic control during oGTT or ipGTT (Figure 23A and 23B, respectively).

5.2 Islets from SIRT3 KO Animals Fed a STD Diet Exhibit Normal Insulin Secretion, whereas Islets from SIRT3 KO Animals Fed a HFHS Diet Secrete Less Insulin in Response to a Wide Array of Secretagogues

Finally, as a direct measure of islet function in response to global SIRT3 deletion, we performed islet perifusion experiments using sixty size-matched islets isolated from individual animals from each cohort. We tested insulin secretion in response to stimulatory glucose and in the presence and absence of known potentiators of insulin secretion, including fatty acids, GLP-1, and GIP. SIRT3 KO islets from animals fed a STD diet secreted modestly but not significantly more insulin compared to their WT controls in response to all conditions in the perifusion, with the exception of a statistically significant increase in response to the depolarizing agent KCl (Figure 24A and 24B). In contrast, islets from SIRT3 KO, HFHS diet-fed animals secreted significantly less insulin compared to their WT controls in response to all secretagogues studied (Figure 25A and 25B), in agreement with the impaired insulin secretion observed during the ipGTT (Figure 23B).

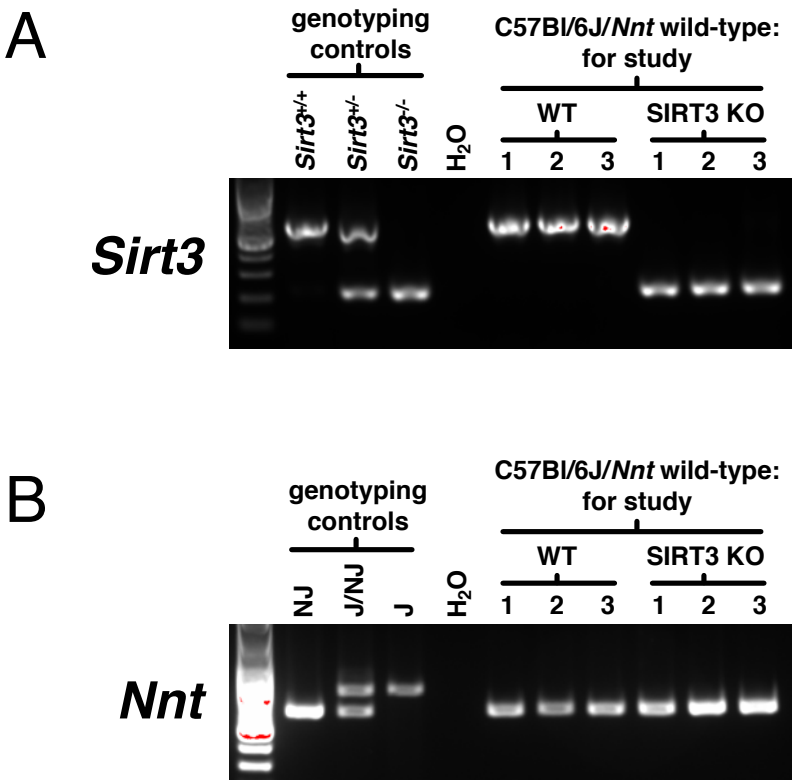

Figure 20: Genotyping confirms the presence of wild-type *Nnt* in the mouse line generated for study.

Genotyping of (A) *Sirt3* alleles and (B) *Nnt* alleles. (A) *Sirt3*$^{+/+}$, *Sirt3*$^{+/-}$, and *Sirt3*$^{-/-}$ genotyping controls are homozygous wild-type, heterozygous, or homozygous knockout, respectively. (B) *Nnt* in the C57Bl/6-NJ, -J/NJ, and -J genotyping controls is homozygous wild-type, heterozygous, or homozygous mutant respectively.

Table 7: Summary of diet-induce obesity (DIO) study.

Static metabolic phenotypes of SIRT3 KO and wild-type (WT) mice fed a standard chow or high-fat/high-sucrose (HFHS) diet. ‡p≤0.05 effect of diet. *p≤0.05 effect of genotype.

study design and summary

diet	standard chow (STD)		high-fat/high-sucrose (HFHS)	
genotype	WT (*N*=13)	SIRT3 KO (*N*=12)	WT (*N*=14)	SIRT3 KO (*N*=10)
study start age (weeks)	11-14	11-14	11-14	11-14
duration of HFHS diet-feeding (weeks)	-	-	12	12

body weight

study start (g)	25.95 ± 0.40	26.71 ± 0.61	26.74 ± 0.53	25.95 ± 0.58
study end (g)	29.48 ± 0.42	30.70 ± 0.67	40.86 ± 1.25‡	38.48 ± 0.85‡

blood glucose (study end)

5-hour fasting (mg/dL)	123.15 ± 5.34	121.58 ± 7.40	200.14 ± 15.01‡	203.30 ± 12.16‡
16-hour fasting (mg/dL)	68.00 ± 2.23	78.25 ± 2.08	108.36 ± 6.45‡	100.20 ± 5.50‡

plasma insulin (study end)

5-hour fasting (ng/mL)	0.27 ± 0.04	0.25 ± 0.07	1.92 ± 0.41‡	0.96 ± 0.16*

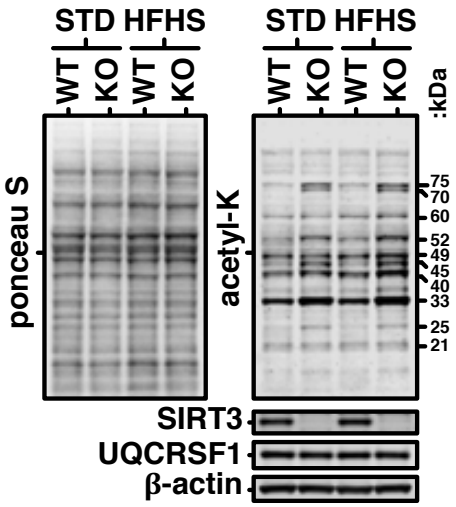

Figure 21: Isolated islets from SIRT3 KO animals exhibit hyperacetylated proteins under both the STD diet-fed and HFHS diet-fed conditions.

Immunoblot detection of lysine acetylation and SIRT3 in isolated islets pooled from SIRT3 KO and wild-type mice fed on STD or HFHS diets. n=3-5 animals per group.

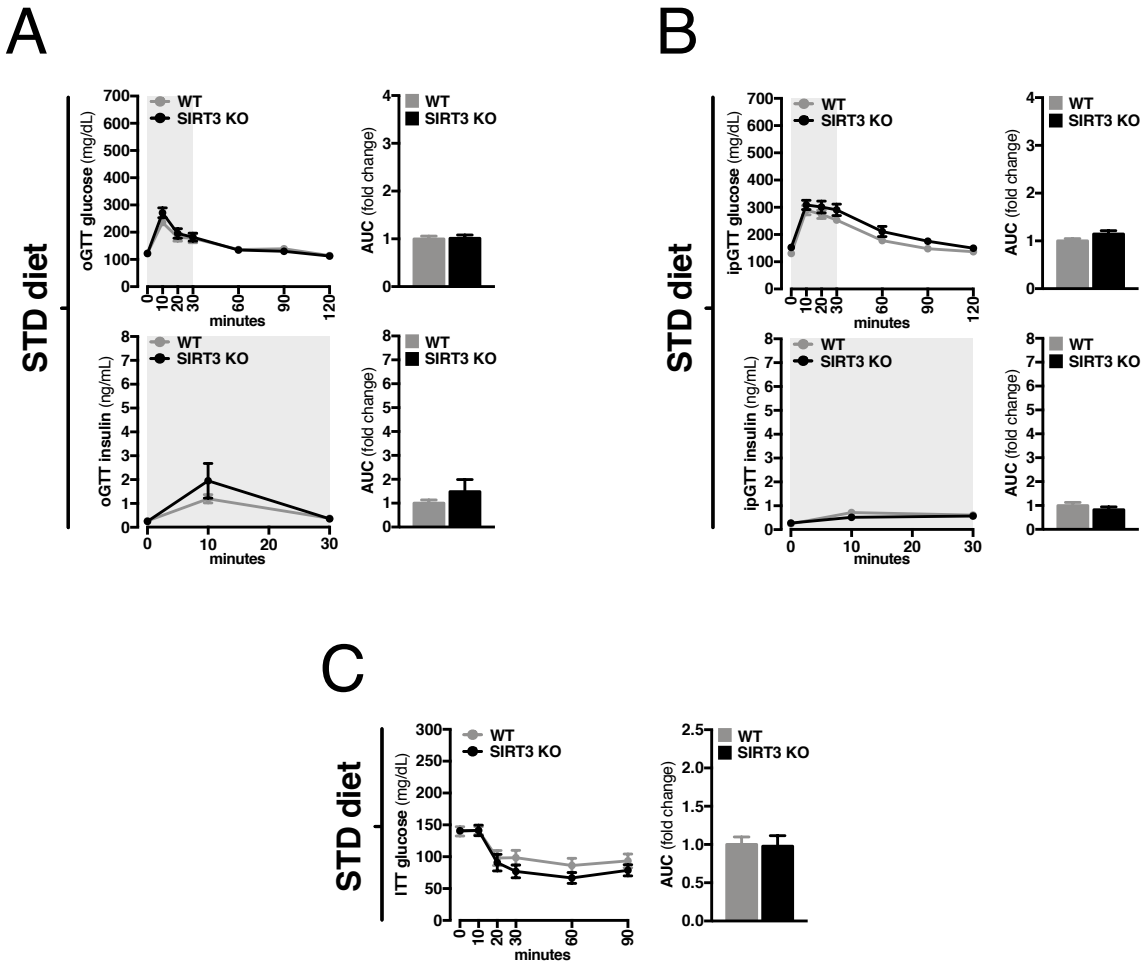

Figure 22: Global SIRT3 deletion does not impair glucose tolerance or insulin tolerance in mice fed a STD diet.

(A) Changes in glucose and insulin levels during an oral glucose tolerance test (oGTT) in STD diet-fed mice. (B) Changes in glucose and insulin levels during an intraperitoneal glucose tolerance test (ipGTT) in STD diet-fed mice. (C) Changes in glucose levels during an insulin tolerance test (ITT) in STD diet-fed SIRT KO and wild-type mice.

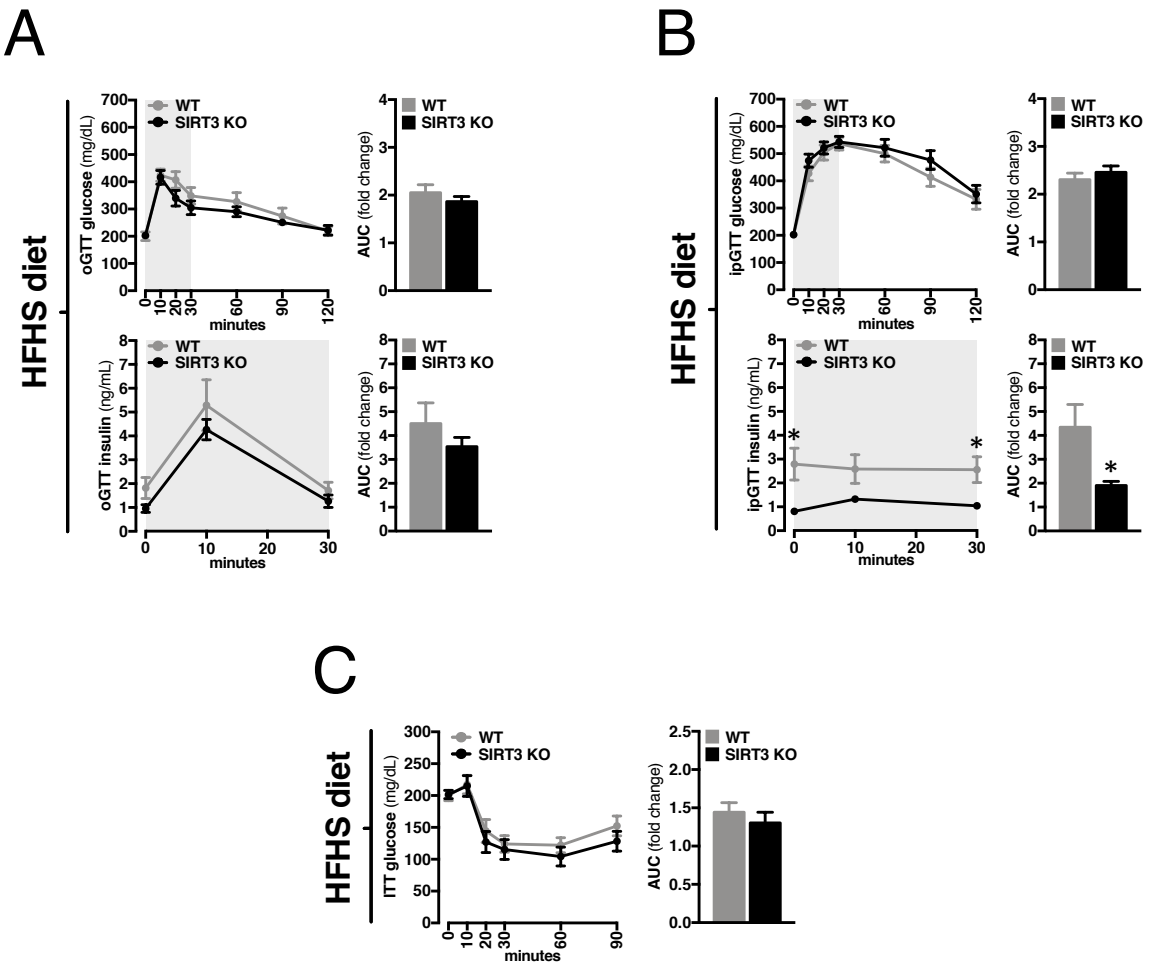

Figure 23: Global SIRT3 deletion does not impair glucose tolerance or insulin tolerance in mice fed a HFHS diet, despite a modest difference in the plasma insulin response following an intraperitoneal (IP) glucose bolus.

(A) Changes in glucose and insulin levels during an oral glucose tolerance test (oGTT) in HFHS diet-fed SIRT3 KO and wild-type mice. (B) Changes in glucose and insulin levels during an intraperitoneal glucose tolerance test (ipGTT) in HFHS diet-fed SIRT3 KO and wild-type mice. (C) Changes in glucose levels during an insulin tolerance test (ITT) in HFHS diet-fed SIRT3 KO and wild-type mice.

A

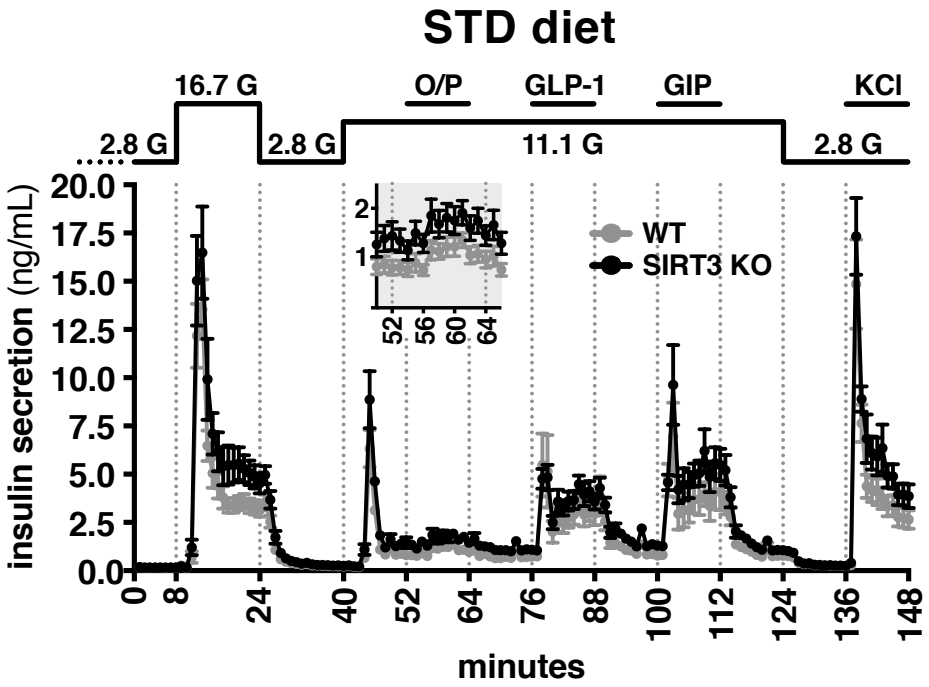
STD diet
16.7 G
O/P
GLP-1
GIP
KCl
2.8 G
2.8 G
11.1 G
2.8 G
WT
SIRT3 KO
insulin secretion (ng/mL)
minutes

B

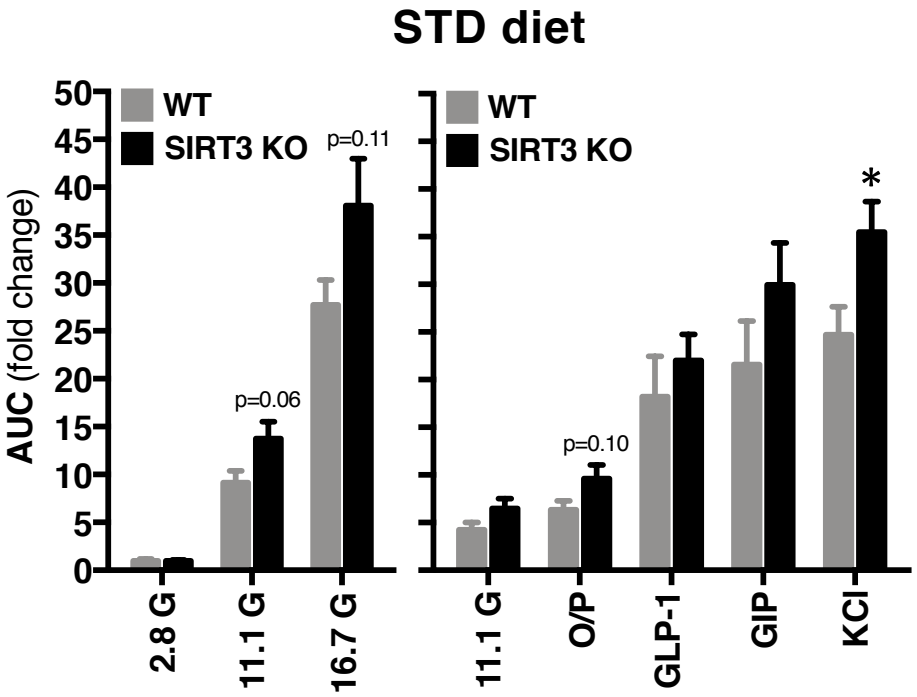
STD diet
WT
SIRT3 KO
p=0.11
p=0.06
p=0.10
*
AUC (fold change)
2.8 G
11.1 G
16.7 G
11.1 G
O/P
GLP-1
GIP
KCl

Figure 24: Perifusion of islets isolated from mice fed a STD diet reveals that insulin secretion in response to multiple secretagogues and potentiators is largely unchanged by global deletion of SIRT3.

(A-B) Perifusion of islets isolated from STD diet-fed mice. (A) Insulin samples collected in 1-minute intervals. Inset shows potentiation of GSIS by O/P. Chambers loaded with sixty size-matched islets from a single animal. (B) AUC of islet perifusion results shown in A. All islets perifused with the following series of conditions: 2.8 mM glucose (2.8 G), 16.7 mM glucose (16.7 G), 11.1 mM glucose (11.1 G), 11.1 G + 0.5 mM oleate/palmitate (O/P), 11.1 G + 0.03 nM GLP-1 (GLP-1), 11.1 G + 0.3 nM GIP (GIP), or 2.8 G + 30 mM KCl (KCl). WT, n=8, SIRT3 KO, n=11. (B) Relative AUC for the islet perifusion insulin secretion response calculated with STD diet-fed WT animals set to 1. Data represent mean ± SE. Statistical comparisons of AUC analyses made using a Two-Way ANOVA with Bonferroni's multiple comparisons test. *$p \leq 0.05$ effect of genotype.

A

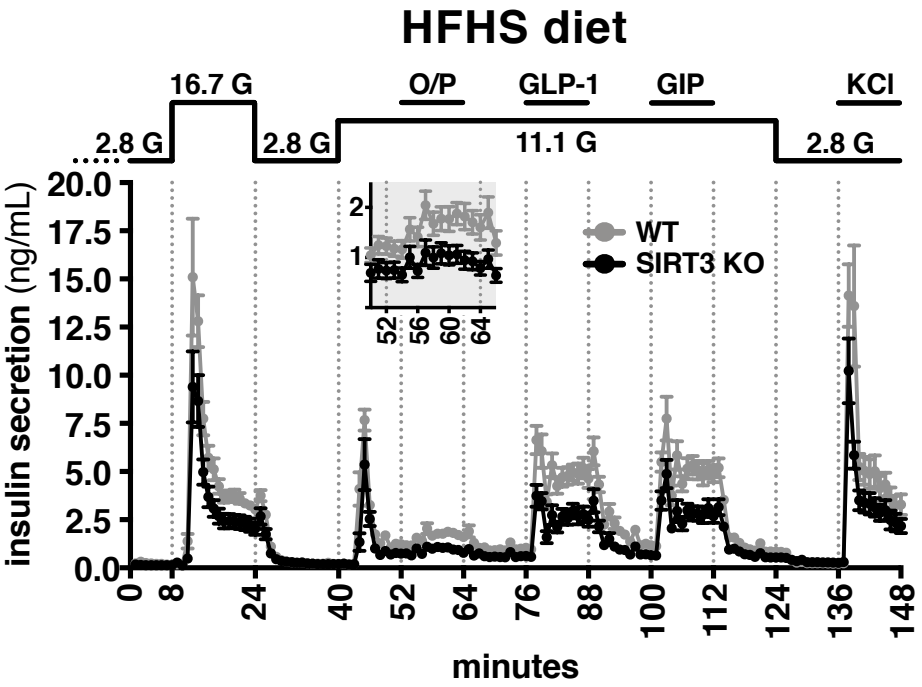
HFHS diet
16.7 G
O/P
GLP-1
GIP
KCl
2.8 G
2.8 G
11.1 G
2.8 G
insulin secretion (ng/mL)
20.0
17.5
15.0
12.5
10.0
7.5
5.0
2.5
0.0
WT
SIRT3 KO
0
8
24
40
52
64
76
88
100
112
124
136
148
minutes

B

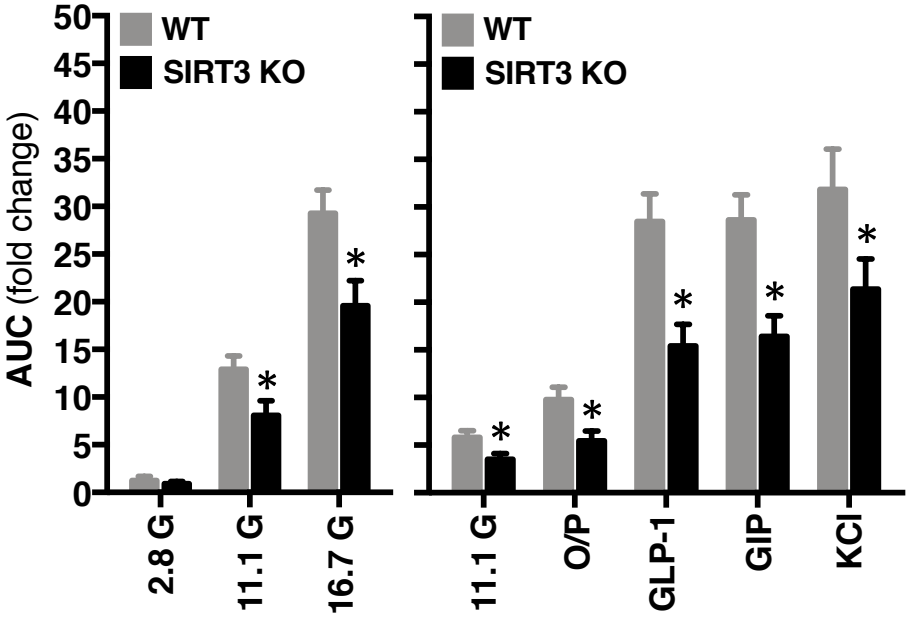
HFHS diet
WT
SIRT3 KO
AUC (fold change)
50
45
40
35
30
25
20
15
10
5
0
2.8 G
11.1 G
16.7 G
O/P
GLP-1
GIP
KCl

Figure 25: Perifusion of islets isolated from mice fed a HFHS diet reveals that SIRT3 KO mice secrete less insulin in response to multiple secretagogues and potentiators.

(A-B) Perifusion of islets isolated from HFHS diet-fed mice. (A) Insulin samples collected in 1-minute intervals. Inset shows potentiation of GSIS by O/P. Chambers loaded with sixty size-matched islets from a single animal. (B) AUC of islet perifusion results shown in A. All islets perifused with the following series of conditions: 2.8 mM glucose (2.8 G), 16.7 mM glucose (16.7 G), 11.1 mM glucose (11.1 G), 11.1 G + 0.5 mM oleate/palmitate (O/P), 11.1 G + 0.03 nM GLP-1 (GLP-1), 11.1 G + 0.3 nM GIP (GIP), or 2.8 G + 30 mM KCl (KCl). WT, n=10, SIRT3 KO, n=10. (B) Relative AUC for the islet perifusion insulin secretion response calculated with STD diet-fed WT animals set to 1. Data represent mean ± SE. Statistical comparisons of AUC analyses made using a Two-Way ANOVA with Bonferroni's multiple comparisons test. *$p \leq 0.05$ effect of genotype.

6. Discussion

Previous studies have implicated the mitochondrial deacetylase, SIRT3, in regulation of β-cell function and survival (Caton et al., 2013; Kim et al., 2015; Zhang et al., 2016; Zhou et al., 2017). However, these studies did not include analyses of global changes in mitochondrial protein acetylation, or effects on metabolism, a major mechanism through which SIRT3 is presumed to exert its biological effects (Baeza et al., 2016). The goal of our study was to fill this void and define the role of the SIRT3-targeted acetylproteome as it pertains to β-cell metabolism and fuel-stimulated insulin secretion. To address these issues, we performed *in vitro* studies with a unique set of cell lines in which CRISPR/Cas9n technology (Ran et al., 2013) was used to completely eliminate endogenous SIRT3 (in contrast to previous studies, which were performed in partial siRNA or shRNA knockdown models), followed by stable overexpression of active or inactive forms of the enzyme. Key findings of the *in vitro* studies were: 1) Manipulation of SIRT3 expression results in clear changes in acetylation of a broad group of mitochondrial enzymes involved in fatty acid oxidation, the TCA cycle, the electron transport chain, and other pathways; 2) These differences had negligible effects on glucose-induced changes in an array of mitochondrial metabolites measured by GC/MS and MS/MS; 3) Glucose and pyruvate-stimulated insulin secretion responses were identical across the full panel of engineered cell lines despite significant differences in mitochondrial protein acetylation;

and 4) Global differences in the SIRT3-targeted acetylproteome did not affect responses to β-cell stress-inducing agents.

In addition, studies in our new global SIRT3 KO, *Nnt* wild-type mouse model revealed that: 1) Acetylation of multiple proteins was increased in islets obtained from SIRT3 KO compared to WT mice, in both the STD diet- and HFHS diet-settings; 2) When fed the STD diet, SIRT3 KO mice given an oral or IP glucose load exhibited glucose excursions and insulin secretion responses indistinguishable from those of WT mice; 3) When fed the HFHS diet, a nutritional stress that caused clear glucose intolerance in both genotypes, SIRT3 KO and WT mice have identical glucose excursions following either an oral or IP glucose load. Despite the identical glucose tolerance curves, insulin levels were lower in SIRT3 KO mice compared to WT mice during the ipGTT, but not the oGTT; and 4) Perifusion studies with islets isolated from both the STD diet- and HFHS diet-fed cohorts corroborated the *in vivo* findings. Thus, there were no significant differences in insulin secretion in islets from SIRT3 KO compared to WT mice fed the STD diet, except for a modest increase in the response to the general depolarizing agent KCl in islets from SIRT3 KO mice. In contrast, islets from SIRT3 KO mice fed the HFHS diet secreted less insulin in response to all secretagogues and potentiators studied, including glucose, fatty acids, GLP-1, GIP, and KCl, relative to islets from WT mice fed the HFHS diet.

Our findings contrast in some respects with those in the literature. For example, partial suppression of SIRT3 in the INS-1 or NIT-1 β-cell lines via siRNA transfection reportedly resulted in increased ROS production and markers of ER stress, decreased cell viability, activation of apoptosis, impaired insulin secretion, and exacerbated palmitate-induced dysfunction (Caton et al., 2013; Zhang et al., 2016). In another study, stable expression of a SIRT3-directed shRNA in the MIN-6 β-cell line decreased glucose-stimulated ATP content, impaired GSIS, and also increased susceptibility to palmitate-induced dysfunction (Zhou et al., 2017). In related studies, overexpression of SIRT3 by plasmid transfection or adenoviral transduction protected insulinoma cells against palmitate-induced dysfunction (Kim et al., 2015; Zhang et al., 2016; Zhou et al., 2017). However, these studies did not report the effects of SIRT3 manipulation on intermediary metabolism. Moreover, with the exception of GRP78 (Zhang et al., 2016) and SOD2 (Zhou et al., 2017), the extent to which partial, siRNA- or shRNA-mediated suppression of SIRT3 expression altered mitochondrial protein acetylation was not investigated. In our own studies with partial siRNA-mediated suppression of SIRT3 in the 832/13 β-cell line, we found little, if any change in mitochondrial protein acetylation measured by anti-acetyllysine immunoblotting, suggesting that incomplete and transient SIRT3 knockdown may not be a reliable approach for assessing the role of protein acetylation in islet cell function. Also, the specificity of the siRNA and shRNA constructs used in the prior studies

was not detailed, opening the possibility that the reported changes in β-cell function could have been due to off-target effects. Finally, the changes in function reported in previous work using stably expressed shRNA constructs (Zhou et al., 2017) could have been driven by clonal variability, as we encountered in the current work and overcame by genetic engineering in polyclonal cell populations. We conclude that the current study, in which we engineered a broad range of SIRT3 activity levels, coupled with large-scale acetylproteomics and targeted metabolomics analyses, provides the first in-depth assessment of the impact of SIRT3 on β-cell function and stress responses. The main conclusion from our *in vitro* studies is that SIRT3 activity clearly modifies the acetylproteome, but has no discernable impact on mitochondrial metabolism, fuel-stimulated insulin secretion, or responses to a variety of stressors, including elevated lipids and apoptosis-inducing agents.

We note that our β-cell lines exhibit a broad dynamic range in which to study the impact of SIRT3 expression; While the KO β-cell line expresses no detectable endogenous rSIRT3, the WT line express ~70-fold more hSIRT3 WT-V5 compared to endogenous rSIRT3 protein in the parental cell line. Thus, in theory, mitochondrial proteins in the KO cells should be maximally hyperacetylated, while mitochondrial proteins in WT cells should be maximally deacetylated. However, even when these cell lines were cultured under conditions to maximally induce acetylation (*e.g.*, 6-12 days of culture in serum-

deprived or pyruvate-supplemented media), SIRT3-dependent changes in mitochondrial protein acetylation had no impact on fuel-stimulated insulin secretion.

Quantitative acetylproteomics revealed significant differences in acetylation of several components of multiple metabolic pathways critical for mitochondrial energy production, including fatty acid oxidation (FAO), the tricarboxylic acid (TCA) cycle, and the electron transport chain (ETC). The most affected proteins in the FAO pathway were subunits A and B of the mitochondrial trifunctional enzyme (HADHA and HADHB), which accounted for 17 of this pathway's 32 SIRT3-targeted lysines. Interestingly, our proteomics analysis also identified Short-Chain 3-Hydroxyacyl-Coenzyme Dehydrogenase (HADH), the enzyme responsible for the penultimate step in β-oxidation of FAs, which has been ascribed a role in insulin secretion. Patients with genetic deficiencies in *HADH* exhibit hyperinsulinemia (Clayton et al., 2001), and siRNA-mediated suppression of HADH in both 832/13 β-cells and mouse islets results in increased basal insulin secretion (Hardy et al., 2007). However, despite significant differences in acetylation of multiple HADH lysines, we found no evidence of increased insulin secretion at basal glucose (2.8 mM) across the three cell lines in multiple experiments. Further, the intracellular concentrations of a broad swath of acylcarnitine species derived from FAO were indistinguishable across the WT, KO, and HY cell lines, suggesting that mitochondrial lipid metabolism is not perturbed. Several enzymes in the

TCA cycle also exhibited differences in acetylation between the SIRT3 expressing and KO lines. These included proteins previously reported to be inhibited by acetylation such as pyruvate dehydrogenase (PDHA1) (Jing et al., 2011), mitochondrial $NADP^+$-dependent isocitrate dehydrogenase (IDH2) (Someya et al., 2010), subunit A of the succinate dehydrogenase complex (SDHA) (Finley et al., 2011), and mitochondrial malate dehydrogenase (MDH2) (specifically acetylation of K239) (Hebert et al., 2013). However, differences in acetylation of these and other TCA cycle components did not appreciably impact glucose-induced changes in organic acids, amino acids, or acylcarnitines, suggesting that glucose metabolism was largely unchanged. With the exception of Complex III, we found differences in acetylation of at least one subunit of each of the ETC complexes (I-V) as well as the ADP/ATP translocase 1 (SLC25A4). Notably, acetylation has been reported to inhibit NADH dehydrogenase and ATP synthase, while deacetylation by SIRT3 restores their activities and ATP production (Ahn et al., 2008; Bao et al., 2010). Our proteomics analysis indicated that acetylation of multiple lysines of an accessory subunit of NADH dehydrogenase (NDUFV3) and acetylation of multiple subunits of ATP synthase (ATP5C1, ATP5F1, ATP5H, ATP5J, and ATP5O) are significantly different between WT and KO cell lines. However, these changes in acetylation did not influence fuel-stimulated insulin secretion or metabolism. Given that a rise in ATP:ADP ratio is an important stimulus/secretion coupling factor for GSIS

(Muoio and Newgard, 2008), this suggests that ETC function remains largely intact despite significant differences in acetylation of multiple ETC complex proteins in response to manipulation of SIRT3.

We also studied global SIRT3 KO mice in order to examine the role of mitochondrial protein acetylation in the primary β-cell, in the presence and absence of nutritional stress. Prior studies of SIRT3 ablation in mice have suggested its involvement in regulation of systemic metabolism and susceptibility to diet-induced metabolic dysregulation (Dittenhafer-Reed et al., 2015; Hirschey et al., 2011; Jing et al., 2011; Lantier et al., 2015; Zhou et al., 2017). Several of those studies have been performed in the 129Sv mouse strain background. We chose to study whole-body deletion of SIRT3 in the C57Bl/6 strain, given its more rapid and robust development of diet-induced obesity and metabolic dysfunction (Almind and Kahn, 2004). At the time that our study was initiated, the SIRT3 knockout mice were in a C57Bl/6J background, which harbors a mutation in mitochondrial nicotinamide nucleotide transhydrogenase (*Nnt*) (Hirschey et al., 2011; Lombard et al., 2007). Mitochondrial NNT catalyzes transhydrogenation between NADH and $NADP^+$. The end products, NAD^+ (necessary for SIRT3 activity) and NADPH (involved in GSIS) could in theory increase the dynamic range of protein acetylation and islet function phenotypes observed in SIRT3 KO and WT mice. In fact, comparison of *Nnt* wild-type and *Nnt* mutant mice reveals a defect in insulin secretion in the latter strain

(Fergusson et al., 2014). Therefore, we bred the wild-type *Nnt* gene back into the C57Bl/6J with global deletion of SIRT3. We selected a high-fat/high-sucrose (HFHS) "Western" diet (45% Kcal from fat/ 35% Kcal from carbohydrates, primarily sucrose) as the dietary stress, due to its potential to drive carbon stress via multiple macronutrients. As expected, we were able to detect hyperacetylation of multiple proteins in SIRT3 KO islets compared to WT islets following 12 weeks of either STD diet- or HFHS diet-feeding. Notably, we did not observe a diet-dependent decrease in SIRT3 expression in these pooled islets, unlike what has been reported in other rodent models in both islet and non-islet tissues (Hirschey et al., 2011; Lantier et al., 2015; Zhang et al., 2016; Zhou et al., 2017).

With STD diet-feeding, SIRT3 KO mice were similar in weight to WT controls and exhibited identical fasting plasma glucose and insulin levels. Glucose excursion in response to either an oral or IP glucose bolus was indistinguishable between genotypes, in contrast to two other studies in which whole-body deletion of SIRT3 was reported to result in significant glucose intolerance, even in animals fed on standard chow diets (Hirschey et al., 2011; Jing et al., 2011). In our study, SIRT3 KO and WT mice fed the STD diet also had identical insulin secretion responses to either an oral or IP glucose load. These findings demonstrate that in the absence of nutritional stress, increased acetylation of pancreatic islet proteins permitted by the absence of SIRT3 is not sufficient to impact

glycemic control or insulin secretion. These findings are consistent with the results from our cell line studies.

HFHS diet-feeding resulted in marked obesity and significant increases in fasting blood glucose compared to STD diet-feeding, in both the SIRT3 KO and WT backgrounds. Fasting plasma insulin levels were significantly lower in the SIRT3 KO compared to WT mice fed the HFHS diet. Glucose tolerance, measured either as oGTT or ipGTT, was markedly impaired by the HFHS diet compared to STD diet-feeding, but was not different in HFHS diet-fed SIRT3 KO and WT mice. This contrasts with prior studies that reported glucose intolerance in SIRT3 KO mice on a 129Sv background in response to chronic feeding of a nutrient-dense diet (Hirschey et al., 2011; Zhou et al., 2017). Notably the feeding period was considerably longer in studies using the 129Sv background (30-55 weeks) compared to the current study in the C57Bl/6J/*Nnt* wild-type background (12 weeks). Insulin secretion in response to the oGTT was not significantly different in SIRT3 KO compared to WT mice. In contrast, insulin levels were lower in response to ipGTT in the SIRT3 KO mice. Identical IP glucose excursions in the two genotypes, occurring in the face of reduced insulin secretion in the SIRT3 KO strain, could have suggested that peripheral insulin sensitivity was enhanced in the SIRT3 KO mice, but an insulin tolerance test did not reveal a significant difference in insulin sensitivity.

The foregoing insulin secretion phenotypes were largely corroborated in perifusion studies of islets isolated from the STD diet- and HFHS diet-fed groups of mice. Here, we were able to control for islet number and size to facilitate the comparison of genotypes. Insulin secretion from islets isolated from STD diet-fed SIRT3 KO mice was not different from that observed with islets from STD diet-fed wild-type controls for all secretagogues tested, with the exception of a statistically significant increase in response to a depolarizing concentration of KCl. Interestingly, islets from HFHS diet-fed SIRT3 KO mice secreted less insulin in response to all secretagogues and potentiators studied relative to islets from HFHS diet-fed wild-type mice, including KCl. The impairment in GSIS is similar to that reported previously in islets isolated from SIRT3 KO animals subjected to chronic overnutrition measured in a static incubation assay (Zhou et al., 2017).

In sum, we find that broad changes in mitochondrial protein acetylation occurring as a function of manipulation of SIRT3 expression are not sufficient to explain changes in islet function observed by other groups. In fact, exaggerated manipulation of SIRT3 expression to broadly and significantly modify the β-cell acetylproteome in β-cell lines has no discernable effect on mitochondrial metabolism, insulin secretion, or responses to external stress-inducing agents. Similarly, global knock out of SIRT3 in mice fed a STD diet has negligible effects on insulin secretion despite clear effects on protein acetylation. Only when global SIRT3 KO animals are subjected to chronic nutrient stress via HFHS

diet-feeding do genotype-specific differences in insulin secretion emerge. It remains to be determined if the modest increase in acetylation observed in islets from HFHS diet-fed versus STD diet-fed SIRT3 KO mice (Figure 21) contributes to impairment of islet cell metabolism or function. A full understanding of this issue requires an assessment of the stoichiometry of lysine acetylation within specific proteins, which was not possible with the proteomics methods used here. In this regard, recent estimates of the stoichiometry of lysine acetylation suggest that for any individual protein only a small percentage of the specific protein molecules in a cell are acetylated on specific lysines, even under conditions of SIRT3 ablation (Weinert et al., 2015). Given that the anti-acetyllysine antibody used in Figure 21 detects only a subset of the most abundant acetylated proteins, more robust changes in acetylation of less abundant proteins could be occurring. However, even if this is the case, the change in insulin secretion observed in HFHS diet-fed SIRT3 KO animals is not sufficient to alter glucose homeostasis during oGTT or ipGTT, suggesting that any such changes in acetylation stoichiometry have limited physiological or pathophysiological significance.

7. Conclusions

The existing literature and the current study suggest that, in specific models of chronic overnutrition, the management of mitochondrial protein acetylation by SIRT3 can modestly exacerbate symptoms of metabolic disease, leading some groups to conclude that SIRT3-activation could be an attractive therapeutic strategy for T2D. For perspective, two of the three studies that examine the effect of chronic overnutrition on SIRT3 KO mice stress the animals for 30 or 55 weeks (Hirschey et al., 2011; Zhou et al., 2017). Given that the 129Sv background strain used in these studies have a maximum lifespan of around 100 weeks (Storer, 1966), these animals were subjected to dietary stress for 30-55% of their normal lifespan, and yet the impact of whole-animal SIRT3 ablation remained modest. In fact, SIRT3 KO animals stressed with chronic overnutrition in the lengthier study do not exhibit exacerbated fasting hyperglycemia (Hirschey et al., 2011), and thus are not worse off in at least one hallmark-metric of T2D (DeFronzo et al., 2015). Further, these modest and inconsistent phenotypes are observed in the global SIRT3 KO animal, while both liver- and skeletal muscle-specific SIRT3 KO mice are phenotypically identical to wild-type mice after 18 weeks of chronic overnutrition (Fernandez-Marcos et al., 2012). In aggregate, these studies fail to convincingly demonstrate that SIRT3 and mitochondrial protein acetylation might play an appreciable role in the development of T2D. Given that the ultimate goal of the aforementioned studies is to determine whether SIRT3 is a

potential therapeutic target for the treatment of T2D, future work should focus on a transgenic mouse engineered with global expression of an inducible transgene for SIRT3 overexpression.

In the first proposed study, these animals should be chronically stressed with a nutrient-dense diet until overtly overweight, glucose intolerant, and insulin resistant. From this starting point, one cohort of animals should have transgenic overexpression of SIRT3 induced, while another cohort should maintain endogenous SIRT3 expression levels. Upon overexpression of SIRT3, both cohorts of animals would continue to be exposed to chronic overnutrition, with serial assessment of metabolic variables to determine if overexpression of SIRT3 prevents further worsening of symptoms, restores healthy systemic metabolism, or is without impact. In this way, SIRT3 overexpression could serve as a surrogate for the proposed pharmacological activation of SIRT3, providing insight into its proposed promise for treatment of T2D. In the event that SIRT3 overexpression has no impact alone, conditions can be added to determine if SIRT3 activation has the potential to synergize with other interventions with well-documented benefits. For example, rather than continuing the dietary stress following overexpression of SIRT3, animals could be given a standard chow diet to determine if SIRT3 overexpression serves to accelerate restoration of healthy metabolic parameters. Another approach could be caloric restriction, an intervention that can remodel the acetylproteome

in a SIRT3-dependent way to promote healthspan (Hebert et al., 2013; Someya et al., 2010). Additionally, following the induced overexpression of SIRT3, animals should be treated with metformin and/or incretin hormones, as these are commonly prescribed therapeutic interventions for T2D (DeFronzo et al., 2015), again searching for an additive or synergistic effect of these agents in the presence of SIRT3 overexpression. Ultimately, the practicality of SIRT3 activation as a potential therapeutic strategy for T2D will depend its benefits (if any) in the context of commonly prescribed diet, exercise, and pharmacological interventions.

Appendix A

human SIRT3 fusion protein gBlock insert sequence (JH507):

TTAATACGACTCACTATAGGGttGAAAGTTTGTACAAAAAAGCAGGCTTAGTTatg

gcgttctggggttggcgcgccgcggcagccctccggctgtggggccgggtagttgaacgggtcgaggccgggggaggcgt

ggggccgtttcaggcctgcggctgtcggctggtgcttggcggcagggacgatgtgagtgcggggctgagaggcagccatgg

ggcccgcggtgagcccttggacccggcgcgccccttgcagaggcctcccagacccgaggtgcccagggcattccggaggca

gccgagggcagcagctcccagtttcttcttttcgagtattaaaggtggaagaaggtccatatctttttctgtgggtgcttcaagtgtt

gttggaagtggaggcagcagtgacaaggggaagctttccctgcaggatgtagctgagctgattcgggccagagcctgccaga

gggtggtggtcatggtgggggccggcatcagcacacccagtggcattccagacttcagatcgccggggagtggcctgtacag

caacctccagcagtacgatctcccgtaccccgaggccatttttgaactcccattcttctttcacaaccccaagccctttttcactttggc

caaggagctgtaccctggaaactacaagcccaacgtcactcactactttctccggctgcttcatgacaaggggctgcttctgcggc

tctacacgcagaacatcgatgggcttgagagagtgtcgggcatccctgcctcaaagctggttgaagctcatggaacctttgcctc

tgccacctgcacagtctgccaaagacccttcccaggggaggacattcgggctgacgtgatggcagacagggttccccgctgcc

cggtctgcaccggcgttgtgaagcccgacattgtgttctttggggagccgctgccccagaggttcttgctgcatgtggttgatttcc

ccatggcagatctgctgctcatccttgggacctccctggaggtggagccttttgccagcttgaccgaggccgtgcggagctcagt

tccccgactgctcatcaaccgggacttggtggggcccttggcttggcatcctcgcagcagggacgtggcccagctgggggacg

tggttcacggcgtggaaagcctagtggagcttctgggctggacagaagagatgcgggaccttgtgcagcgggaaactggga

agcttgatggaccagacaaaaACCCAGCTTTCTTGTACAAAGTGGTccccTATCCCTAACCCTC

TCCTCGGTC

References

Ahn, B.H., Kim, H.S., Song, S., Lee, I.H., Liu, J., Vassilopoulos, A., Deng, C.X., and Finkel, T. (2008). A role for the mitochondrial deacetylase Sirt3 in regulating energy homeostasis. Proc Natl Acad Sci U S A *105*, 14447-14452.

Almind, K., and Kahn, C.R. (2004). Genetic determinants of energy expenditure and insulin resistance in diet-induced obesity in mice. Diabetes *53*, 3274-3285.

An, J., Muoio, D.M., Shiota, M., Fujimoto, Y., Cline, G.W., Shulman, G.I., Koves, T.R., Stevens, R., Millington, D., and Newgard, C.B. (2004). Hepatic expression of malonyl-CoA decarboxylase reverses muscle, liver and whole-animal insulin resistance. Nat Med *10*, 268-274.

Anderson, K.A., Huynh, F.K., Fisher-Wellman, K., Stuart, J.D., Peterson, B.S., Douros, J.D., Wagner, G.R., Thompson, J.W., Madsen, A.S., Green, M.F., et al. (2017). SIRT4 Is a Lysine Deacylase that Controls Leucine Metabolism and Insulin Secretion. Cell Metab *25*, 838-855 e815.

Anello, M., Lupi, R., Spampinato, D., Piro, S., Masini, M., Boggi, U., Del Prato, S., Rabuazzo, A.M., Purrello, F., and Marchetti, P. (2005). Functional and morphological alterations of mitochondria in pancreatic beta cells from type 2 diabetic patients. Diabetologia *48*, 282-289.

Asfari, M., Janjic, D., Meda, P., Li, G., Halban, P.A., and Wollheim, C.B. (1992). Establishment of 2-mercaptoethanol-dependent differentiated insulin-secreting cell lines. Endocrinology *130*, 167-178.

Ashcroft, F.M., Harrison, D.E., and Ashcroft, S.J. (1984). Glucose induces closure of single potassium channels in isolated rat pancreatic beta-cells. Nature *312*, 446-448.

Ashcroft, S.J., Hammonds, P., and Harrison, D.E. (1986). Insulin secretory responses of a clonal cell line of simian virus 40-transformed B cells. Diabetologia *29*, 727-733.

Baeza, J., Smallegan, M.J., and Denu, J.M. (2016). Mechanisms and Dynamics of Protein Acetylation in Mitochondria. Trends Biochem Sci *41*, 231-244.

Banting, F.G., and Best, C.H. (1922). The Internal Secretion of the Pancreas. Journal of Laboratory and Clinical Science *7*, 251-256.

Banting, F.G., Best, C.H., Collip, J.B., Campbell, W.R., and Fletcher, A.A. (1922). Pancreatic Extracts in the Treatment of Diabetes Mellitus. Can Med Assoc J *12*, 141-146.

Bao, J., Scott, I., Lu, Z., Pang, L., Dimond, C.C., Gius, D., and Sack, M.N. (2010). SIRT3 is regulated by nutrient excess and modulates hepatic susceptibility to lipotoxicity. Free Radic Biol Med *49*, 1230-1237.

Baum, J., Simons, B.E., Jr., Unger, R.H., and Madison, L.L. (1962). Localization of glucagon in the alpha cells in the pancreatic islet by immunofluorescent technics. Diabetes *11*, 371-374.

Benjamini, Y., Drai, D., Elmer, G., Kafkafi, N., and Golani, I. (2001). Controlling the false discovery rate in behavior genetics research. Behav Brain Res *125*, 279-284.

Bryan, J., Crane, A., Vila-Carriles, W.H., Babenko, A.P., and Aguilar-Bryan, L. (2005). Insulin secretagogues, sulfonylurea receptors and K(ATP) channels. Curr Pharm Des *11*, 2699-2716.

Calvo, S.E., Clauser, K.R., and Mootha, V.K. (2016). MitoCarta2.0: an updated inventory of mammalian mitochondrial proteins. Nucleic Acids Res *44*, D1251-1257.

Carrico, C., Meyer, J.G., He, W., Gibson, B.W., and Verdin, E. (2018). The Mitochondrial Acylome Emerges: Proteomics, Regulation by Sirtuins, and Metabolic and Disease Implications. Cell Metab *27*, 497-512.

Caton, P.W., Richardson, S.J., Kieswich, J., Bugliani, M., Holland, M.L., Marchetti, P., Morgan, N.G., Yaqoob, M.M., Holness, M.J., and Sugden, M.C. (2013). Sirtuin 3 regulates mouse pancreatic beta cell function and is suppressed in pancreatic islets isolated from human type 2 diabetic patients. Diabetologia *56*, 1068-1077.

Chick, W.L., Warren, S., Chute, R.N., Like, A.A., Lauris, V., and Kitchen, K.C. (1977). A transplantable insulinoma in the rat. Proc Natl Acad Sci U S A *74*, 628-632.

Choudhary, C., Kumar, C., Gnad, F., Nielsen, M.L., Rehman, M., Walther, T.C., Olsen, J.V., and Mann, M. (2009). Lysine acetylation targets protein complexes and co-regulates major cellular functions. Science *325*, 834-840.

Clayton, P.T., Eaton, S., Aynsley-Green, A., Edginton, M., Hussain, K., Krywawych, S., Datta, V., Malingre, H.E., Berger, R., and van den Berg, I.E. (2001). Hyperinsulinism in short-chain L-3-hydroxyacyl-CoA dehydrogenase deficiency reveals the importance of beta-oxidation in insulin secretion. J Clin Invest *108*, 457-465.

Cooper, H.M., Huang, J.Y., Verdin, E., and Spelbrink, J.N. (2009). A new splice variant of the mouse SIRT3 gene encodes the mitochondrial precursor protein. PLoS One *4*, e4986.

Coore, H.G., and Randle, P.J. (1964). Regulation of insulin secretion studied with pieces of rabbit pancreas incubated in vitro. Biochem J *93*, 66-78.

DeFronzo, R.A., Ferrannini, E., Groop, L., Henry, R.R., Herman, W.H., Holst, J.J., Hu, F.B., Kahn, C.R., Raz, I., Shulman, G.I., et al. (2015). Type 2 diabetes mellitus. Nat Rev Dis Primers *1*, 15019.

Dittenhafer-Reed, K.E., Richards, A.L., Fan, J., Smallegan, M.J., Fotuhi Siahpirani, A., Kemmerer, Z.A., Prolla, T.A., Roy, S., Coon, J.J., and Denu, J.M. (2015). SIRT3 mediates multi-tissue coupling for metabolic fuel switching. Cell Metab *21*, 637-646.

Dobbins, R.L., Chester, M.W., Stevenson, B.E., Daniels, M.B., Stein, D.T., and McGarry, J.D. (1998). A fatty acid- dependent step is critically important for both glucose- and non-glucose-stimulated insulin secretion. J Clin Invest *101*, 2370-2376.

Dorfer, V., Pichler, P., Stranzl, T., Stadlmann, J., Taus, T., Winkler, S., and Mechtler, K. (2014). MS Amanda, a universal identification algorithm optimized for high accuracy tandem mass spectra. J Proteome Res *13*, 3679-3684.

Efrat, S., Linde, S., Kofod, H., Spector, D., Delannoy, M., Grant, S., Hanahan, D., and Baekkeskov, S. (1988). Beta-cell lines derived from transgenic mice expressing a hybrid insulin gene-oncogene. Proc Natl Acad Sci U S A *85*, 9037-9041.

Ferdaoussi, M., Dai, X., Jensen, M.V., Wang, R., Peterson, B.S., Huang, C., Ilkayeva, O., Smith, N., Miller, N., Hajmrle, C., et al. (2015). Isocitrate-to-SENP1 signaling amplifies insulin secretion and rescues dysfunctional beta cells. J Clin Invest *125*, 3847-3860.

Fergusson, G., Ethier, M., Guevremont, M., Chretien, C., Attane, C., Joly, E., Fioramonti, X., Prentki, M., Poitout, V., and Alquier, T. (2014). Defective insulin secretory response to intravenous glucose in C57Bl/6J compared to C57Bl/6N mice. Mol Metab *3*, 848-854.

Fernandez-Marcos, P.J., Jeninga, E.H., Canto, C., Harach, T., de Boer, V.C., Andreux, P., Moullan, N., Pirinen, E., Yamamoto, H., Houten, S.M., et al. (2012). Muscle or liver-specific Sirt3 deficiency induces hyperacetylation of mitochondrial proteins without affecting global metabolic homeostasis. Sci Rep *2*, 425.

Ferrara, C.T., Wang, P., Neto, E.C., Stevens, R.D., Bain, J.R., Wenner, B.R., Ilkayeva, O.R., Keller, M.P., Blasiole, D.A., Kendziorski, C., et al. (2008). Genetic networks of liver metabolism revealed by integration of metabolic and transcriptional profiling. PLoS Genet *4*, e1000034.

Finley, L.W., Haas, W., Desquiret-Dumas, V., Wallace, D.C., Procaccio, V., Gygi, S.P., and Haigis, M.C. (2011). Succinate dehydrogenase is a direct target of sirtuin 3 deacetylase activity. PLoS One *6*, e23295.

Goldsmith, P.C., Rose, J.C., Arimura, A., and Ganong, W.F. (1975). Ultrastructural localization of somatostatin in pancreatic islets of the rat. Endocrinology *97*, 1061-1064.

Gooding, J.R., Jensen, M.V., Dai, X., Wenner, B.R., Lu, D., Arumugam, R., Ferdaoussi, M., MacDonald, P.E., and Newgard, C.B. (2015). Adenylosuccinate Is an Insulin Secretagogue Derived from Glucose-Induced Purine Metabolism. Cell Rep *13*, 157-167.

Grodsky, G.M., Batts, A.A., Bennett, L.L., Vcella, C., McWilliams, N.B., and Smith, D.F. (1963). Effects of Carbohydrates on Secretion of Insulin from Isolated Rat Pancreas. Am J Physiol *205*, 638-644.

Guarente, L. (2000). Sir2 links chromatin silencing, metabolism, and aging. Genes Dev *14*, 1021-1026.

Hardy, O.T., Hohmeier, H.E., Becker, T.C., Manduchi, E., Doliba, N.M., Gupta, R.K., White, P., Stoeckert, C.J., Jr., Matschinsky, F.M., Newgard, C.B., et al. (2007). Functional genomics of the beta-cell: short-chain 3-hydroxyacyl-coenzyme A dehydrogenase regulates insulin secretion independent of K+ currents. Mol Endocrinol *21*, 765-773.

Hebert, A.S., Dittenhafer-Reed, K.E., Yu, W., Bailey, D.J., Selen, E.S., Boersma, M.D., Carson, J.J., Tonelli, M., Balloon, A.J., Higbee, A.J., et al. (2013). Calorie restriction and SIRT3 trigger global reprogramming of the mitochondrial protein acetylome. Mol Cell *49*, 186-199.

Henquin, J.C., Ravier, M.A., Nenquin, M., Jonas, J.C., and Gilon, P. (2003). Hierarchy of the beta-cell signals controlling insulin secretion. Eur J Clin Invest *33*, 742-750.

Hirschey, M.D., Shimazu, T., Goetzman, E., Jing, E., Schwer, B., Lombard, D.B., Grueter, C.A., Harris, C., Biddinger, S., Ilkayeva, O.R., et al. (2010). SIRT3 regulates mitochondrial fatty-acid oxidation by reversible enzyme deacetylation. Nature *464*, 121-125.

Hirschey, M.D., Shimazu, T., Jing, E., Grueter, C.A., Collins, A.M., Aouizerat, B., Stancakova, A., Goetzman, E., Lam, M.M., Schwer, B., et al. (2011). SIRT3 deficiency and mitochondrial protein hyperacetylation accelerate the development of the metabolic syndrome. Mol Cell *44*, 177-190.

Hohmeier, H.E., Mulder, H., Chen, G., Henkel-Rieger, R., Prentki, M., and Newgard, C.B. (2000). Isolation of INS-1-derived cell lines with robust ATP-sensitive K+ channel-dependent and -independent glucose-stimulated insulin secretion. Diabetes *49*, 424-430.

Huang, M., and Joseph, J.W. (2014). Assessment of the metabolic pathways associated with glucose-stimulated biphasic insulin secretion. Endocrinology *155*, 1653-1666.

IDF (2017). IDF Diabetes Atlas, 8th edn. (Brussels, Belgium: International Diabetes Federation).

Imai, S., Armstrong, C.M., Kaeberlein, M., and Guarente, L. (2000). Transcriptional silencing and longevity protein Sir2 is an NAD-dependent histone deacetylase. Nature *403*, 795-800.

Iynedjian, P.B., Pilot, P.R., Nouspikel, T., Milburn, J.L., Quaade, C., Hughes, S., Ucla, C., and Newgard, C.B. (1989). Differential expression and regulation of the glucokinase gene in liver and islets of Langerhans. Proc Natl Acad Sci U S A *86*, 7838-7842.

Jensen, M.V., Joseph, J.W., Ilkayeva, O., Burgess, S., Lu, D., Ronnebaum, S.M., Odegaard, M., Becker, T.C., Sherry, A.D., and Newgard, C.B. (2006). Compensatory responses to pyruvate carboxylase suppression in islet beta-cells. Preservation of glucose-stimulated insulin secretion. J Biol Chem *281*, 22342-22351.

Jensen, M.V., Joseph, J.W., Ronnebaum, S.M., Burgess, S.C., Sherry, A.D., and Newgard, C.B. (2008). Metabolic cycling in control of glucose-stimulated insulin secretion. Am J Physiol Endocrinol Metab *295*, E1287-1297.

Jing, E., Emanuelli, B., Hirschey, M.D., Boucher, J., Lee, K.Y., Lombard, D., Verdin, E.M., and Kahn, C.R. (2011). Sirtuin-3 (Sirt3) regulates skeletal muscle metabolism and insulin signaling via altered mitochondrial oxidation and reactive oxygen species production. Proc Natl Acad Sci U S A *108*, 14608-14613.

Jing, E., O'Neill, B.T., Rardin, M.J., Kleinridders, A., Ilkeyeva, O.R., Ussar, S., Bain, J.R., Lee, K.Y., Verdin, E.M., Newgard, C.B., et al. (2013). Sirt3 regulates metabolic flexibility of skeletal muscle through reversible enzymatic deacetylation. Diabetes *62*, 3404-3417.

Joseph, J.W., Jensen, M.V., Ilkayeva, O., Palmieri, F., Alarcon, C., Rhodes, C.J., and Newgard, C.B. (2006). The mitochondrial citrate/isocitrate carrier plays a regulatory role in glucose-stimulated insulin secretion. J Biol Chem *281*, 35624-35632.

Kaeberlein, M., McVey, M., and Guarente, L. (1999). The SIR2/3/4 complex and SIR2 alone promote longevity in Saccharomyces cerevisiae by two different mechanisms. Genes Dev *13*, 2570-2580.

Kall, L., Canterbury, J.D., Weston, J., Noble, W.S., and MacCoss, M.J. (2007). Semi-supervised learning for peptide identification from shotgun proteomics datasets. Nat Methods *4*, 923-925.

Kim, M., Lee, J.S., Oh, J.E., Nan, J., Lee, H., Jung, H.S., Chung, S.S., and Park, K.S. (2015). SIRT3 Overexpression Attenuates Palmitate-Induced Pancreatic beta-Cell Dysfunction. PLoS One *10*, e0124744.

Kim, S.C., Sprung, R., Chen, Y., Xu, Y., Ball, H., Pei, J., Cheng, T., Kho, Y., Xiao, H., Xiao, L., et al. (2006). Substrate and functional diversity of lysine acetylation revealed by a proteomics survey. Mol Cell *23*, 607-618.

Kimmel, J.R., Hayden, L.J., and Pollock, H.G. (1975). Isolation and characterization of a new pancreatic polypeptide hormone. J Biol Chem *250*, 9369-9376.

Lamont, B.J., Li, Y., Kwan, E., Brown, T.J., Gaisano, H., and Drucker, D.J. (2012). Pancreatic GLP-1 receptor activation is sufficient for incretin control of glucose metabolism in mice. J Clin Invest *122*, 388-402.

Langerhans, P. (1869). Beitrage Zur Mikroskopischen Anatomie De Bauchspeicheldrusse. Inaugural-dissertation. (Berlin).

Lantier, L., Williams, A.S., Williams, I.M., Yang, K.K., Bracy, D.P., Goelzer, M., James, F.D., Gius, D., and Wasserman, D.H. (2015). SIRT3 Is Crucial for Maintaining Skeletal Muscle Insulin Action and Protects Against Severe Insulin Resistance in High-Fat-Fed Mice. Diabetes *64*, 3081-3092.

Lesack, K., and Naugler, C. (2011). An open-source software program for performing Bonferroni and related corrections for multiple comparisons. J Pathol Inform *2*, 52.

Lin, S.J., Defossez, P.A., and Guarente, L. (2000). Requirement of NAD and SIR2 for life-span extension by calorie restriction in Saccharomyces cerevisiae. Science *289*, 2126-2128.

Lombard, D.B., Alt, F.W., Cheng, H.L., Bunkenborg, J., Streeper, R.S., Mostoslavsky, R., Kim, J., Yancopoulos, G., Valenzuela, D., Murphy, A., et al. (2007). Mammalian Sir2 homolog SIRT3 regulates global mitochondrial lysine acetylation. Mol Cell Biol *27*, 8807-8814.

Matschinsky, F.M., and Ellerman, J.E. (1968). Metabolism of glucose in the islets of Langerhans. J Biol Chem *243*, 2730-2736.

McDonnell, E., Crown, S.B., Fox, D.B., Kitir, B., Ilkayeva, O.R., Olsen, C.A., Grimsrud, P.A., and Hirschey, M.D. (2016). Lipids Reprogram Metabolism to Become a Major Carbon Source for Histone Acetylation. Cell Rep *17*, 1463-1472.

Mulder, H. (2017). Transcribing beta-cell mitochondria in health and disease. Mol Metab *6*, 1040-1051.

Newgard, C.B., and Matschinsky, F. (2001). Substrate control of insulin release. In Handbook of Physiology, Vol. A, J. Jefferson, ed. (Oxford University Press).

Odegaard, M.L., Joseph, J.W., Jensen, M.V., Lu, D., Ilkayeva, O., Ronnebaum, S.M., Becker, T.C., and Newgard, C.B. (2010). The mitochondrial 2-oxoglutarate carrier is part of a metabolic pathway that mediates glucose- and glutamine-stimulated insulin secretion. J Biol Chem *285*, 16530-16537.

Patterson, J.N., Cousteils, K., Lou, J.W., Manning Fox, J.E., MacDonald, P.E., and Joseph, J.W. (2014). Mitochondrial metabolism of pyruvate is essential for regulating glucose-stimulated insulin secretion. J Biol Chem *289*, 13335-13346.

Poitout, V., and Robertson, R.P. (2008). Glucolipotoxicity: fuel excess and beta-cell dysfunction. Endocr Rev *29*, 351-366.

Prado, C.L., Pugh-Bernard, A.E., Elghazi, L., Sosa-Pineda, B., and Sussel, L. (2004). Ghrelin cells replace insulin-producing beta cells in two mouse models of pancreas development. Proc Natl Acad Sci U S A *101*, 2924-2929.

Praz, G.A., Halban, P.A., Wollheim, C.B., Blondel, B., Strauss, A.J., and Renold, A.E. (1983). Regulation of immunoreactive-insulin release from a rat cell line (RINm5F). Biochem J *210*, 345-352.

Prentki, M., and Madiraju, S.R. (2012). Glycerolipid/free fatty acid cycle and islet beta-cell function in health, obesity and diabetes. Mol Cell Endocrinol *353*, 88-100.

Prentki, M., Matschinsky, F.M., and Madiraju, S.R. (2013). Metabolic signaling in fuel-induced insulin secretion. Cell Metab *18*, 162-185.

Ran, F.A., Hsu, P.D., Lin, C.Y., Gootenberg, J.S., Konermann, S., Trevino, A.E., Scott, D.A., Inoue, A., Matoba, S., Zhang, Y., et al. (2013). Double nicking by RNA-guided CRISPR Cas9 for enhanced genome editing specificity. Cell *154*, 1380-1389.

Rardin, M.J., Newman, J.C., Held, J.M., Cusack, M.P., Sorensen, D.J., Li, B., Schilling, B., Mooney, S.D., Kahn, C.R., Verdin, E., et al. (2013). Label-free quantitative proteomics of the lysine acetylome in mitochondria identifies substrates of SIRT3 in metabolic pathways. Proc Natl Acad Sci U S A *110*, 6601-6606.

Rogina, B., and Helfand, S.L. (2004). Sir2 mediates longevity in the fly through a pathway related to calorie restriction. Proc Natl Acad Sci U S A *101*, 15998-16003.

Ronnebaum, S.M., Ilkayeva, O., Burgess, S.C., Joseph, J.W., Lu, D., Stevens, R.D., Becker, T.C., Sherry, A.D., Newgard, C.B., and Jensen, M.V. (2006). A pyruvate cycling pathway involving cytosolic NADP-dependent isocitrate dehydrogenase regulates glucose-stimulated insulin secretion. J Biol Chem *281*, 30593-30602.

Schwer, B., North, B.J., Frye, R.A., Ott, M., and Verdin, E. (2002). The human silent information regulator (Sir)2 homologue hSIRT3 is a mitochondrial nicotinamide adenine dinucleotide-dependent deacetylase. J Cell Biol *158*, 647-657.

Sol, E.M., Wagner, S.A., Weinert, B.T., Kumar, A., Kim, H.S., Deng, C.X., and Choudhary, C. (2012). Proteomic investigations of lysine acetylation identify diverse substrates of mitochondrial deacetylase sirt3. PLoS One *7*, e50545.

Someya, S., Yu, W., Hallows, W.C., Xu, J., Vann, J.M., Leeuwenburgh, C., Tanokura, M., Denu, J.M., and Prolla, T.A. (2010). Sirt3 mediates reduction of oxidative damage and prevention of age-related hearing loss under caloric restriction. Cell *143*, 802-812.

Spegel, P., Sharoyko, V.V., Goehring, I., Danielsson, A.P., Malmgren, S., Nagorny, C.L., Andersson, L.E., Koeck, T., Sharp, G.W., Straub, S.G., et al. (2013). Time-resolved metabolomics analysis of beta-cells implicates the pentose phosphate pathway in the control of insulin release. Biochem J *450*, 595-605.

Stein, D.T., Esser, V., Stevenson, B.E., Lane, K.E., Whiteside, J.H., Daniels, M.B., Chen, S., and McGarry, J.D. (1996). Essentiality of circulating fatty acids for glucose-stimulated insulin secretion in the fasted rat. J Clin Invest *97*, 2728-2735.

Sterner, D.E., and Berger, S.L. (2000). Acetylation of histones and transcription-related factors. Microbiol Mol Biol Rev *64*, 435-459.

Storer, J.B. (1966). Longevity and gross pathology at death in 22 inbred mouse strains. J Gerontol *21*, 404-409.

Tan, M., Peng, C., Anderson, K.A., Chhoy, P., Xie, Z., Dai, L., Park, J., Chen, Y., Huang, H., Zhang, Y., et al. (2014). Lysine glutarylation is a protein posttranslational modification regulated by SIRT5. Cell Metab *19*, 605-617.

Taus, T., Kocher, T., Pichler, P., Paschke, C., Schmidt, A., Henrich, C., and Mechtler, K. (2011). Universal and confident phosphorylation site localization using phosphoRS. J Proteome Res *10*, 5354-5362.

Thorens, B., Sarkar, H.K., Kaback, H.R., and Lodish, H.F. (1988). Cloning and functional expression in bacteria of a novel glucose transporter present in liver, intestine, kidney, and beta-pancreatic islet cells. Cell *55*, 281-290.

Tissenbaum, H.A., and Guarente, L. (2001). Increased dosage of a sir-2 gene extends lifespan in Caenorhabditis elegans. Nature *410*, 227-230.

Toye, A.A., Lippiat, J.D., Proks, P., Shimomura, K., Bentley, L., Hugill, A., Mijat, V., Goldsworthy, M., Moir, L., Haynes, A., et al. (2005). A genetic and physiological study of impaired glucose homeostasis control in C57BL/6J mice. Diabetologia *48*, 675-686.

Verdin, E., and Ott, M. (2015). 50 years of protein acetylation: from gene regulation to epigenetics, metabolism and beyond. Nat Rev Mol Cell Biol *16*, 258-264.

Vizcaino, J.A., Csordas, A., Del-Toro, N., Dianes, J.A., Griss, J., Lavidas, I., Mayer, G., Perez-Riverol, Y., Reisinger, F., Ternent, T., et al. (2016). 2016 update of the PRIDE database and its related tools. Nucleic Acids Res *44*, 11033.

Wagner, G.R., and Hirschey, M.D. (2014). Nonenzymatic protein acylation as a carbon stress regulated by sirtuin deacylases. Mol Cell *54*, 5-16.

Wagner, G.R., and Payne, R.M. (2013). Widespread and enzyme-independent Nepsilon-acetylation and Nepsilon-succinylation of proteins in the chemical conditions of the mitochondrial matrix. J Biol Chem *288*, 29036-29045.

Wang, Q., Zhang, Y., Yang, C., Xiong, H., Lin, Y., Yao, J., Li, H., Xie, L., Zhao, W., Yao, Y., et al. (2010). Acetylation of metabolic enzymes coordinates carbon source utilization and metabolic flux. Science *327*, 1004-1007.

Watt, M.J., Hoy, A.J., Muoio, D.M., and Coleman, R.A. (2012). Distinct roles of specific fatty acids in cellular processes: implications for interpreting and reporting experiments. Am J Physiol Endocrinol Metab *302*, E1-3.

Weinert, B.T., Moustafa, T., Iesmantavicius, V., Zechner, R., and Choudhary, C. (2015). Analysis of acetylation stoichiometry suggests that SIRT3 repairs nonenzymatic acetylation lesions. EMBO J *34*, 2620-2632.

Yates, J.R., 3rd (2015). Pivotal role of computers and software in mass spectrometry - SEQUEST and 20 years of tandem MS database searching. J Am Soc Mass Spectrom *26*, 1804-1813.

Zhang, H.H., Ma, X.J., Wu, L.N., Zhao, Y.Y., Zhang, P.Y., Zhang, Y.H., Shao, M.W., Liu, F., Li, F., and Qin, G.J. (2016). Sirtuin-3 (SIRT3) protects pancreatic beta-cells from endoplasmic reticulum (ER) stress-induced apoptosis and dysfunction. Mol Cell Biochem *420*, 95-106.

Zhao, S., Xu, W., Jiang, W., Yu, W., Lin, Y., Zhang, T., Yao, J., Zhou, L., Zeng, Y., Li, H., et al. (2010). Regulation of cellular metabolism by protein lysine acetylation. Science *327*, 1000-1004.

Zhou, Y., Chung, A.C.K., Fan, R., Lee, H.M., Xu, G., Tomlinson, B., Chan, J.C.N., and Kong, A.P.S. (2017). Sirt3 Deficiency Increased the Vulnerability of Pancreatic Beta Cells to Oxidative Stress-Induced Dysfunction. Antioxid Redox Signal.

Biography

Brett Steven Peterson

Born to Steven and Karen Peterson on November 20, 1987 in Stoneham, Massachusetts.

Education

Duke University Graduate School, Durham, NC – Ph.D. in Pharmacology, 2018
Northeastern University, Boston, MA – B.S. in Biology, *magna cum laude*, 2011

Publications

Peterson BS, Campbell JE, Ilkayeva O, Grimsrud PA, Hirschey MD, Newgard CB. Broad remodeling of the acetylproteome by SIRT3 manipulation fails to affect insulin secretion or β-cell metabolism in the absence of overnutrition. *Submitted for publication.*

Jensen MV, Gooding JR, Ferdaoussi M, Dai X, **Peterson BS**, MacDonald PE, Newgard CB. Metabolomics Applied to Islet Nutrient Sensing Mechanisms. Diabetes Obes Metab, 2017. 19 Suppl 1: p. 90-94.

Anderson KA, Huynh FK, Fisher-Wellman K, Stuart JD, **Peterson BS**, Douros JD, Wagner GR, Thompson JW, Madsen AS, Green MF, Sivley RM, Ilkayeva OR, Stevens RD, Backos DS, Capra JA, Olsen CA, Campbell JE, Muoio DM, Grimsrud PA, Hirschey MD. SIRT4 is a Lysine Deacylase That Controls Leucine Metabolism and Insulin Secretion. Cell Metab (2017) 25(4): p. 838-855 e15

Hayes HL, **Peterson BS**, Haldeman JM, Newgard CB, Hohmeier HE, Stephens SB. Delayed apoptosis allows islet β-cells to implement an autophagic mechanism to promote cell survival. PLoS ONE (2017) 12(2): e0172567.

Chhoy P, Anderson KA, Hershberger KA, Huynh FK, Martin AS, McDonnell, **Peterson BS**, Starzenski LA, Backos DS, Fritz KS, Hirschey MD. Chapter 5: Deacetylation by SIRT3 Relieves Inhibition of Mitochondrial Protein Function. Proteins and Cell Regulation. Volume 10: Sirtuins (2016). Edited by Riekelt H. Houtkooper.

Ferdaoussi M, Dai X, Jensen MV, Wang R, **Peterson BS**, Huang C, Ilkayeva O, Smith N, Miller N, Hajmrle C, Spigelman AF, Wright RC, Plummer G, Suzuki K, Mackay JP, van de Bunt M, Gloyn AL, Ryan TE, Norquay LD, Brosnan MJ, Trimmer JK, Rolph TP, Kibbey RG, Manning Fox JE, Colmers WF, Shirihai OS, Neufer PD, Yeh ET, Newgard CB, MacDonald PE. Isocitrate-to-SENP1 signaling amplifies insulin secretion and rescues dysfunctional β cells. J Clin Invest (2015) 125(10):3847–3860.

McDonnell E, **Peterson BS**, Bomze HM, Hirschey MD. SIRT3 regulates progression and development of diseases of aging. Trends Endocrinol Metab. 2015 Sep;26(9):486-92.

Tan M, Peng C, Anderson KA, Chhoy P, Xie Z, Dai L, Park JS, Chen Y, Huang H, Zhang Y, Ro J, Wagner GR, Green MF, Madsen AS, Schmiesing J, **Peterson BS**, Xu G, Ilkayeva OR, Muehlbauer MJ, Braulke T, Mühlhausen C, Backos DS, Olsen CA, McGuire PJ, Pletcher SD, Lombard DB, Hirschey MD, Zhao Y. Lysine Glutarylation Is a Novel Protein Modification Regulated by SIRT5. Cell Metab (2014) vol. 19 (4) pp. 605-617